Characterization of Photonic Materials Using Thermal Lens Technique

Achamma Kurian

International School of Photonics,
Cochin University of Science and Technology,
Kochi 682 022, India

Characterization of Photonic Materials Using Thermal Lens Technique.
PhD thesis in the field of Photonics.

Author:

Achamma Kurian

Research Fellow, International School of Photonics,

Cochin University of Science and Technology, Kochi 682022, India.

E- mail: achammakurian@rediffmail.com

Permanent affiliation:

Department of Physics, Catholicate College, Pathanamthitta, India.

Research Advisor:

Dr V P Nampoori

Professor, International School of Photonics,

Cochin University of Science and Technology, Kochi 682022, India.

E- mail: vpnnampoori@cusat.ac.in

G78602

R
535.14
A CH

Front Cover:

Thermal lens effects showing the blooming of the laser beam cross section- a schematic
representation.

Back Cover:

Photograph showing the experimental set up to record   thermal lens signal.

To my husband Dr. Mathew Varughese

and my children Shon and Shema,

whom are such an important part of my life.

Certificate

Certified that the research work presented in the thesis entitled, *"Characterization of Photonic Materials Using Thermal Lens Technique" is* based on the original work done by Mrs. Achamma Kurian under my guidance in the International School of Photonics, Cochin University of Science and Technology, Kochi 682 022 and has not been included in any other thesis submitted previously for the award of any degree.

Kochi

12 July, 2002

Dr. V. P. N. Nampoori

Declaration

Certified that the work presented in the thesis entitled, *"Characterization of Photonic Materials Using Thermal Lens Technique"* is based on the original work done by me under the guidance of Prof. V. P. N. Nampoori in the International School of Photonics, Cochin University of Science and Technology, Kochi 682 022, and has not been included in any other thesis submitted previously for the award of any degree.

Kochi

12 July, 2002

Achamma Kurian

Acknowledgements

It is with deep sense of gratitude that I express my heart felt thanks to Prof. V. P. N. Nampoori for the supervision, guidance and support, without which I would not have accomplished this task.

I sincerely appreciate Prof. V. M. Nandakumaran, Director, International School of Photonics, CUSAT for his help in completing this work. Thanks to Prof. C. P. Girijavallabhan, who devoted his precious time for the meaningful discussions. I also wish to acknowledge Dr. P. Radhakrishnan and Mr.C M. Basheer for their timely help.

It is a pleasure to convey my indebtedness and sincere thanks to all research scholars of ISP for their interest and priceless help all through my Ph.D Programme.

With a deep sense of gratitude, I thank Bindhu, Hari and Nibu for their concern and timely support. I also owe to Preetha and Jean of Chemistry Department, CUSAT for their numerous help when it really matters.

Financial assistance under F. I. P. from University Grants Commission, Government of India is greatly appreciated.

Financial support from the Netherlands University Federation For International Collaboration (NUFFIC) is also acknowledged.

I extend my sincere thanks to the Principal and Manager of Catholicate College, Pathanamthitta for their encouragement and help.

I have no words to express my gratitude to my family whose constant encouragement and patience helped me in the successful completion of this work.

Achamma Kurian

Preface

One of the major achievements in the field of science and technology during the second half of the twentieth century was the invention of lasers in 1960. Laser, which generates coherent, monochromatic, intense and directional light beam, is the dream source of spectroscopists and optical scientists. Initial phase of laser research, known as the period of solution in search of a problem, has triggered a number of advancements in almost all fields of human knowledge and activities – Physics, Chemistry, Biology, Archeology, Geology, Medicine, Entertainment and Consumer devices and the list expands day by day.

Laser resolution gave birth to another revolution in the field of Communication and Information Technology. Capabilities of photons to compute, to transmit information and to get guided through optical fibre have opened up a new branch of technology called Photonics. The capabilities of optics based computers in high speed parallel processing and in ultrahigh dense connectivity have made Photonics an integral part of the fifth level computers, which fuses IT with logical processing.

Breakthrough in optical computing was possible due to the development of Non Linear Optics (NLO) that made laser a wonder source of light. Hence, synthesis and characterization of NLO materials form an integral part of Photonics based research. There exist a number of techniques to characterize optical and thermal properties of materials of which Thermo-Optic method is one of the prominent one.

The work described in the present thesis deals with the use of one of the thermo-optic phenomena called Thermal Lens (TL) effect, to investigate optical and thermal properties of a class of photonic materials namely laser dyes in solution as well as in solid matrices. When the energy of radiation matches with that of a transition between the ground state and an

excited state of the molecule a photon is absorbed. The excited molecule can eventually return to the ground state by radiative or non-radiative transition. The nonradiative de-excitation causes local heating in the sample along the beam path. The heating results in the creation of a refractive index gradient, which causes the effect of thermal blooming, or thermal lensing in the medium. This thermal lens causes a significant deviation of the probe beam path. Measurements of a change in the divergence of a laser beam after the blooming of the thermal lens allows determination of absorbance in the range $10^{-7}-10^{-6}$.

There are different configurations for the thermal lens setup. In single beam experiment, the same laser is used as both the excitation source and probe beam. In dual beam configuration, separate lasers are used as the pump and probe beams. Dual beam TL technique is more advantageous since only a single wavelength (probe) is always detected and there need be no correction for the spectral response of the optical elements and detector. Moreover one can record TL spectra only by dual beam setup. The important feature of thermo optical spectroscopy is its non-destructivity nature of analysis that provides the studies of fluorescent materials, the analysis of biological objects, the remote analysis and on-line determination in the flow. TL effect has been exploited for a number of measurements such as evaluation of triplet and fluorescence quantum yield in solid and liquid phases, study of the multiphoton processes, determination of thermal diffusivity of various samples and calorimetric trace analysis. Thermal lens spectrometry is 100-1000 times more sensitive than conventional spectrophotometry.

The eight chapters of the thesis describe the details of the work carried out and the results obtained therein.

Chapter 1 reviews the history and development of the TL effect, outlines different theoretical models along with the theory of TL spectroscopy. Applications of TL effect have been specially emphasized in this chapter.

Chapter 2 gives a detailed account of the experimental setup used for the present studies. For the study of TL effect, both pulsed and continuous wave (CW) lasers are used. Pulsed laser such as Optical Parametric Oscillator (OPO) and continuous lasers such as diode pumped solid-state laser and Argon ion laser are used as the excitation beam. He-Ne laser is used as the probe beam in the TL setup. The details of the detectors such as Digital storage oscilloscope, Lock-in amplifier, Monochromator-PMT assembly, Photodetectors, etc., used in different studies are detailed in this chapter.

Chapter 3 describes the use of dual beam thermal lens technique for the evaluation of fluorescence quantum yield of dye-doped polymers. Solid-state lasers provide an alternative to conventional liquid lasers because of their various technical and economical advantages. Luminescence quantum efficiency is one of the most important optical properties of fluorescent materials. The TL method, for evaluating quantum yield, offers significant advantages over conventional methods because the absolute values of quantum yield can be measured and no standard sample is required. TL method can be effectively used to study the variation of fluorescence quantum yield of Rhodamine 6G doped PMMA for a range of concentrations. The photodegradation of the dye molecules under cw and pulsed laser excitation are also studied using the present method details of which are included in this chapter.

Chapter 4 deals with intermolecular transfer of electronic energy, which has become a powerful tool for obtaining information about molecular excited states not obtainable by ordinary spectroscopic methods. Without electronic energy transfer, the photosynthetic process in plants could not be as efficient as it is or might not operate at all. Excitation energy transfer processes are important controlling factors in fields ranging from radiation physics to biology.

Energy transfer from a donor molecule to an acceptor molecule in a dye mixture affects the operation and spectral output of the dye laser. The energy transfer rate and the distance between molecules like

Rhodamine6G- Rhodamine B and Fluorescein – Rhodamine B are evaluated using this method. The variation of quantum yield with pH of Fluorescein and Rhodamine B are discussed in detail in this chapter.

Chapter 5 gives a detailed account of the nonlinear absorption process occurring in organic liquid like aniline. Two photon induced thermal lens spectra of aniline are recorded using Optical Parametric Oscillator (OPO). The overtone frequencies are also determined using this technique. The thermal lens spectra of Rhodamine B and Crystal Violet are also discussed in this chapter.

Chapter 6 describes a method of implementing AND, OR and NAND optical logic gates using dual beam thermal lens technique. The rapid growth of the Internet demands faster speeds and larger bandwidths than electronic circuits can provide. The speed of computers has now become a pressing problem as electronic circuits reach their miniaturization limit. This can be overcome by using optical data processing. Logic gates are the building blocks of any digital system. An optical logic gate is a switch that controls one light beam with another. Optical media used in this experiments are chemically stabilized Rhodamine 6G doped PMMA.

Chapter 7 presents the use of TL technique as a tool to study the rate of inorganic chemical reactions like that of potassium iodide – potassium persulphate. The reaction is monitored using lock-in amplifier and from the reaction curve we can calculate the reaction rate. Argon ion laser is used as the pump source for this study.

Chapter 8 gives a general conclusion and future prospects of the work carried out in the present thesis.

Publications in Journals

1) Study of energy transfer in organic dye pairs using thermal lens technique
   Achamma Kurian, K P Unnikrishnan, Pramod Gopinath, V P N Nampoori and C P G Vallabhan, *J. of Nonlinear Optical Physics & Materials*, 10, 415-421 (2001).

2) Thermal lens spectrum of organic dyes using Optical Parametric Oscillator
   Achamma Kurian, K P Unnikrishnan, D. Sajan George, Pramod Gopinath, V P N Nampoori and C P G Vallabhan, Spectrochimica Acta *Part A* (in press).

3) Effect of pH on quantum yield of fluorescein using thermal lens technique
   Achamma Kurian, Nibu A George, D. Sajan George, K P Unnikrishnan, Binoy Paul, Pramod Gopinath, V P N Nampoori and C P G Vallabhan,
   J. Opt. Soc. India, (in press)

4) Realization of logic gates using thermal lens technique
   Achamma Kurian, Nibu A George, Thomas Lee S, D. Sajan George, K P. Unnikrishnan, V P N Nampoori and C P G Vallabhan, *Laser Chemistry*, (in press)

5) Application of laser beam deflection technique to study the diffusion process in electrolyte solutions
   Achamma Kurian, C.V. Bindhu. S. S. Harilal, Riju C Issac, V P N Nampoori and C. P. G. Vallabhan, *Pramana J. of Physics*, 43, 401-406 (1994).

6) Realization of NAND & XOR logic gates using Thermal lens effect

Achamma Kurian, K P Unnikrishnan, Pramod Gopinath, Binoy Paul, V P N Nampoori and C P G Vallabhan, Photonic systems & Applications, 27-30, Nov. 2001, Singapore, *Proccedings of SPIE*, PP 100-106.

7) Nonlinear absorption and optical limiting in solutions of some rare earth substituted phtahlocyanines

K P Unnikrishnan, Jayan Thomas, Binoy Paul, **Achamma Kurian**, Pramod Gopinath, V P N Nampoori and C P G Vallabhan, *J. of Nonlinear Optical Physics & Materials*,10, 113, (2001).

8) Two and three photon absorption in rhodamine 6G methanol solutions using pulsed thermal lens technique

C.V.Bindhu, S.S.Harilal, **Achamma Kurian**, V P N Nampoori and C P G Vallabhan, *J. of Nonlinear Optical Physics& Materials*,10, 113 , (1998).

9) Studies on two photon absorption of aniline using thermal lens effect,

Achamma Kurian, K P Unnikrishnan, Thomas Lee S, D. Sajan George, , V P N Nampoori and C P G Vallabhan (communicated to *J. of Nonlinear Optical Physics & Materials*).

10) Studies on fluorescence efficiency and photodegradation of Rhodamine 6G doped PMMA using thermal lens technique,

Achamma Kurian, Nibu A George, Binoy Paul, V P N Nampoori and C P G Vallabhan, (communicated to *Laser Chemistry*).

CONTENTS

1

Thermal lens spectroscopy - An overview

This chapter introduces different photophysical processes taking place in an illuminated medium. Various photothermal phenomena that characterize the photo-induced thermal state of materials are also briefly described in the introduction. The relevant theoretical treatment of photo-induced thermal lens effect that forms the foundation of this work is discussed in this chapter. Recent advancements in the field of thermal lens spectroscopy and it's applications are also outlined.

1.1 Introduction

The science and technology of photonics is an edifice resting on two strong pillars viz., (1) the theory of light-matter interaction and (2) synthesis and characterization of photonic materials. The fifth generation computer which fuses information technology and logical programming demand fast computation and parallel processing, leading to dense connectivity. It is an accepted fact that photon-based photonic technology will provide a helping hand in this regard through the development of appropriate photonic materials and their characterization. Materials, which exhibit efficient optical nonlinearities, fluorescence quantum yield and large thermal diffusivity are potential candidates for efficient photonic materials.

The knowledge about thermal and optical properties of materials can be achieved through a systematic study of light-matter interaction. Such studies can be made by monitoring radiative or nonradiative processes taking place in a medium, which contain a number of excited state atoms or molecules. This chapter gives a brief introduction to various processes taking place due to light-matter interaction with special reference to thermo-optic effects.

1.2 Processes of light-matter interaction

The absorption of photon by a molecule (A) of a sample in accordance with their spectroscopic properties may follow a variety of effects so that the excited state molecule will lose its energy either by radiative processes or by non-radiative deactivation processes. If the photon energy is sufficient enough, direct photochemical decomposition of the molecule can be achieved. Schematic representations of relevant processes are given below.

A + hv*   (fluorescence)

A + heat (nonradiative decay)

A + hv ———→ A* ——→ B ——→ B* + A   (energy transfer)

A**(Excited state absorption)

Chemical reaction
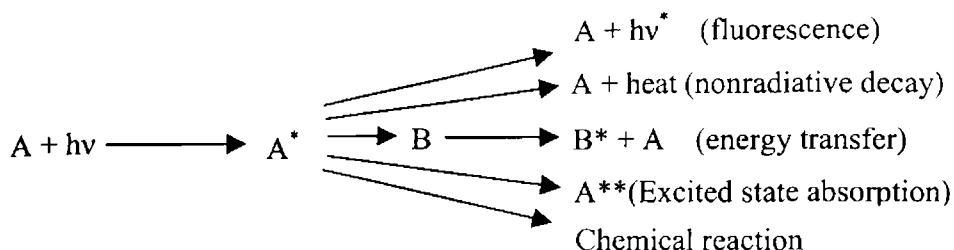
1.2.1 Fluorescence

When a molecule in the excited state returns to the ground state radiatively, the emission probability is maximum from the lowest vibrational level of the first excited singlet state, regardless of the vibrational levels or the electronic states to which the molecule is originally excited (figure 1.1). Therefore the fluorescence maximum occurs at lower energy due to the Stokes' shift. This is the difference between the energy of the excitation and emission maxima that indicates the energy dissipated during the lifetime of the excited state before returning to the ground state. Stokes' shift can be represented as

$$\text{Stokes' shift} = 10^7 \left(\frac{1}{\lambda_{ex}} - \frac{1}{\lambda_{em}} \right) \text{nm}^{-1} \tag{1.1}$$

where λ_{ex} and λ_{em} are the maximum wavelength for excitation and emission. The rate of emission depends on the molecular environment and the structure of molecule.

1.2.2 Non-radiative Transition

Once the molecule is in an exited state (S_1) it has a lifetime in the range of nano seconds, which depends upon a number of competing factors. It may non-radiatively return to the ground state by internal conversion (IC), or may undergo intersystem crossing (ISC) to the triplet state, as shown in figure 1.1.
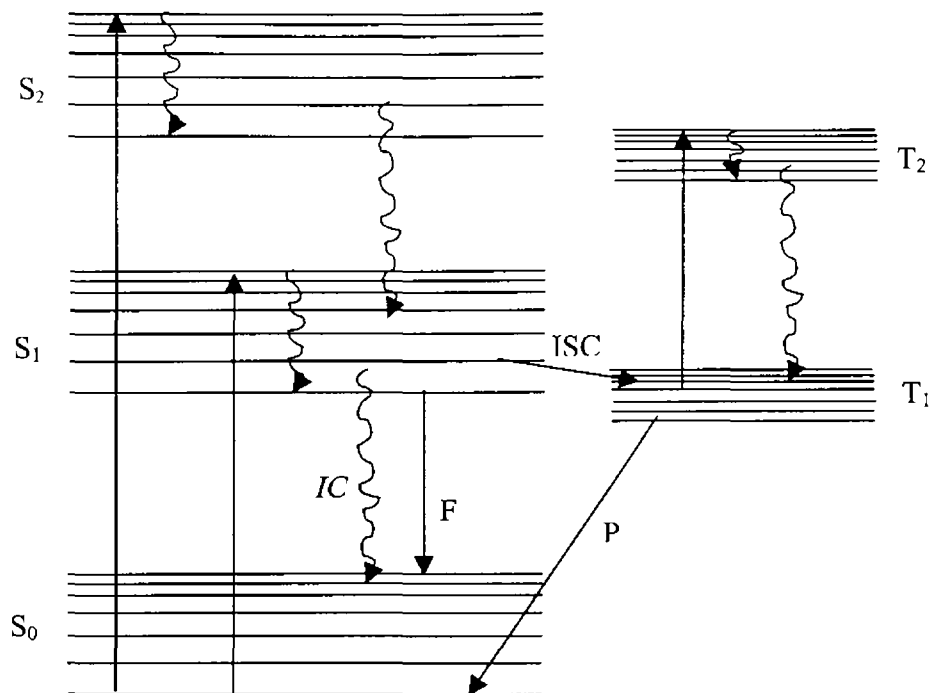
Figure 1.1 Energy level diagram of typical dye molecule illustrating several optical and kinetic processes (A-absorption, IC-internal conversion, F-fluorescence, P-phosphorescence and ISC-intersystem crossing)

However, IC cross-section is prominent factor in the case of de-excitation from S_n to S_1 (n>1) and it has low probability for transition between S_1 and S_0. It should be noted that direct absorption to triplet state is spin forbidden. Major component of nonradiative relaxations appears through de-excitation to various vibronic levels, ISC etc.

1.2.3 Energy transfer

Energy transfer represents another channel whereby the excited molecule can dispose its energy. The excited molecule (D^*) may transfer its energy to another molecule A, so that

$$A + D^* \rightarrow D + A^*$$
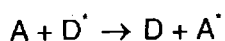
This process can be considered as either quenching of the excited state molecules D^* (A is called the quencher) or to generate A^* indirectly rather than by optical excitation. The molecule D is said to be the donor while A is the acceptor molecule. For the transfer of energy to occur, A^* should be lower in energy than D^* and it must takes place within the excited lifetime of the donor. Of the two types of transfer, in trivial process, the light emitted by the donor travels through the solution and is absorbed by the acceptor. In the other type of transfer, removal of energy from D^* occurs simultaneously with its appearance in A. In this process of nonradiative transfer, absorption spectrum of A must overlap with the fluorescence spectrum of D.

Most of the spectroscopic techniques are based on the detection of photons so that only radiative relaxation processes are monitored directly. Information regarding the nonradiative process is extracted indirectly from the data of radiative transitions. However the results obtained thus may not be reliable as far as nonradiative processes are concerned. Direct information about such process can be obtained by employing techniques of the thermo-optic effect. An added advantage is that this method will provide both optical and thermal properties of the medium directly. Salient features of the thermo-optic spectroscopy are described in the following section.

1.3   Photothermal Spectroscopy

Photothermal Spectroscopy belongs to a class of highly sensitive techniques, which can be used to measure optical absorption and thermal characteristics of a sample. The basis of photothermal spectroscopy is photo-induced changes in the thermal state of the sample due to optical absorption by molecules and the subsequent nonradiative relaxation processes that results in heating of the sample, which in turn modifies its thermal state. Photothermal signals will not be affected by scattered or reflected light unlike conventional optical signal detection. Hence photothermal spectroscopy measures optical absorption more precisely in scattering solutions, solids and at interfaces. The large signal to noise ratio of thermo-optic techniques makes it an effective tool to study the surface and absorption properties of materials, particularly for solids. There are different photothermal mechanisms that can be used for the physical and chemical analyses of materials, such as photoacoustic spectroscopy, photothermal deflection, photothermal lens spectroscopy etc. These are briefly described in the following sections.

1.3.1 Photoacoustic spectroscopy
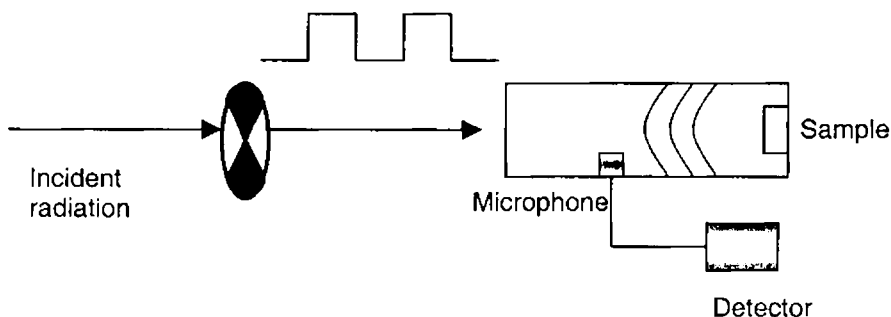
Figure 1.2   Photoacoustic effect

When light (short light pulse or modulated light beam) is absorbed by the sample, non-radiative relaxation produces local heating. This induces local expansion in the irradiated region. This thermal energy is coupled to the coupling gas in the photoacoustic cell, which causes a transient or periodic pressure change in this cell. This generates acoustic signal that can be detected using a sensitive microphone. Photoacoustic effect has been applied to detect phase transitions, fluorescent properties of laser dyes, nonlinear optical properties of materials, imaging, depth profiling etc. A good treatment of this topic is available in standard books [1].

1.3.2 Photothermal deflection

Photothermal deflection method or mirage technique is a sensitive method to evaluate the thermal, optical and transport properties of matter in all its states. In this method, the sample is excited with a mechanically modulated optical radiation. The nonradiative de-excitation of molecules produce periodic local heating of the specimen which in turn produces refractive index variation in the coupling medium.
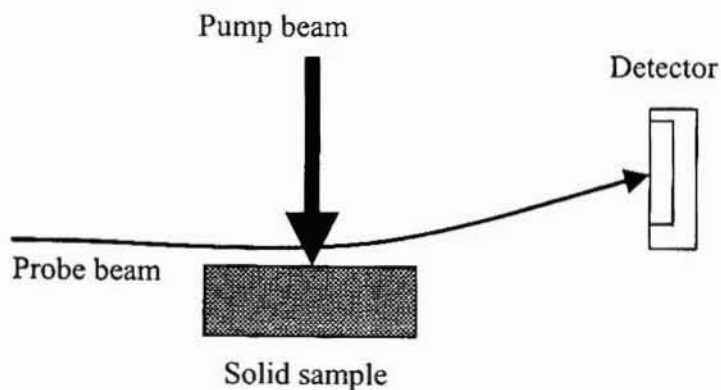
Figure 1.3 Photothermal deflection

This refractive index variation can be probed using a low power laser radiation (probe beam), the deflection of which depends on the optical and thermal properties of the sample. Depending on the pump-probe configuration, photothermal deflection technique can be employed in two ways, either in transverse photothermal deflection method or in collinear photothermal deflection method. Photothermal deflection technique has been successfully used to evaluate thermal properties of materials, surface imaging, phase transition studies etc [2].

1.3.3 Thermal lens effect

The first photothermal spectroscopic method to be applied for sensitive chemical analysis was photothermal lens spectroscopy. The photothermal lens effect was discovered by Gordon et al. in 1965 [3]. In this technique the sample is illuminated using a gaussian beam having intensity distribution across the beam as

$$I_r = I_0 e^{-2r^2/\omega^2} \tag{1.1}$$

where ω is the beam radius. A part of the incident radiation is absorbed by the sample and subsequent nonradiative decay of excited state population results in local heating of the medium. The temperature distribution in the medium mimics the beam profile of the excitation beam and hence a refractive index gradient is created in the medium. Due to this modification in refractive index, the medium mimics a lens, called thermal lens (TL). Figure 1.4 shows the schematic diagram of TL effect. The thermal lens generally has a negative focal length since most materials expand upon heating and hence have negative temperature coefficient of refractive index. This negative lens causes beam divergence and the signal is

detected as a time dependent decrease in power at the center of the beam at far field.
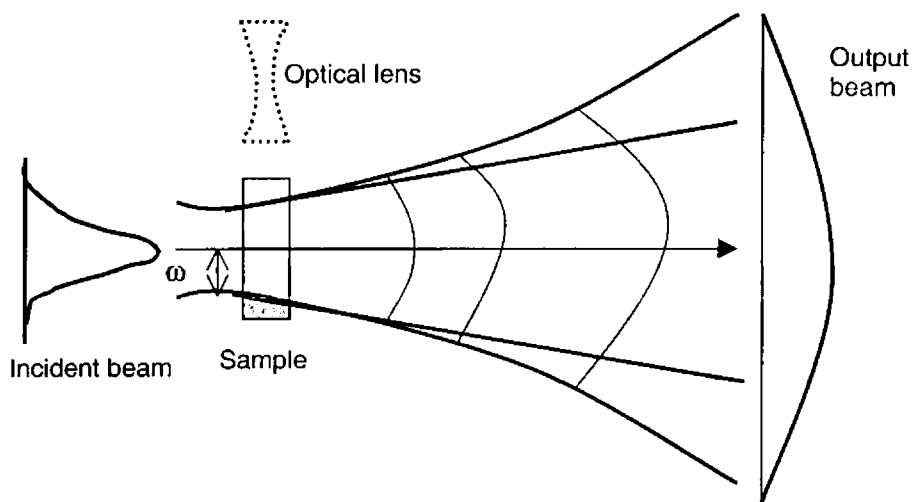
Figure 1.4   Block diagram of Thermal lens effect

1.4 Historical developments of thermal lens studies

Gordon and his coworkers observed TL effect quite accidentally during their study of laser Raman scattering of pure liquids. The resulting investigations predicted the most important application of the measurements of small absorbance. The first use of the intra-cavity thermal lens to measure the absorptivity of liquids was reported by Leite et al [4] in 1964. Solimini (1966) [5] refined the apparatus and measured the absorption coefficients of 27 organic liquids. In 1967 Callen et al [6] reported the observation of a pattern of concentric rings, which is now recognized as arising due to spherical aberration of the thermal lens. Similar observations were reported by Dabby et al in 1970 [7] and

Akhmanov et al [8]. Carman and Kelly [9] studied the time evolution of thermal lens and recorded the growth of thermal lens by a movie camera. But the problem with the intra-cavity method was that the beam propagation altered the character of the photothermal lens element and the intra-cavity apertures. The first extra-cavity photothermal lens apparatus was used by Rieckhoff in 1966 [10]. However, he misinterpreted the results as nonlinear sample absorption.

The most important advance in thermal lens technique was introduced by Hu and Whinnery in 1973 [11,12]. The authors demonstrated that maximum divergence of the laser beam could be obtained for a given sample by positioning the sample at a distance of one confocal length from the minimum beam waist of the laser, which results in sensitive absorbance measurements. Later, an extensive application and refinement of the thermal lens technique were carried out by Dovichi and Harris [13-16]. They introduced procedures needed for reliable and reproducible measurements of thermal lens signal. The authors constructed a differential thermal lens spectrophotometer for canceling the back absorbance of the sample matrix or the solvent. When the sample, with negative thermal coefficient of refractive index, is placed beyond the beam waist, a diverging beam is created and when it is placed at an equal distance before the beam waist, a converging beam is resulted. Therefore, when two cells filled with identical samples are placed symmetrically about a beam waist, a cancellation of about 99% of TL signal is observed. Hence, signal due to the matrix or solvent can be optically subtracted from that of the sample automatically, if blank sample is placed $\sqrt{3}$ times confocal distance before and after the beam waist. Using this experimental arrangement, an improved sensitivity was reported.

All the works described above used the single beam TL measurement method. The first reports of dual beam thermal lens measurements were from the

work of Grabiner et al [17] and Flynn [18] (1974) who used a He-Ne laser to probe the time resolved formation of thermal lens. The first application of dual beam TL technique to spectroscopic absorption measurements was the work of Long et al [19] who used repetitively chopped (13 Hz) tunable cw dye laser. The 13 Hz modulation frequency was selected on the basis of the practical low frequency limit for lock-in amplifier. Several other optical arrangements for the dual beam thermal lens technique have been suggested. Moacanin et al showed the counter propagating pump and probe beams through the sample. But in this arrangement care should be taken to avoid pump beam from entering probe laser cavity. Rojas et al [20] developed a dual beam thermal lens optical fibre spectrometer which is capable of measuring sensitive TL spectra at a location remote from the pump laser such as in an environmentally–controlled glove box for actinide chemistry studies and remote environmental analysis. Franko and Tran [21] constructed a cw dual-wavelength pump-probe configuration TL spectrometer that was capable of measuring thermal lens signal at two different wavelengths. The advantage of this dual–wavelength setup included its ability to correct for solvent background absorption and its improved selectivity. Swofford et al [22-24] investigated the dependence of the magnitude of thermal lens on the parameters of the experimental design in a dual beam TL setup. The authors observed very good agreement between measured and calculated signal in the repetitively chopped TL experiment.

A novel fiber optic modified thermal lens detector in combination with capillary electrophoresis that facilitate the use of microlitre volumes of samples was demonstrated by Seidel and Faubel [25]. Imasaka et al [26] constructed TL spectrophotometer [TLS] consisted of a couple of optical fibers. Franko and Tran described various analytical thermal lens instruments such as differential thermal lens, multiwavelength and spectral tunable instruments, circular dichroism

spectropolarimeters and miniaturized instruments. Recently Franko demonstrated differential IR TLS and microscopic TLS, with improved sensitivity [27-35]. Leach and Harris [36,37] and Amador-Hernandez et al demonstrated sensitivity of three orders of magnitude in supercrictical fluids [38,39], which opened new possibilities for using TLS in combination with supercrictical fluid extraction or chromatography.

The pulsed laser thermal lens has made possible the study of a wide variety of nonlinear optical effects. One of the important phenomena is two-photon absorption, by which a molecule is promoted to an excited state at twice the frequency of the incident light as a result of simultaneous absorption of two photons. Since the rate of this weak process depends on laser intensity, the use of pulsed laser combined with a sensitive detection method is required. Long et al [19] was the first to recognize TL technique as a possible detection scheme for two-photon absorption. Twarowski and Kliger studied two-photon absorption of benzene with a pulsed nitrogen pumped dye laser [40,41]. Rasheed etal recorded fifth CH overtone spectra of some organic molecules using dual beam TL method [42]. Bindhu et al investigated some novel applications of TL effect [43-50]. This includes the study of multiphoton absorption processes occurring in liquids, optical limiting properties of C_{60} and C_{70}, fluorescence quantum yield of dyes in different organic solvents, thermal diffusivity of organic liquids and sea water. The details of the theory and experimental arrangement for two-photon absorption are given in chapter 5.

1.5 Theory of Thermal lens effect

The thermal lens effect has been theoretically derived under a variety of experimental conditions [51-73]. Existing theoretical models range from relatively simple formulations to complex and sophisticated versions. These models cover

thermal lens effect, which are generated under different excitation conditions (pulsed and cw excitation), different pump/probe geometries (single and dual beam, collinear and crossed beam configuration, pump–probe displacements) and different sample conditions (stationary and flowing samples). The thermal lens effect has been theoretically derived under aberrant and parabolic models. Sheldon et al [51] were the first to consider the aberrant nature of the thermally induced lens. They used the diffraction theory to find the intensity at the beam center in the far field. Parabolic and aberrant lens models were both derived for single beam or coaxial two beam experiments in which the probe beam and pump beam radii are same in the sample cell. These models of thermal lens describing its effect upon the propagation of the probe beam assume that the sample is thick and hence the surrounding medium has no influence on the heat flow away from the probed region of the sample. Therefore for thin samples these assumptions are not valid. Wu and Dovichi [52] developed a Fresnel diffraction theory for steady state thermal lens in thin films. Fang and Swofford [24] postulated mismatched configuration and in this two beam configuration maximum sensitivity was predicted when the sample is placed at $\sqrt{3}$ times the confocal distance from the beam waist. Shen et al [53] and others modified the theory for mode mismatched configuration and constructed a dual beam mode-mismatched TL spectrometer that can be used for steady-state measurements and time resolved studies. With this apparatus they determined the trace of copper in water. Viyas and Gupta modified the theory for flowing samples [59-61].

The theoretical procedure can be divided into three parts. (I) The heat equation must be solved for the particular boundary conditions of the system to generate a temperature distribution within the sample. (2) The temperature

distribution must be converted into a refractive index profile. (3) The interaction of the beam with the refractive index profile is used to predict a change in the beam intensity profile. The different models differ primarily in the last step. A simple paraxial approximation theory is usually used to predict changes in the beam centre intensity and in the beam spot size [3, 11,12]. This paraxial approximation is a closed- form solution of ray tracing through a parabolic temperature rise near the beam axis.

1.5.1 Background

In a thermal lens experiment, a Gaussian laser beam illuminates a weakly absorbing sample. Nonradiative decay of excited states within the sample produces a temperature field that mimics the intensity profile of the laser beam. Expansion of the heated sample leads to a change in refractive index that acts to defocus the laser beam. Either the change in the beam spot size or the change in the beam centre intensity may be monitored to estimate the strength of the thermal lens.

1.5.2 Assumptions

A number of assumptions are involved in the model of the thermal lens.

(1) The laser beam is in the TEM_{00} mode so that the beam cross section
is gaussian.

(2) The spot of the laser beam remains constant over the length of the sample cell.

(3) The sample is homogeneous and satisfies Beer's law.

(4) The thermal conduction is the main mechanism of heat transfer and the temperature rise produced within the sample does not induce convection.

(5) Refractive index change of the sample with temperature, $\dfrac{dn}{dT}$, is constant over the temperature rise induced by the laser.

(6) Detection of the intensity profile of the laser beam is undertaken in the far field.

(7) The strength of the thermal lens is not sufficient to induce a change in the beam profile within the sample.

Consider a gaussian beam passing through an element of an absorbing sample in which the heat flow is radial and the beam is turned on during the time interval $0 \le t \le t_0$. The heat generated per unit length [54]

$$Q(r)dr = \frac{2\alpha E_0}{\pi\omega^2}\exp(\frac{-2r^2}{\omega^2})$$ (1.2)

where α is the absorption coefficient of the medium. E_0 is the total energy in each laser pulse and ω is the beam radius at time $t = 0$.

The temperature rise of the laser-irradiated region [57,58] is obtained as

$$T(r,t) = \frac{2\alpha E_0}{\pi\rho c_p(\omega^2 + 8Dt)}\exp(\frac{-2r^2}{\omega^2 + 8Dt})$$ (1.3)

where D is the thermal diffusivity given as

$$D = \frac{\omega^2}{4t_c}$$ (1.4)

The solution of equation for cw excitation is given as [60, 61]

$$T(r,t) = \frac{2\alpha P(1 + \cos \omega t)}{\pi\rho c_p(\omega^2 + 8Dt)}\exp(\frac{-2r^2}{\omega^2 + 8Dt})$$ (1.5)

Due to nonuniform radial temperature distribution, time dependent refractive index gradient formed inside the sample can be expressed as

$$n(r,t) = n_0 + (\frac{\partial n}{\partial t})T(r,t) \tag{1.6}$$

where n_0 is the refractive index at time $t=0$

Consequently, the irradiated sample acts like a lens, which affects the laser beam intensity profile by altering the radius ω. The relative change in the beam intensity is proportional to the relative changes in power of the beam reaching the detector and hence is a direct measure of the thermal lens strength.

The photothermal lens signal is obtained by monitoring the probe laser power that passes through a pinhole placed far from the sample. The photothermal lens will either focus or defocus the probe laser beam so that the power at the center of the beam will either increase or decrease. This change in power is maximized when the sample is placed at one confocal distance, $z_0 = \dfrac{\pi \omega_0^2}{\lambda}$ on either side of the focal point. In this case, the relative change in power monitored past the pinhole aperture is [11,12]

$$s(t) = \frac{\omega_2^2(t) - \omega_2^2(0)}{\omega_2^2(0)} \tag{1.7}$$

where $\omega_2(0)$ is the radius of the beam at time $t=0$ and $\omega_2(t)$ is the time dependent radius of a beam induced by a thermal lens given as [74,75]

$$\omega_2^2(t) = \omega_0^2[(1 - \frac{z_2}{f(t)})^2 + \frac{z_2^2}{z_0^2}(1 - \frac{z_1}{f(t)})^2] \tag{1.8}$$

$f(t)$ is the focal length of the thermal lens.

Considering the approximation $Z_2 >> Z_1$,

$$s(t) = \frac{2\, z_1}{f(t)} \tag{1.9}$$

The steady state focal length of the induced lens is given as [11,12]

$$f_\infty = \frac{\pi k \omega^2}{PA\,(dn\,/\,dt)} \tag{1.10}$$

where k is the thermal conductivity (W cm^{-1} K^{-1}), P is the laser power (W), A is the sample absorbance, and dn/dt is the refractive index change with temperature. The thermal lens signal for pulsed excitation [36,60-62]

$$S_p = \frac{4\ln(10)AE_0 Z_1}{\pi k \omega^2 t_c}\left(\frac{\partial n}{\partial T}\right)\frac{1}{(1+2t/t_c)^2} \tag{1.11}$$

For cw excitation

$$S_c = \frac{2\ln(10)APZ_1}{\pi k \omega^2}\left(\frac{\partial n}{\partial T}\right)\frac{1}{(1+t_c/2t)^2} \tag{1.12}$$

1.6   Sensitivity of Thermal lens technique

The sensitivity of TL signal can be understood by comparing it with conventional spectrophotometric measurements. Consider the transmission of optical radiation through an absorbing medium and let I_0 be the incident intensity, then the transmitted intensity, I_t is given as

$$I_t = I_0 e^{-\alpha cl} \tag{1.13}$$

where c is the concentration of the solution and l is the length of the medium. The transmittance of the medium can be defined as

$$T = \frac{I_t}{I_0} = 10^{-A} \qquad (1.14)$$

Hence absorbance is given by

$$A = 1 - T \qquad (1.15)$$

$$= 1 - 10^{-A} \cong 2.303A \qquad (1.16)$$

In TL technique the thermal gradient established after optical absorption and thermal relaxation of the sample results in a change in intensity at the beam center owing to the induced beam divergence. The thermal lens signal is expressed as the relative change in power

$$S = \frac{I_0 - I}{I} = \frac{\Delta I}{I} = \frac{2.30 AP}{\lambda k} (-\frac{dn}{dT}) \qquad (1.17)$$

where I_0 and I are the transmitted power before and after the formation of the thermal lens respectively, A is the absorbance, P is the laser power, λ is the pump laser wavelength, k is the thermal conductivity and $\dfrac{dn}{dT}$ is the samples temperature coefficient of refractive index. Equation (1.17) is written as [32]

$$\frac{\Delta I}{I} = 2.303AE \qquad (1.18)$$

where $E = \dfrac{P(-dn/dt)}{\lambda k} \qquad (1.19)$

Comparing eqn. (1.16) and (1.18) for the same absorbance, the thermal lens signal is increased by a factor E, called the enhancement factor.

The enhancement factor is a function of the thermodynamic and optical properties of the medium and on the power used to excite the sample. Thus the sensitivity of the photothermal method can be increased by using solvents with high refractive index gradient and low thermal conductivity for a given power.

With both cw and pulsed excitation, water is a poor solvent while organic solvents like carbon tetrachloride induce larger enhancement factors [74,75]. The TL signal is inversely proportional to the square of the excitation beam waist, while the sensitivity is independent of the beam size. The selectivity of TLS is hindered by the limited wavelength range of available lasers and is most frequently confined to single wavelength only. The selectivity of TL technique can be improved by using OPO based TL setup, the details are given in chapter 5.

1.7 Measurement approach

1.7.1 Single beam Thermal lens configuration

Figure 1.5 shows the schematic representation of single beam thermal lens setup. In single-beam TL spectrometer, the same laser is used to excite the sample and to probe the thermal lens created. The first analytical application of single beam thermal lens spectroscopy was the trace level determination ofCu(II) with an EDTA complex reported by Dovichi and Harris [13]. This method is perhaps the most well known and used of all the photothermal spectroscopy methods. In single beam TL spectrometer, the laser beam is focused with a lens and modulated with a chopper or a shutter. After passing through the sample, the beam center intensity is usually measured in the far field with a photodiode

placed behind the pinhole. The photo diode output is fed into storage oscilloscope, which gives the transient change in the beam center intensity.

The single beam measurement method can be used to produce a differential TL experiment. Reference and unknown samples are located on opposite sides of the beam waist so that TL strength of the two samples are
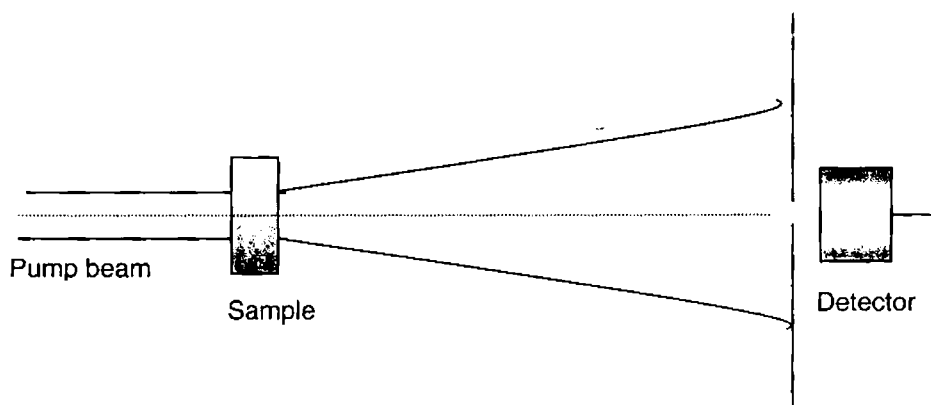
Figure 1.5 Schematic representation of single beam thermal lens setup.

subtracted by their opposite effects on the far field beam spot size. The differential configuration has immunity from laser power fluctuations but is limited to weak TL. The sensitivity of TL can be enhanced by keeping the sample at one confocal distance past the probe beam waist. Since one beam is used to probe the TL, there is decrease in power at the beam radius. The relative simplicity of the apparatus coupled with the low solution absorption detection limits, make it highly attractive for trace analysis applications.

1.7.2 Dual beam thermal lens configuration

The two-laser photothermal lens apparatus was used before the extra-cavity single laser method was invented. Dual beam instrumentation can be of two types, collinear and transverse configuration. In collinear configuration, good spatial overlapping of both beams is necessary for optimal sensitivity. The pump beam is used to generate the thermal lens in the medium. Another laser of low intensity is used to probe the lens formed. The pump beam is modulated while the probe is not. Separate lenses are used to focus the beams. The alignment and combination of the two beams is facilitated by a dichroic mirror.

The generated TL produces fluctuations in the intensity of the probe beam that can be sensitively monitored by signal averaging devices like lock-in amplifier and boxcar averager

In transverse thermal lens experiment, the excitation beam is focused on to the sample perpendicular to the probe beam. The monitored volume is defined by the intersection of two laser beams and is usually of the order of picolitres. This alignment is useful for samples, which are available in a very low concentration and in small volume and for chromatographic detection. Franko and Tran [34] using this configuration detected amino acids at a femtomole level, which corresponds to only 50 molecules. The authors used a prism to ensure a good overlap and counter propagation between the pump and probe beams.

Dual beam thermal lens setup is given in chapter 2. Dual beam technique is more advantageous since only a single wavelength (probe) is always detected

and no correction for the spectral response of the optical elements and detector are required. Moreover TL spectra can be recorded only by dual beam setup.

1.8 Advantages in using Photothermal Lens Spectrometry

- Photothermal signals are relatively linear and independent of excitation and probe laser beam focus geometries
- Excitation energy or power dependent signals may be easily measured and modeled, yielding information regarding ground and excited state absorption cross sections and relaxation rate constants
- Data is complimentary to relaxation kinetic measurements but yield more information
- Sensitivity allows the use of thin optical cells.

1.9 Recent applications

1.9.1 Differential TLS in the infrared region

Latest progress in TL technique is the construction of TL signal spectrometers, which operate in the IR region [76,77]. Franko constructed differential IR TLS spectrometer [35], which enables better cancellation of the blank signal when two identical sample cells, containing the solvent in which the analyte is dissolved, are placed symmetrically with respect to the probe beam waist. With this setup they determined organophosphate and carbamate pesticides extracted into organic solvents and they determined pesticides at the ng ml^{-1}. However, working in the IR spectral region imposes certain limitations in the instrumental design.

1.9.2 Microscopic TLS

The possibility of focusing laser beam to points smaller than 1 μm in diameter opens an area of new applications of TLS. This includes the measurements of absorbance on the microscopic level and eventually inside a single living cell. Application and development of microscopic TLS represents an important contribution to general trends towards miniaturization of analytical instrumentation [78,79]. Use of microscopic TLS demonstrated the measurements of pigments and colour distribution in a 5 μm- thick slice of human hair measuring 125 μm in diameter.

1.9.3 Foodstuff analysis

Applications of TLS to foodstuff analysis were governed by the need for new analytical tools to control the quality of foodstuffs and eventual adulteration. Franko [35] using IR TL spectrometer detected the adulteration of fruit juices and low quality of olive oils. With this setup they identified trans unsaturated fatty acids, free fatty acids, etc.

1.9.4 Analysis of environmental samples

TLS is best suited for the analysis of liquid samples. Various organic pollutants, heavy metals and biologically active compounds can be detected with high sensitivity. Further more the high sensitivity of TLS technique has been successfully combined with separation techniques such as HPLC and ion chromatography or bio-recoganation methods such as biosensors. Philip et al

[80] studied the effect of phosphorus in saline solution and Power and Langford [81] studied the brown colouration of fresh water due to the dissolved organic matters, which are detrimental to the environment.

1.9.5 Trace detection

The high absorbance sensitivity of these methods has opened up new areas of trace chemical analysis based on optical absorption spectroscopy. The first study of the application of TL technique to trace determination in solution was done by Dovichi and Harris [13] in 1979. They developed a low power (cw) thermal lens spectrometer to study the determination of Cu^{2+} having a molar absorption coefficient of 47 mol^{-1} dm^3 cm^{-1}. Grabiner et al [17] designed a collinear dual beam arrangement using Q- switched CO_2 laser -and they suggested that excellent sensitivity of TL technique could prove to be valuable for the detection of trace concentration of absorbing species in atmospheric samples. Mori et al [81] using similar setup carried out the trace determination of NO_2 and Long and Bialkowski [82] conducted a quantitative determination of CF_2Cl_2. Using this setup they evaluated the TL signal in flowing gas samples. Nakanishi et al [84] constructed a compact TL spectrometer using a near- infrared semiconductor laser and applied it to the trace analysis of phosphorus at sub-micromolar levels.

1.9.6 Measurements of absolute absorption coefficients

The high sensitivity of thermo-optic spectroscopy methods has led to applications for analysis of low absorbance samples. Using this method, concentrations lower than 10^{-7} M of these strongly absorbing chromophores may be measured in standard cuvettes. These limits of detection are slightly higher than those obtained using laser excited fluorescence spectroscopy and are 2-3 orders of magnitude better than that obtained using conventional transmission

spectroscopy. The low molar absorption detection limits coupled with the fact that the volume being probed can be very small, results in extremely small numbers of molecules being detected.

1.9.7 Measurement of Fluorescence Quantum yield

Hu and Whinnery [11] were the first to demonstrate that thermal lens spectrometer could be used to measure the fluorescence quantum yield of organic dyes using a reference standard. More details of these measurements are discussed in chapter 3 of this thesis. Terazima and Azumi [85-88] carried out a series of investigations for the measurements of quantum yield of triplet formation and triplet lifetime of different species in the liquid and solid phase using time resolved TL technique. The photodissociation of iodine has been studied by Lebedkin and Klmov [89].

1.9.8 Chemical kinetics of solution

Dual beam thermal lens technique has been successfully employed for the study of the reaction kinetics in solutions. Haushalter and Moris [90] monitored the reaction of the enzyme-catalysed oxidation of dopamine by polyphenyloxidase. The details of this application are given in chapter 7. TL spectroscopy has been used to measure thermal diffusion coefficients, sample temperatures, bulk sample flow rates, specific heats, volume expansion coefficients, and heterogeneous thermal conductivities in solids. Detailed experimental techniques, analysis of results and conclusions drawn there from are given in subsequent chapters.

References

1. A. Rosencwaig, Photoacoustics and Photoacoustic Spectroscopy, Wiley, New York, (1980).
2. Photoacoustic and Photothermal phenomena I 11,Ed. D. Bicanic, Proceedings of the 7th international Topical meeting, Netherlands, (1991).
3. J. P. Gordon, R. C. C. Lette, R. S. Moore, S. P. S. Porto and J.R. Whinnery, *J. Appl. Phys.* 9, 501 (1964).
4. R. C. C. Lette, R. S. Moore and J. R. Whinnery, *Appl. Phys. Lett.* 5, 141 (1964).
5. D. Solimini, *J. Appl. Phys.* 37, 3314 (1966).
6. W. R. Callen, B. G. Huthand R. H. Pantell, *Appl. Phys. Lett.* 11, 103 (1967).
7. F. W. Dabby, T. K. Gustafson, J. R. Whinnery and Y. Kohanzadeh and P. L. Kelly, *Appl. Phys. Lett.* 16, 362 (1970).
8. S. A. Akhamov, D. P. Krinadach, A. V. Migulin, A. P. Sukorukov and R. V. Khokhlov, *IEEE J. Quant. Elect.* 4, (1968) 568.
9. R. L. Carman and P.L. Kelly, *Appl. Phys. Lett.* 12, 241 (1968).
10. K. E. Rieckhoff, *Appl. Phys. Lett.* 9, 87 (1966).
11. C. Hu and J. R. Whinnery, *Appl. Opt.* 12, 72 (1973).
12. J. R. Whinnery, *Acc. Chem. Res.* 7, 231 (1974).
13. N. J. Dovichi and J. M. Harris, *Annal. Chem.* 51, 728 (1979).
14. N. J. Dovichi and J. M. Harris, *Annal. Chem.* 52, 2338 (1980).
15. N. J. Dovichi and J. M. Harris, *Annal. Chem.* 53, 106 (1981).
16. N. J. Dovichi and J. M. Harris, *Annal. Chem.* 53, 689 (1981b).
17. F. R. Grabiner, D. R. Siebart and G. W. Flynn, *Chem. Phys. Lett.* 17. 189 (1972).
18. G. W. Flynn, *Chemical and biological application of lasers*, Ed; C. B. Moore, Academic press, New York, p 163-201 (1974).
19. M. E. Long, R. L. Swofford and A.C. Albrecht, *Science* 191, 183 (1976).
20. D. Rojas, R. J. Silva, J. D. Spear and R. E. Russo, *Anal. Chem.* 63, 1927 (1991).
21. C. D. Tran, *Analyst.* 12, 1417, (1987).
22. R. L. Swofford and J. A. Morrell, *J. Appl. Phys.*, 49, 3667 (1978).
23. H. L. Fang, R. L. Swofford, *J. Appl. Phys.* 50, 6609 (1979).
24. H. L. Fang, R. L. Swofford, *The thermal lens in absorption spectroscopy*, in D. S. Kliger (Ed), Ultra sensitive laser Spectroscopy. Academic press, New York, 1983.
25. B. S. Seidel and W. Faubel, *J. Chromatography A*, 817, 223 (1998).
26. T. Imasaka, K. Nakanishi and N. Ishibashi, *Anal. Chem.* 59, 1554 (1987).
27. M. Franko, C. D. *Tran, Anal. Chem.* 60, 1925 (1988).
28. M. Franko, C. D. Tran, *Appl. Spectrosoc.* 43, 661 (1989).
29. C. D. Tran, *Photoacoustic and photothermal phenomena in: proceedings of the 5th International Topical meeting*, P. Hess and J. Pelzl (Eds.) Springer-Verlag, New York (1987).
30. M. Xu and C. D. Tran, *Anal. Chem.* 62, 2467 (1990).
31. M. Franko, D. Bicanic, Z. Bozoki and H. Jalink, *Appl. Spectrosoc.* 48, 1457 (1994).
32. M. Franko and C. D. Tran, *Rev. Sci. Instrum*, 62, 2430 (1991).
33. M. Franko and C. D. Tran, *Rev. Sci. Instrum*, 62, 2439 (1991).
34. M. Franko and C. D. Tran, *Rev. Sci. Instrum*, 67, 1 (1996).
35. M. Franko, *Talanta*, 54,1 (2001).

36. R. A. Leach and J. M. Harris, *Anal. Chem.* 56, 1481 (1984).
37. R. A. Leach and J. M. Harris, *Anal. Chem.* 56, 2801 (1984).
38. J. A. Hernandez, J. M. F. Romero, G. R. Ramos and M. D. L Castro, *Anal Chim.Acta* 390, 163 (1999).
39. J. Amador-Hernandez, J. M. Fernandez-Romero and M. D. L. Castro, *Talanta* 49, 813 (1999).
40. A. J. Twarowski and D. S. Kliger, *Chem. Phys.* 20, 253 (1977a).
41. A. J. Twarowski and D. S. Kliger, *Chem. Phys.* 20, 259 (1977b).
42. T. M. A. Rasheed , V. P. N. Nampoori and Sathyianandan, Chem. Phys. 108, 349 (1986).
43. C. V. Bindhu, S, S, Harilal, *Anal. Sci*, 17, 141 (2001).
44. C. V. Bindhu, S, S, Harilal, V. P. N. Nampoori and C. P. G. Vallabhan, *Current Sci.* 74,764 (1998).
45. C. V. Bindhu, S, S, Harilal, V. P. N. Nampoori and C. P. G. Vallabhan, *Opt. Eng.*
46. C. V. Bindhu, S, S, Harilal, A. Kurian, V. P. N. Nampoori and C. P. G. Vallabhan, *J. Nonlinear Opt. Phys. Mats.* 7, 531 (1998).
47. C. V. Bindhu, S, S, Harilal, R. C. Issac, V. P. N. Nampoori and C. P. G. Vallabhan, *J. Phys. D Appl. Phys.* 29, 1074 (1996).
48. C. V. Bindhu, S, S, Harilal, R. C. Issac, V. P. N. Nampoori and C. P. G. Vallabhan, *Pramana-J. Phys.* 44, 225 (1995).
49. C. V. Bindhu, S, S, Harilal, R. C. Issac, V. P. N. Nampoori and C. P. G. Vallabhan, *Pramana-J. Phys.* 44, 231 (1995).
50. C. V. Bindhu, S, S, Harilal, R. C. Issac, V. P. N. Nampoori and C. P. G. Vallabhan, *Mod. Phys. Lett. B* 9, 1471 (1995).
51. S.J. Sheldon, L. V. knight and J. M. Thorne, *Appl. Opt.* 21, 1663 (1982).
52. S. Wu and N. J. Dovicni, *J. Appl. Phys.*, 67, 1170 (1990).
53. S. Shen, A. J. Soroka and R. D. Snook. *J. Appl. Phys.*, 78, 700 (1995).
54. A. E. Siegman, *Lasers*, Oxford University press (1986).
55. R. Raymond, T. Bailey, F. R. Cruickshank, D. Pugh and W. Johnstone, *J. C. S. Faraday 2*, 76, 633 (1980).
56. R. Raymond, T. Bailey, F. R. Cruickshank, D. Pugh and W. Johnstone, *J. C. S. Faraday 2*, 1387 (1981).
57. H. S. Carslaw and J. C. Jaeger, *Operational methods in Applied Mathematics* 2nd ed. Dover Publications New York, , pp. 393 (1948).
58. G. N. Watson, *Bessel Functions*, 2nd ed. Macmillan, Newyork, ,p393 (1948).
59. R. Guphta in *Photothermal Investigations of solids and Fluids* ed. J. A. Sell (Academic, New York, (1988).
60. R. Vyas and R. Guptha, *Appl. Opt.* 27, 4701 (1988).
61. Q. He, R. Vyas and R. Guptha, *Appl. Opt*, 36, 1841 (1997).
62. J. M. Harris, *Thermal lens effect*, in; E. H. Piepmeier (d) Analytical applications of lasers, Wiley, New York, 1986, p. 451.
63. S. E. Bialkowski, *Photothermal spectroscopy methods for chemical analysis* in: J. D. Winefordner (Ed), Chemical Analysis, vol. 134, Wiley, New York 1996.
64. J. R. Whinnery, D. T. Miller and F. Dabby, IEEE J. Quant. Elect. 3, 282 (1967).
65. J. Shen, D. R. Lowe and R. D. Snook, *Chem. Phys.* 165, 385 (1992).
66. M. L. Baesso J. Shen and R. D. Snook, *Chem. Phys. Lett.* 197, 255 (1992).

67. M. L. Baesso J. Shen and R. D. Snook, *J. Appl. Phys.* 75, 3732 (1994).
68. J. Shen, M. L. Baesso and R. D. Snook, *J. Appl. Phys.* 75, 3738 (1994).
69. R. D. Snook and D. R. Lowe, *Analyst*, 120, 2051 (1995).
70. T. Catunda, M. L. Baesso, Y. Messaddeq and M. A. Aegerter, *J. Non- Crystalline solids*, 213&214, 225 (1997).
71. M. L. Baesso, A. C. Bento, A. A. Andrade, T. Catunda, J. A. Sampaio and S. Gama, *J. Non-Crystalline solids*, 219, 165 (1997).
72. M. L. Baesso, A. C. Bento, et al *J. Appl. Physics*, 85, 8112 (1999).
73. S. M. Lima, T. Catunda, M. L. Baesso, L. D. Vila, Y. Messaddeq, E. B. Stucchi and S. J. L. Ribeiro, *J. Non- Crystalline solids*, 247, 222 (1999).
74. S. M. Lima, T. Catunda, R. Lebullenger, A. C. hernades, M. L. Baesso, A. C. Bento ,and L. C. M. Miranda, *Phys. Rew.* B, 60, 15173 (1999).
75. S. M. Colombe and R. D. Snook, *Analytica Chimica Acta*, 390, 155 (1999).
76. M. Franko, P. Van De Bovenkamp and D. Bicanic, *J. Chromatogr. B Biomed. Sci. Appl.* 718,47 (1998).
77. M. Sikovec, M. Novic and M. Franko, *J. Chromatogr.* A 706, 121 (1995).
78. S. L. Nickolaisen and S. E. Bialowski, *Anal. Chem.* 57, 758 (1985).
79. A. Harata, T. Kitamori and T. Sawada, *J. Jap. Soc.* 68, 606 (1995).
80. T. Philip, T. S. Chen and D. B. Nelson, *J. Agric. Food Chem.* 37, 90 (1989).
81. J. F. Power and C. H. Langford, Anal. Chem. 60, 842 (1988).
82. K. Mori, T. Imasaka, and N. Ishibashi, *Anal. Chem.* 55, 1075 (1983).
83. G. R. Long and S. E. Bialkowski, *Anal. Chem.* 56, 2806 (1984).
84. K. Nakanishi, T. Imasaka, and N. Ishibashi, *Anal. Chem.* 57, 1219 (1985).
85. M. Terazima, and T. Azumi, *Chem. Phys. Lett.* 141, 237 (1987).
86. M. Terazima, and T. Azumi, *Chem. Phys. Lett.* 145, 286 (1988).
87. M. Terazima, H. Kanno and T. Azumi, *Chem. Phys. Lett.* 173, 327 (1990).
88. M. Terazima, M. Horiguchi and T. Azumi, *Anal. Chem.* 61, 883 (1989).
89. S. F. Lebedkin and A. D. Klmov, *Chem. Phys. Lett.*190, 313 (1992).
90. J. P. Haushalter and M. D. Morris, *Appl. Spect.* 34, 445 (1980).

2

Experimental details

This chapter describes the general experimental methods used in the work presented in this thesis. A brief idea of the different laser systems and detectors used in the study are also presented in this chapter.

2.1 Introduction

To generate thermal lens in the medium, the molecules of the medium are excited to the higher energy states using either pulsed or cw lasers. The excited molecules relax their energy by the generation of heat and light. The heat released results in the change in the refractive index in the medium and the refractive index gradient is formed due to the intensity distribution of the cross section of incident light beam. The induced refractive index in the medium creates a lens like behavior called thermal lens. Another laser beam is used to detect the presence of the thermal lens [TL]. TL signal thus formed is processed using different equipments such as Digital storage oscilloscope, Lock-in amplifier etc. The absorption spectrum and fluorescence spectrum of the medium are also recorded for further evaluation of the parameters like fluorescence quantum yield, energy transfer rates etc.

2.2 Laser systems

The laser as a source of coherent optical radiation has made it possible to investigate nonlinear interaction of optical radiation with atoms and molecules. The Optical Parametric Oscillator, diode pumped solid state laser, argon ion laser and He-Ne laser are the laser sources used for the investigation of thermal lens studies described in this thesis.

2.2.1 Optical Parametric Oscillator (OPO)

Pulsed laser used for the studies described in chapter 4 and 5 is a tunable solid-state Optical Parametric Oscillator (Quantaray mopo-700) having wide range tunability from 450 to 2 m [1]. Most lasers are single wavelength devices or have only a restricted range of multiple wavelengths. The widely used

wavelength tunable coherent radiation sources are dye lasers. But each dye has a rather limited tuning range of about 5 to 20 nm in the visible part of the spectrum. Moreover, optical parametric devices provide wide and continuous wavelength coverage, easy and rapid wavelength tunability, high-energy output and the added advantage of being of solid state.

OPO is based on a nonlinear optical process that involves energy conversion of a pump beam of fixed frequency ω_p into two lower energy beams, the signal at ω_s and the idler at ω_i. so that

$$\omega_p = \omega_s + \omega_i$$

$$\frac{1}{\lambda_p} = \frac{1}{\lambda_s} + \frac{1}{\lambda_i}$$

or

$$\lambda_s = \frac{\lambda_p}{1 - \frac{\lambda_p}{\lambda_i}}$$

as λ_i increases λ_s decreases and vice versa. Figure 2.1 shows the schematic diagram of Optical Parametric Oscillator. It is composed of a nonlinear crystal placed within an optical resonator to form feedback for these signal or idler or both. The nonlinear material used in this Optical Parametric Oscillator is BBO (Barium Borate). BBO has broad transparency, large optical nonlinearity, large birefringence, high optical damage threshold and large fracture temperature. The third harmonic of Nd: YAG laser at 355 nm is generated by mixing the fundamental output at 1064 nm with the second harmonic at 532 nm in the nonlinear material BBO [2]. The signal and idler exhibit strong coherence are highly monochromatic and have a spectrum consisting of one or more longitudinal modes. OPO obtains gain from a nonlinear conversion rather than an

atomic transition. The output of OPO is greater than 40 mJ of energy and 10 Hz repetition rate over most visible wavelength, with conversion efficiencies in excess of 20% at single wavelength. As indicated earlier we can use both λ_i and λ_s as tuned out put so that effective tunability is enhanced.
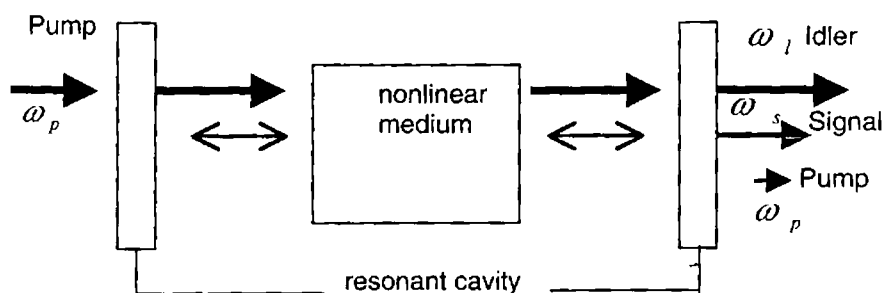
Figure 2.1 Schematic diagram of optical parametric oscillator where only a pump wave of frequency ω_p is used to interact with a nonlinear optical medium to generate widely tunable signal ω_s and idler radiation of frequency ω_i.

2.2.2   Diode pumped solid state laser (DPSS)

One of the cw lasers employed for the thermal lens studies (chapter 3, 6 and 7) is the diode pumped solid state laser (Uniphase BWT-50) having an out put of 50 mW [3]. Diode pumped lasers have many advantages over the old style arc lamp or flash lamp based systems. The diode pumped systems are smaller, consume less power and they have less waste of heat. Neodymium doped Yttrium vanadate (Nd:YVO$_4$) is the most efficient and excellent laser crystal for DPSS lasers, due to its good physical, optical and mechanical properties. Nd:YVO$_4$ has

moderate power, low threshold, large stimulated emission cross-section at lasing wavelength, high slope efficiency, wide absorption peak at pump wavelength, low intrinsic optical loss, high laser induced damage threshold, strong polarized output and good physical, optical and mechanical properties as well. Comparing with Nd:YAG, Nd:YVO$_4$ has higher absorption coefficient at pumping wavelengths, which means that Nd:YVO$_4$ with shorter lengths (such as 1mm) can be used to constructe more compact lasers. Furthermore, the wider absorption bandwidth permits a less pump wavelength drift due to the variations of temperature or aging of diode. These features guarantee Nd:YVO$_4$ as one kind of laser host which is most suitable to construct more compact and significantly more efficient DPSS lasers.

2.2.3   Argon ion laser

Another cw laser used for the present studies is Argon ion laser having a power of 4 W (Spectra Physics model Liconix-5000 series). All the wavelengths of light emitted by the Argon laser can be operated in multi-mode and single line operation is also possible by tuning prism. Every wavelength is a monochromatic light source of itself and each wavelength has a very narrow bandwidth. The two dominant wavelengths, of 514 and 488 nm make up about 67% of the total beam output power. The other wavelengths are 496.5, 476.5 and 456 nm. The out put has a Gaussian profile and has a frequency stability of 60 MHz per degree Celsius and good stability when used in the light control mode [4]. When the laser is first turned on, a delay allows for temperature stabilization. Then a pulse of high voltage (8 kilovolts DC) ionizes the argon gas. Upon ionization, high DC current (45 Amps) and about 600 volts DC across the gas filled tube maintains a sufficient discharge to keep the gas ionized. This Argon laser tube has a tungsten bore which has a high melting point and allows the laser to operate at

higher power levels with longer tube life. Argon lasers require tap water cooling and separate three phase 220 AC volt and 50 Amps electrical line [5, 6].

2.2.4   He-Ne laser

This continuous- wave gas laser have exceptional temporal and spatial coherence, good polarization, good pointing stability over and above, it is cheap. 632.8 nm radiation from He-Ne (Uniphase Model No. 1507) having a Gaussian intensity profile was used as the probe beam in the experimental studies. The output of the laser is 2 mW and it is intensity stabilized [7].

2.3 Detectors

2.3.1 Digital Storage Oscilloscope (DSO)

The digital storage oscilloscope used for the present study is Tektronix, TDS220 (100 MH$_z$). The maximum sampling rate is 1 GS/s [8]. Digital oscilloscopes sample signals using a fast analog-to-digital converter (ADC). At evenly spaced intervals, the ADC measures the voltage level and stores the digitized value in high-speed dedicated memory. The shorter the intervals, the faster the digitizing rate, and the higher the signal frequency which can be recorded. The greater the resolution of the ADC, the better the sensitivity to small voltage changes. The more memory, the longer the recording time. Multiple signals associated with intermittent and infrequent events can be captured and analyzed instantly. Captured waveforms can be expanded to reveal minute details such as fast glitches, overshoot on pulses, and noise. These captured waveforms can be analyzed in either the time or frequency domains. It has internally adjustable pretrigger viewing, superior measurement accuracy, quiick hardcopies on printers and plotters, archives for later comparison or analysis, waveform

mathematics and spectral analysis and completely programmable and automatic setups.

2.3.2 Lock-in amplifier

Lock-in amplifier is an extremely important and powerful measuring tool used to measure voltage amplitudes as small as few nano volts while ignoring noise signals thousands of times larger. The lock-in amplifier used for both TL and fluorescence studies were Standford Research Systems S R 850 [9]. Lock-in amplifiers use the process of synchronous detection to recover signals that have been buried in noise. They act as extremely narrow pass band filters with the pass band centre point selected by a reference signal [10, 11].
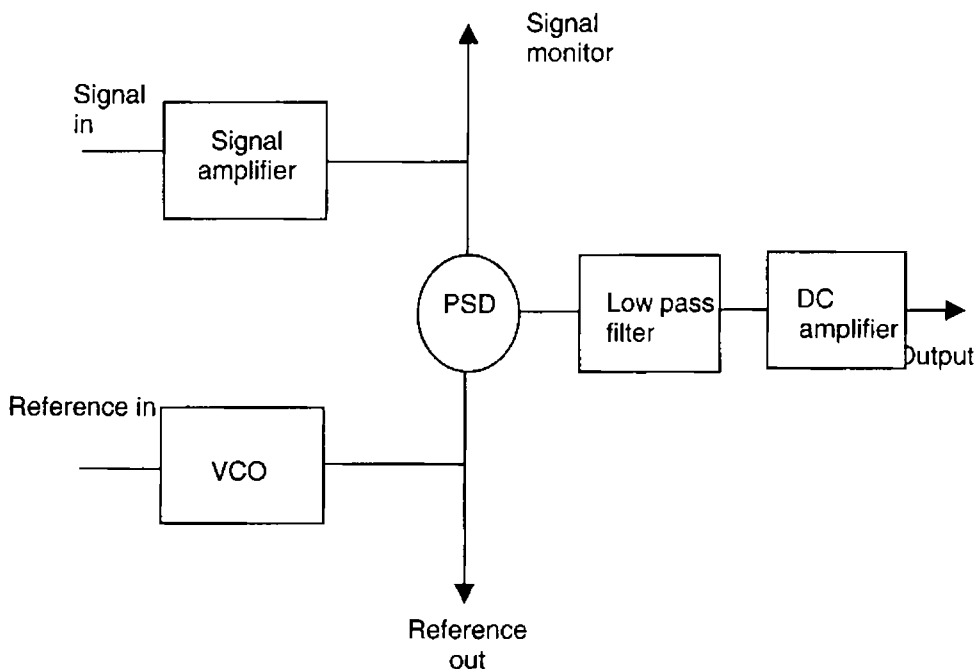
Figure 2 .2 Block diagram of the lock-in amplifier

The signal amplifier is a voltage amplifier with variable filters. The voltage-controlled oscillator (VCO) is able to synchronize with an external reference signal. It also contains a phase- shifting circuit that allows to shift its signal from 0° to 360° with respect to the reference. The phase sensitive detector (PSD) is a circuit, which takes in two voltages as inputs and produces an output, which is the product of the two inputs. The low-pass filter is an RC filter and the dc amplifier is a low frequency amplifier.

2.3.3   Photodetector

Optical detection is a process in which optical signals are converted into electrical signals and photodetectors are the key components of such detection systems. Photodetectors like photodiodes and photomultiplier tubes are used to extract information contained in the optical beams as well as to monitor the presence of light.

Photomultiplier tube (PMT)

In a photomultiplier tube electrons ejected by a   photosensitive cathode   are accelerated to secondary electrodes known as dynodes (figure 2.2). When impacting electrons have sufficient kinetic energy, additional electrons are released from the dynodes. The newly released electrons are also accelerated by the applied fields to the next dynode, thus generating even more electrons. Finally, they are collected and passed to the external circuits. Since more and more electrons are emitted by the successive dynode stages, more electrons reach the external circuit. This means that there is an internal current gain in the PMTs. The internal gain is dependent upon the electron emission efficiency, the geometry of the dynodes, and the applied voltage.
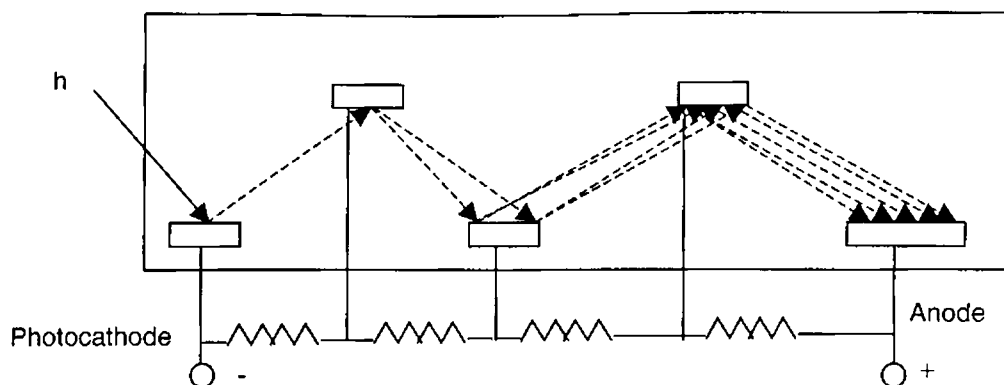
Figure 2.3 Schematic diagram of a photomultiplier tube.

The presence of this gain is the main advantage of the PMTs over vacuum diodes. The spectral characteristics of PMTs are determined by the spectral sensitivity of the photocathodes. To liberate electrons from a photocathode, the photon energy must be greater than the work function of the material. The speed of response of PMTs is determined by the time of flight of electrons from the photocathode to the dynodes. In order to have the advantage of the available bandwidth the electrodes must be impedance matched with the other circuit elements [14]. The operating voltage for this PMT is -750 V (1.7 – 2.1 KV). The Model Thron MI PMT with S-20 cathode is used in our studies [15].

2.3.4   Monochromators

Monochromator is another important tool for both research and education purposes. A monochromator is a spectrometer capable of measuring a single wavelength which can be scanned through a wide wavelength range. Monochromator consists of fixed entrance and exit slits, fixed focusing mirrors and a rotatable diffraction grating. As the grating rotates different wavelength is

focused onto the exit slit. The spectral resolution depends on the widths of the slits, the choice of grating and focal length. Grating monochromators may have planar or concave gratings. Planar gratings are produced mechanically and may contain imperfections in some of the grooves. Concave gratings are usually produced by holographic methods and imperfections are usually rare. Imperfections of the gratings are major sources of stray light transmission by the monochromators, and of ghost images from the grating. For this reason the holographic gratings are preferable for the study of emission spectroscopy. Another important characteristic of the grating monochromators is that the transmission efficiency depends upon polarization of the light. Therefore, the emission spectrum of the sample can be shifted in wavelength and altered in shape, depending upon the polarization conditions chosen to record. In the present work we used the following monochromators.

2.3.4.1 Spex- 1m monochromator

Spex, Model 1704 is a 1 meter scanning spectrometer having a maximum resolution of 0.05 A [12]. The monochromator covers a spectral range 350-950 nm using a grating with 1200 grooves per mm blazed at 500 nm and spectral band pass 0.1 A. The entrance and exit silts on the front of the spectrometer are controlled by micrometer type knob above the slits. The scan rate of the monochromator is adjusted by using microprocessor controlled spex compudrive (CD2A) arrangement. Spex compudrive has got a key board control over the spectrometer which not only provides repeat scan over the spectral regions but also gives the scan status and spectrometer position. The main advantages of CD2A compudrive are, the start and end positions of the scan, rate, repetitions, delay between repetitions, recorder scale and marker frequency can be programmed (9). The output of the spex monochromator is coupled to a

thermoelectrically cooled photo multiplier tube (Thorn EMI, model KQB 9863, rise time 2 ns, quantum efficiency 22%).

2.3.4.2 McPherson- 0.2 m monochromator

The monochromator of the unit is the McPherson Model No. 275 [13]. This model is a 0.2m, f/2 instrument. Bilaterally adjustable slit assemblies allow resolutions as high as 0.4nm with a 1200G/mm grating and a maximum bandpass of 16nm. McPherson provides innovative electronics for detector operation and signal level amplification. The wavelength range of a monochromator varies with the choice of grating and this model can scan from 200 nm to 600 nm.

2.3.5 Spectrophotometer

Absorption spectra are recorded by JASCO-570/UV/VIS/NIR spectrophotometer [16] which covers a wavelength range of 190 nm to 2600 nm.

2.3.6 Power meters

The detection and measurement of laser power can be classified as photon detection and thermal detection. Photon detectors such as silicon photocells directly convert the energy of individual photons into a voltage or current. Thermal detectors convert light into heat and then into electric signal.

Model 407A (Spectra-Physics) [17] power meter is a thermopile detector that withstands 20 KW/cm^2 average power density. This model is capable of measuring power from a few milliwatts upto>20 W.

Model 1815-C (Newport) [18] optical power meter that provides optical measurement from nanowatts to kilowatts.

Model 55 PM (Liconix) [19] optical power meter having a maximum of 300 mW is also used in the studies.

2.4 Accessories (Other components of experimental setup)

2.4.1 Chopper

For double beam cw thermal lens measurements, the argon ion laser beam was modulated using a mechanical chopper (EG&G Parc model 192 or SR540, Stanford Research Systems). Mechanical chopper is the simplest form of a modulator consisting of a rotating slotted disk placed in the path of light beam. It offers 100% modulation depths for frequencies from a few Hz to 5-8 KHz [20, 21].

2.4.2 Sample cell

The sample cells used for thermal lens studies are 1mm and 3 mm quartz cuvettes and for fluorescence studies are 10 mm cuvette.

2.4.3 Optical fibre

Thermal lens signal is coupled to the monochromator through an optical fibre (200μm core, NA 0.22) with minimum loss in transmission. Use of OF makes the experimental configuration geometrically flexible.

2.4.4 Vibration free table

The experimental setup was arranged on a locally made vibration isolated table (Hallmarc) so that errors due to any stray vibrations are minimised.

2.5   Experimental setup

Both continuous and pulsed laser excitations have been used for the measurements of weak absorbance, determination of fluorescence quantum yield, thermal diffusivity of different solvents, study of multiphoton processes and excitation energy transfer between molecules etc.

2.5.1   Pulsed laser thermal lens setup

The experimental set up (dual beam) for the transient thermal lens studies is shown in figure 2.4. Pulsed laser photothermal lens technique has allowed a number of applications involving the study of radiationless de-exciation processes. The high irradiance at the focus can induce nonlinear absorption effects. The absorbed energy is proportional to the integrated irradiance raised to the power of the number of photons absorbed. In this configuration separate lasers are used for pump and probe beams. This dual beam technique is more advantageous since only a single wavelength (probe) is always detected and there needed no correction for the spectral response of the optical elements and detector. Moreover one can record TL spectra only by dual beam setup.

The pulsed laser used for the present study is an Optical Parametric Oscillator with tunable output in the range 450-620 nm. OPO is characterized by pulses of about 10 ns width with a Gaussian profile. The repetition rate was 10 Hz. A long focal length lens (400mm) is used for focusing the excitation beam so that the spot size inside the cuvette remains more or less constant.
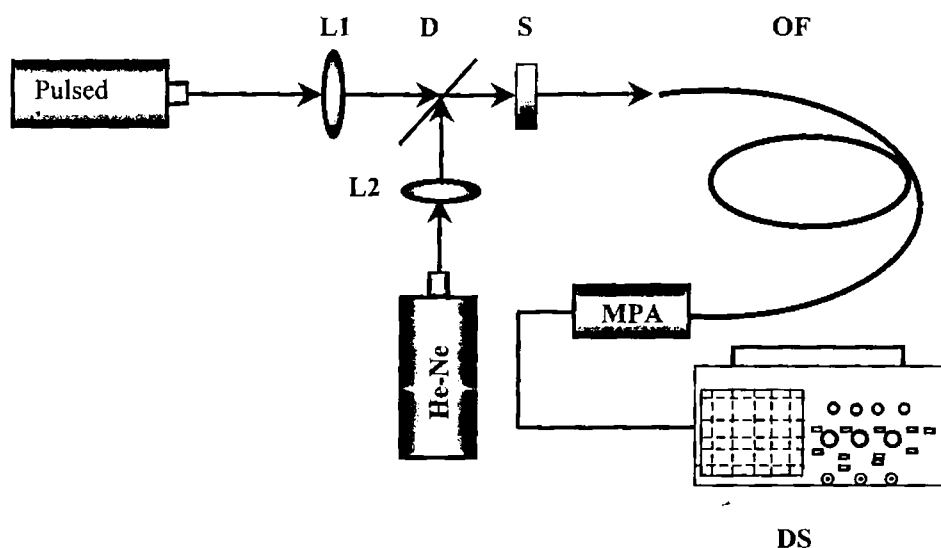
Figure 2.4 The block diagram of the experimental arrangement for the pulsed Thermal lens effect. L_1, L_2– Lens; DM - Dichoric Mirror; S - Sample; OF - Optic Fibre; MPA - Monochromator-PMT assembly; DSO- Digital Storage Oscilloscope.

The excitation energy at the sample cell was varied from 0.3mJ to 3mJ by using optical density filters. Radiation of wavelength 632.8 nm from a low power (1.5 mw) intensity stabilized He-Ne laser source is used as the probe beam. Accurate alignment of the laser beams is essential for better results.

In collinear arrangement first, fix the path of the pump laser beam by locating it at two points in space with an appropriate visible method and marking this with irises closed down to their minimum apertures. The second laser beam

is then centered on these irises (using a dichroic mirror) using the appropriate visible method and opening the irises to a suitable diameter to ensure accurate alignment. The probe beam was focused by a 20 mm focal length lens. The TL signal is detected by sampling the intensity of the centre portion of the probe beam through a small aperture. The polished tip of the optical fibre mounted on XYZ translator is placed at the beam center in the far field which serves simultaneously as the finite aperture as well as a light guide for the probe beam to a monochromator − photomultiplier tube (PMT) assembly. The advantage of using optical fibre in the detector system is that remote detection of signals is possible apart from the geometrical flexibility in the configuration of the experimental setup. The monochromator-photomultiplier assembly tuned to the probe wavelength (632.8 nm) provides further filtering of the signal. The TL signal is detected as the relative change in the intensity of the probe beam centre at far field and processed using a 100 MHz digital storage oscilloscope, which provides a complete time domain representation of the signal. A synchronous trigger pulse from the Nd: YAG driver laser operated at 10 Hz is used to trigger the oscilloscope. The present work is done at a temperature of 26 ° C. The thermal lens signal outputs are normalized to account for the spectral profile of the OPO output. This dual beam technique is more advantageous since only a single wavelength (probe) is always detected and there needed no correction for the spectral response of the optical elements and detector. Moreover, the dual beam TL setup can be used to record TL spectrum unlike in the case of single beam setup.

2.5.2 Continuous wave thermal lens setup

Continuous wave (cw) thermal lens spectrometry has proved to be a valuable technique to study thermal and optical properties of transparent materials. Eversince

the earlier report of the TL effect the sensitivity of the technique has been improved by changing the experimental configuration. [22-24]. The excitation source was 532 nm from a Diode Pumped Nd: YVO_4 laser or 488 nm radiation from an Argon ion laser. The excitation beam was focused with a 400 mm focal length lens.

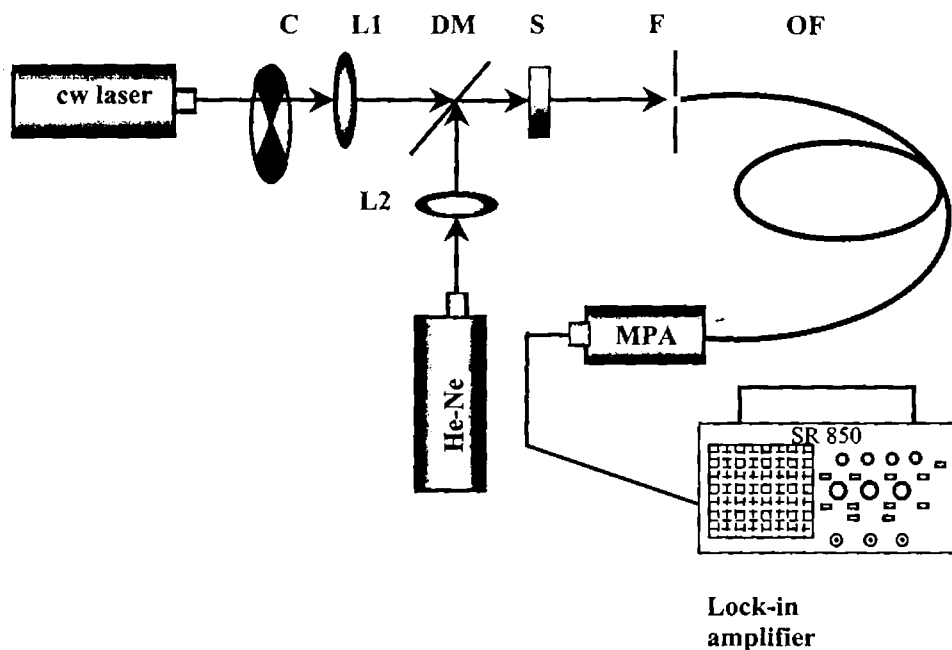*Figure 2.5 Schematic diagram of the cw thermal lens set up. L_1, L_2– Lens; DM - Dichoric Mirror; C- chopper; S - Sample; OF - Optic Fibre; MPA - Monochromator-PMT assembly.*

The probe beam was focused by a 200 mm focal length lens. The sample cell was a 1mm / 3 mm optical path length quartz cuvette and was positioned at the optimum

distance from the waist of the probe beam. The probe beam is made to pass collinearly through the sample using a dichroic mirror. A filter is placed in the path of the emergent beams, which allow only the 632.8 nm wavelengths to reach the detector system. An optical fibre mounted on XYZ translator serves as finite aperture. The center of the probe beam is coupled to the monochromator - photomultiplier tube (PMT) assembly using an optic fibre placed 2m away from the sample. The output from PMT is connected to a 47 KΩ impedance matching circuit and then processed using a dual phase digital lock-in amplifier (SR 850).
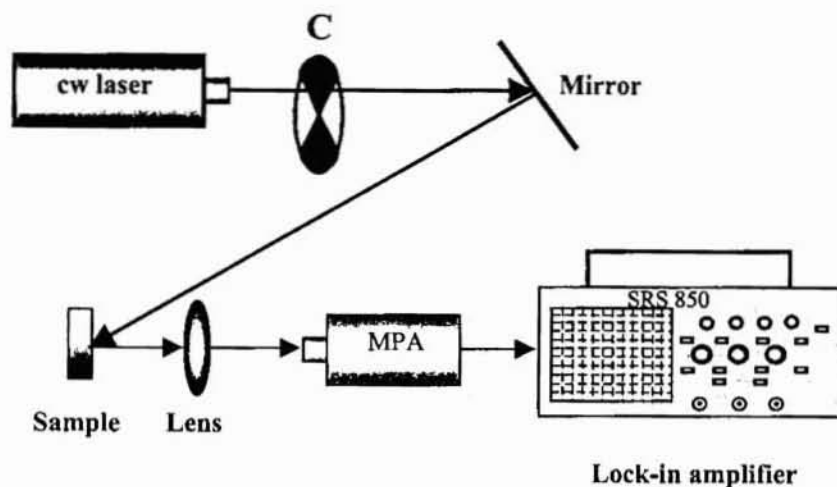
2.5.3 Fluorescence studies

Figure 2.6 Schematic diagram of the fluorescence setup. The sample can be dye solution /solid sample in the form of discs.

Continuous wave laser source is used for the fluorescence study. Solution is taken in the cell. In this configuration fluorescence emission from the front surface of the cell is collected and focused by a lens to the entrance slit of a 1m Spex / McPherson monochromator, which is coupled to a PMT having an S20 cathode. The PMT output is fed to a lock-in amplifier .The emission wave length is scanned in the specified region (490-640 nm). Dye doped polymer samples are moulded in the form of a disc.

References

1. Instruction manual, Optical Parametric Oscillator, Model Quantaray mopo-700.
2. L. K. Cheng, W. R. Bosenberg and C. L. Tang, *Appl. Phys. Lett.* 53, 175 (1988).
3. Instruction manual, Diode pumped solid-state laser, Model Uniphase BWT-50.
4. Instruction manual, Argon ion laser, Spectra physics, Model Liconix 5000 series.
5. O. Svelto, Principles of Lasers, New York, Plenum Press, 1976.
6. A. E. Siegman, Lasers, Mill Valley, CA: University Science Books, 1986.
7. Instruction manual, He-Ne laser, Uniphase, Model No. 1507.
8. Instruction manual, Tektronix Model TDS 220.
9. Instruction manual, Standford Research Systems, Model SR850.
10. R. Wolfson, *Am. J. Phys.* 59, 569 (1991).
11. J. H. Scofield, *Am. J. Phys.* 62, 129 (1994).
12. Instruction manual, Spex CD2A compudrive (Spex,USA).
13. Instruction manual, Mcpherson monochromator Model no.275.
14. C. Chen, Elements of optoelectronics &fiber optics, IRWIN, USA,1996.
15. D. R. Carter, Photomultiplier Hand book, 1987.
16. Instruction manual, spectrophotometer JASCO-570/UV/VIS/NIR.
17. Instruction manual, Power meter Spectra-Physics Model 407A.
18. Instruction manual, Power meter Newport-Model 1815-C.
19. Instruction manual, Power meter Liconix-Nodel 55PM
20. Instruction manual, Mechanical chopper, Eg&g Parc model 192.
21. Instruction manual, Mechanical chopper, Standford Research Systems, Model SR540.
22. C. Hu and J. R. Whinnery, *Appl. Opt.* 12,72 (1973).
23. S. J. Sheldon, L. V. Knight and J. M. Thorne, *Appl. Opt.* 21, 1663 (1982).
24. T. Higaishi, T. Imasaka and N. Ishibashi, *Anal. Chem.* 55, 1907 (1983).

3

Study of thermo-optic properties of dye doped polymer

This chapter describes the use of thermal lens technique as a quantitative method to determine absolute fluorescence quantum efficiency and concentration quenching of fluorescence emission from dye doped polymer. Samples considered for the experiments are rhodamine 6G doped Poly(methyl methacrylate) (PMMA) prepared with different concentrations of the dye. The fluorescence quantum yield strongly depends on the concentration of the dye. The accurate measurement of thermo-physical properties of materials, such as thermal diffusivity, is an integral part of heat transfer and thermal processing. This chapter also presents a laser-based thermal lens technique to measure the thermal diffusivity of dye doped PMMA. Thermal lens technique is also used to study the photodegradation of the dye.

3. 1 Introduction

From the mid 60s, dye lasers have been attractive sources of coherent tunable visible radiation because of their unique operational flexibility. The salient features of dye lasers are its tunability with emission from near ultraviolet to the near infrared. High gain, broad spectral bandwidth enabled pulsed and continuous wave operation [1, 2]. Although dyes have been demonstrated to lase in the solid, liquid or gas phases, liquid solutions of dyes in suitable organic solvents have been the most frequently used laser media. This is because the active medium can be obtained in high optical quality, the cooling is achieved by using a flow system and the medium is self repairable to a certain extent. Nevertheless, the use of liquid solutions in dye lasers entails a number of inconveniences, mainly related to the need of employing large volumes of organic solutions of dyes that are both toxic apart from being expensive. Furthermore, each dye has a limited range of tunability from 5 nm to 20 nm so that the dye has to be changed for different wavelength regions. This, together with the need of complex and bulky cell designs for the continuous circulation of the solution has restricted the use of these laser systems outside the laboratory.

From the early days of development of dye lasers, attempts were made to overcome the problems posed by dye solutions, by incorporating dye molecules into solid matrices. A solid state dye laser avoids the problems of toxicity and flammability and they are compact, versatile and easy to operate and maintain. The first observations of stimulated emission from solid matrices doped with organic dyes were reported as early as 1967 and 1968 by Soffer and Mcfarland [3] and Peterson and Snavely [4] respectively. Since laser dyes were in most cases merely dispersed, the results were not very encouraging due to the low lasing efficiencies and fast dye photodegradation. In recent years, the synthesis

of high performance dyes and the implementation of new ways of incorporating the organic molecules into the solid matrix have resulted in significant advances towards the development of practical tunable solid-state laser [5-36]. The use of a synthetic polymer host presents advantages as these materials show much better compatibility with organic laser dyes and are amenable to inexpensive fabrication techniques. Furthermore, new modified dye doped polymers have been developed with laser radiation threshold comparable to or higher than that of laser- damage resistant inorganic glasses and crystals. These polymers provide an opportunity for the production of polymer elements that can effectively control the characteristics of laser radiation. Hence, adequate knowledge of thermal and optical properties of dye doped polymers is important in identifying suitable laser media. Apart from its use as active laser media dye doped polymers find many applications in the modern photonic technology [37-44]. In the present investigation, the absolute value of fluorescence quantum yield, the effect of concentration of the dye on its fluorescence efficiency in the matrix and thermal diffusivity of the medium are evaluated. The mechanisms responsible for the photostability of the dye in the matrix are also studied. Details of these studies are presented in this chapter.

3. 2   Materials

3.2.1   Polymer (PMMA)

The basic requirements imposed in a polymeric host for laser dye molecules are its good optical transparency at pump and lasing wavelengths, good solubility of the dye in the material and resistance to pump laser radiation. The polymer (poly methly methacrylate) (Figure 3.1) has been most frequently used for laser dyes

due to its excellent optical transparency in the visible region and its relatively high laser damage resistance [7,10].

$$-\left[CH_2-\underset{\underset{\underset{OCH_3}{|}}{\overset{\overset{CH_3}{|}}{\underset{\|}{C}}}{\overset{|}{C}}=O}-CH_2-\underset{\underset{\underset{OCH_3}{|}}{\overset{\overset{CH_3}{|}}{\underset{\|}{C}}}{\overset{|}{C}}=O}\right]-$$
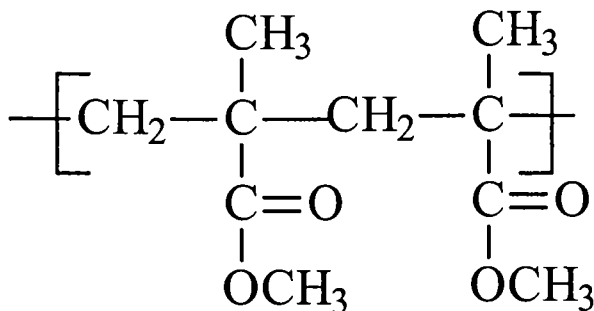
Figure 3.1 Structure of PMMA

3.2.2 Dyes (Rhodamine 6G)

Present work in dye doped polymer has been carried out with dyes of the Xanthene family. Rhodamine dyes, with emission in the yellow-red region of the spectrum, are known for their excellent lasing performance in liquid solution. Hence they are the obvious candidates for the development of dye lasers in solid state. For the present investigations, the well-known dye Rhodamine 6G chloride (Exciton) (structure is given in figure 3.2) [45] is used. Numerous studies on this dye in liquid medium as well as incorporated into different matrices have been reported in the literature [2, 46-59]. The rigid planar molecular structure of rhodamine 6G favours high fluorescence efficiency. It has monoethylamino groups, methyl substituents adjacent to the two amino substituents and the carboxyl group on the pendent 9-phenyl substituent is esterified [58, 59,60]. The methyl substituents have no influence on either absorption or emission spectrum of the dye.
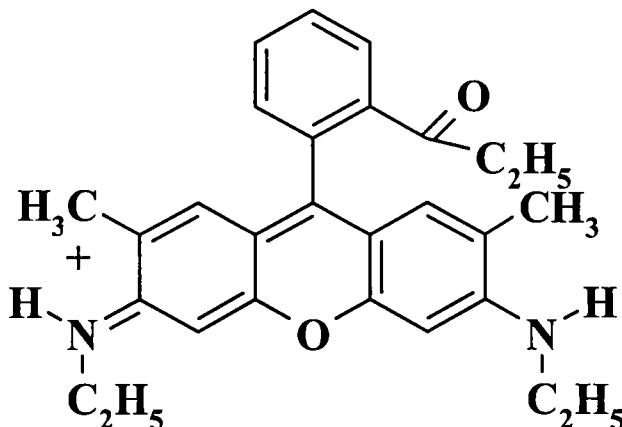
Figure 3.2 Structure of Rhodamine 6G

Since the amino groups are not fully alkylated the absorption maximum depends on the solvent and their fluorescence spectra resemble the mirror image of the long- wavelength absorption band [2].

3. 3   Method of preparation of dye doped polymer samples

Methyl methacrylate (MMA) (Merck) is washed three times with (2 vol %) aqueous sodium hydroxide to remove the inhibitor and then twice with distilled water. An accurately weighed amount of rhodamine 6G chloride is dissolved in a mixture of MMA and ethanol taken in the ratio 4:1 to give a concentration of 1.5×10^{-3} mol l^{-1}. Since rhodamine 6G has limited solubility in MMA ethyl alcohol is added, it being a good solvent for the dye and enhances the optical damage threshold. Apart from being a good solvent ethyl alcohol enhances the value of dielectric constant, which increases the conversion efficiency. From the stock

solution, sample solutions with different concentrations ranging from 1.5 x 10⁻³ mol l⁻¹ to1 x10⁻⁴ mol 1⁻¹ are prepared. Then 1.5 gm/l of benzoyl peroxide (CDH chemicals) (0.15% by weight), which is a free-radical initiator, is added to each sample solution. The mixture is then taken in glass bottles and is kept in a constant temperature bath maintained at 50° C for polymerisation. After about 48 hours completely polymerized samples are taken out and kept for one week for drying. Care is taken to see that dye is homogeneously distributed in the polymer matrix. The dried samples are then cut into pieces of 2 mm thickness. The disc shaped samples thus obtained are initially lapped using different grades of silicon carbide to obtain a smooth surface quality. This is followed by the polishing process employing fine grade Alumina ($Al_2 O_3$) powder. The various grades for polishing include 1,0.5, 0.3 microns on TEXMET polishing cloth. All these ensured minimum loss due to scattering as all the samples are made to good optical finish. Plain undoped PMMA samples are also prepared under the same experimental conditions and this is used as a reference sample to record the optical absorption spectrum.

3. 4   Measurement of fluorescence Quantum yield

3.4.1 Methods using a standard reference

Fluorescence quantum efficiency is one of the most important optical properties of fluorescent materials and it is the essential parameter in determining the lasing characteristics of the active laser medium. The fluorescence quantum yield ϕ is the ratio of the total energy emitted per quantum of energy absorbed.

Most methods presently followed using conventional technique for determining the absolute quantum yield of fluorescence by comparing emissions from fluorescent solutions with radiations scattered by a the standard scatterer

magnesium oxide plate [61], under conditions of identical geometry. But relative-scattering methods are tedious and suffer from poor reproducibility [62]. Another method for determining absolute fluorescence quantum yield given by Weber and Teale [63] was based on a comparison of the radiation emitted by fluorescent solutions with that scattered by a solution of macromolecules, attenuating the incident radiation to the same extent. The macromolecules behave as pure dipolar scatterers of the incident radiation, and after correction for the polarization of the scattered radiation, are equivalent to a material of unit quantum efficiency. By comparing fluorescent solutions with solution of the standard scatterer under identical conditions the quantum efficiency can be written as [62]

$$\phi = \frac{(dF/dE)\lambda_0}{(dS/dE)_{\lambda_0}} \frac{(3+P_t)}{(3+P_s)} \frac{f(\lambda_0)}{f(\Delta\lambda)} \tag{3.1}$$

where dF/dE is the slope of the plot of fluorescent intensity vs absorbance of the compound under investigation, dS/dE is the slope of the plot of intensity of scattered radiation against apparent absorbance for the standard scatterer, P_t and P_s are the polarization of fluorescence and scattered radiation respectively and $f(\lambda_0)/f(\Delta\lambda)$ is a correction factor for the difference in detector response to the wavelength of scattered radiation and fluorescence radiation. In these kinds of measurements it is necessary to introduce corrections for the spectral sensitivity of the detection system. Pure optical measurements also demand calibration of the detector. The use of fluorescence lifetime is also inadequate, especially for multilevel energy systems, as it depends both on the value of nonradiative lifetime and fluorescence decay time. Even after the various corrections for system geometry, re-absorption, polarization etc, the accuracy of

the quantum yield values obtained from photometric measurements is rather poor [64]. It is in this context that an alternate technique using photothermal effect is employed to evaluate absolute quantum efficiency of luminescent samples.

The introduction of photothermal techniques to measure the quantum efficiency has brought new perspectives to obtain more accurate values for this parameter. These methods are based on the principle that light absorbed and not lost by subsequent emission results in sample heating and are therefore complementary to the purely optical procedures [65- 74].

3.4.2 Quantum yield measurements using thermal lens technique

The application of photothermal lensing effect for the measurement of quantum yield was first introduced by Brannon and Madge [75]. Since then, the technique has been used to determine this parameter in fluorescent solutions [76] and fluorescent polymers [6]. In these experiments single beam configuration has been used to evaluate this parameter. In the present experimental setup dual beam thermal lens technique is used to find the fluorescence quantum efficiency of dye doped polymer since this method is more sensitive than single beam configuration [77].

3.4.3 Theory

The method to evaluate the fluorescence quantum yield of materials is based on the principle of conservation of energy. Let P_0 be the power of the incident pump beam and P_t the power of the transmitted beam. The absorbed power is the sum of the laser power degraded to heat, P_{th}, and luminescence emission P_l, provided there occurs no photochemical reaction. Hence,

$$P_0 = P_{th} + P_l + P_t \qquad (3.2)$$

so that the transmission ratio is given by

$$T = \frac{P_t}{P_o} \qquad (3.3)$$

Absorbance is given by

$$A = 1 - T \qquad (3.4)$$

Thus the absorbed power is given by

$$AP_o = P_{th} + P_l \qquad (3.5)$$

Then, $\qquad P_l = AP_o - P_{th} \qquad (3.6)$

The emission quantum yield by definition

$$Q_f = \frac{P_f / <V_f>}{(P_0 - P_t)/V_0} \qquad (3.7)$$

Here V_0 is the laser frequency and $<V_f>$ is the mean luminescence emission frequency, evaluated as [73]

$$<V_f> = \frac{\int V_f dn(V_f)}{\int dn(V_f)} \qquad (3.8)$$

The quantity *dn (V_f)* in photons/sec is the number of photons emitted in an incremental bandwidth centered at V_f. Rewriting the expression for emission quantum yield, eq. 3.7 becomes

$$Q_f = \frac{V_0}{<V_f>}(1 - \frac{P_{th}}{AP_0}) \qquad (3.9)$$

The ratio $\dfrac{V_0}{<V_f>}$ takes into account of the stokes shift, which entails some deposition of heat in the sample even for 100% fluorescence quantum yield. The absorption A may be measured with an ordinary spectrophotometer. Brannon and Madge [76] developed a comparison method in which thermal lensing measurements are made on both the fluorescent sample and nonluminescent reference absorber. The concentrations of sample 's' and reference 'r' are carefully adjusted to give identical photometric transmission. With identical incident light levels, the fluorescent sample, of course, produces solution heating. For the reference sample,

$$A^r P_0^r = P_{th}^r \tag{3.10}$$

Hence we can write

$$Q_f = \frac{V_0}{<V_f>}(1 - \frac{A^r P^r}{A^s P^s} \frac{P_{th}^s}{P_{th}^r}) \tag{3.11}$$

where A^s is the absorption coefficient of the luminescent sample, A^r is the absorption coefficient of the nonluminescent reference, P_{th}^s is the thermal power generated in the sample and P_{th}^r is the thermal power generated in the reference absorber. The absorption coefficient A may be measured with an ordinary spectrophotometer and P_{th} can be measured using thermal lens technique. Eqn. (3.11) assumes that the same solvent and the same excitation laser wavelength are used for the sample and the reference.

In using this method, care must be taken to maintain the ratio $\dfrac{A^r P^r}{A^s P^s}$ near unity and to work with reasonably dilute solutions. Otherwise a systematic error occurs when the sample and reference solutions are of considerably different optical densities [76]. Another problem encountered in measuring light absorption

coefficient A^s using spectrophotometer is high apparent transmittance, which results from the low fluorescence, received by the detector from measurements on a fluorescent sample. This causes uncertainty in the quantum yield values.

The problem can be solved if a quenched luminescent sample is used as the reference absorber because the quenched sample has the same light absorption coefficient as the luminescent sample. In the case of a totally fluorescent quenched sample we can consider that the entire excitation energy is converted into nonradiative relaxation process. Hence the fluorescence quantum yield is given by [75],

$$Q_f = \frac{P_f}{AP_0}\frac{\lambda_f}{\lambda} = (1 - \frac{P_{th}}{P_\alpha})\frac{\lambda_f}{\lambda} \qquad (3.12)$$

where $P_\alpha = AP_0$ and hence this can be rewritten as

$$Q_f = \left(1 - \frac{\eta}{\eta_\alpha}\right)\frac{\lambda_f}{\lambda} \qquad (3.13)$$

Here the ratio of the fluorescence peak wavelength λ_f to excitation wavelength λ takes into account of the stokes shift. P_{th} is directly proportional to TL signal η_α corresponding to the concentration at which the fluorescence intensity is quenched completely. The thermal lens signal η has been measured as the variation of light intensity at far field at the centre of the probe beam [78].

3.4.4 Experimental

The details of the experimental setup are given in chapter 2. Laser radiation at 532 nm wavelength from a Diode Pumped Nd: YVO$_4$ laser is used as the pump beam to generate the thermal lens in the medium. Radiation of wavelength 632.8 nm from a low power (1 mw) intensity stabilized He-Ne laser source is used as the probe beam. The pump beam is intensity modulated at 5 Hz using a

mechanical chopper. Sample in the form of disc having a thickness of 2 mm is kept in the pump beam path. The probe beam is made to pass collinearly through the sample using a dichroic mirror. An optical fibre mounted on XYZ translator serves as the finite aperture. The other end of the fibre is coupled to a monochromator- PMT assembly that is set at 632.8 nm. The signal output from PMT is processed using a dual phase lock-in amplifier.

The absorption spectra of the sample having different concentrations are recorded using a UV-VIS-IR spectrophotometer. For the fluorescence study, the front surface emission is collected and focused by a lens to the entrance slit of a McPherson monochromator, which is coupled to a PMT. The PMT output is fed to a lock-in amplifier. The emission wavelength is scanned in the specified region (500-640 nm).

3.4.5 Results and discussion

The absorption spectra of the solid sample at different concentrations are given in figure 3.3. At low concentration dye-dye interaction is negligible because of the large average distance between them. As we increase the concentration, absorption spectra contain contributions from monomers and aggregates which make the spectrum broader at higher concentrations. Fluorescence of a molecule depends on the structure and environment of the molecule. Figure 3.4 shows the fluorescence spectrum of the polymer sample for different dye concentrations. At low concentrations, dyes dissolve completely into monomers and obviously the dye-dye interaction and the intermolecular interactions between dye molecules and macromolecules are negligible. Hence, at very low concentration, fluorescence intensity increases linearly with increasing concentration.
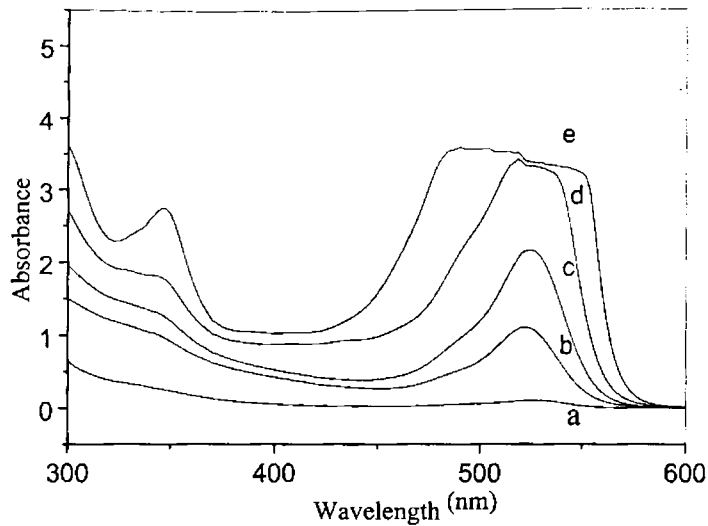
Figure 3.3   Absorption spectrum of rhodamine 6G doped PMMA for various concentrations in m mol l^{-1} (a) 0.4 (b) 0.54 (c) 0.7 (d) 0.8 (e) 0.9
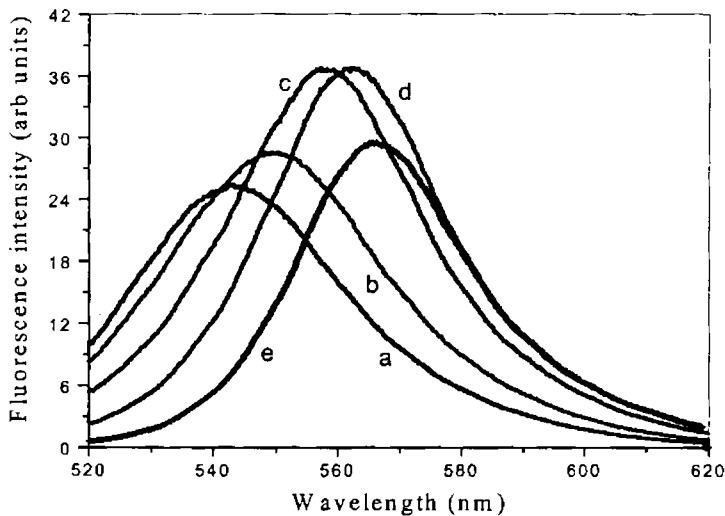

Figure 3.4   Fluorescence spectra of rhodamine 6G doped PMMA for various concentrations in m mol l^{-1} (a) 0.4 (b) 0.54 (c) 0.7 (d) 0.8 (e) 0.9

At higher concentrations fluorescence intensity reaches a limiting value and then decreases with further increase in concentration. Several factors are responsible for this behaviour.

This can be related to the phenomenon of re-absorption and re-emission, which ultimately reduces fluorescence emission. With increasing dye concentration the formation of dimers and higher aggregates decreases the fluorescence emission by a combination of monomer-dimer / higher aggregates energy transfer and absorption of radiation by non-fluorescent dimers / higher aggregates [60]. This transfer of energy between molecules by collisional mechanism makes the nonradiative part prominent and hence fluorescence decreases.
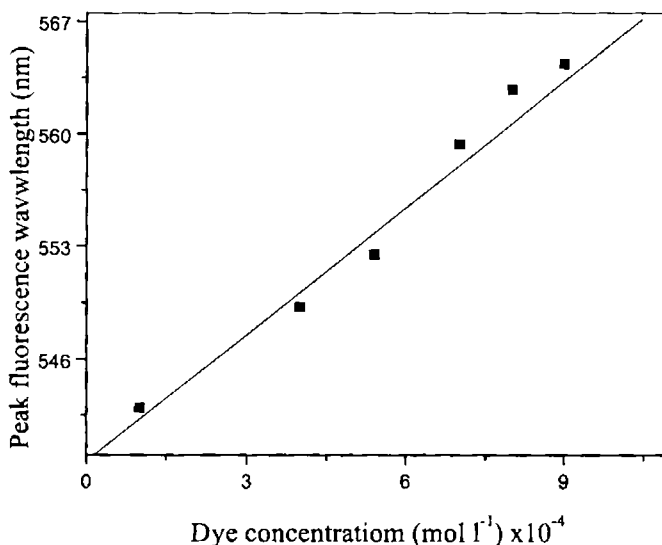

Figure 3.5   The concentration dependence of peak fluorescence wavelength of rhodamine 6G doped PMMA.

However, in the present case, re-absorption and emission are the probable causes for the reduction in fluorescence intensity at higher concentrations. The observed shift in the fluorescence emission peak (figure 3.5) follows the same profile. Figure 3.5 gives the variation of peak fluorescence wavelength as a function of concentration. It can be seen that peak fluorescence wavelength increases with concentration. The low frequency tail of the absorption spectrum of the dye molecule overlaps with the high frequency end of its fluorescence spectrum. The fluorescence from the excited state dye molecule is reabsorbed by the ground state molecule. This process increases with increase in concentration, which results in decrease in fluorescence and shifts the fluorescence peak to smaller energies [2,60,75-78].
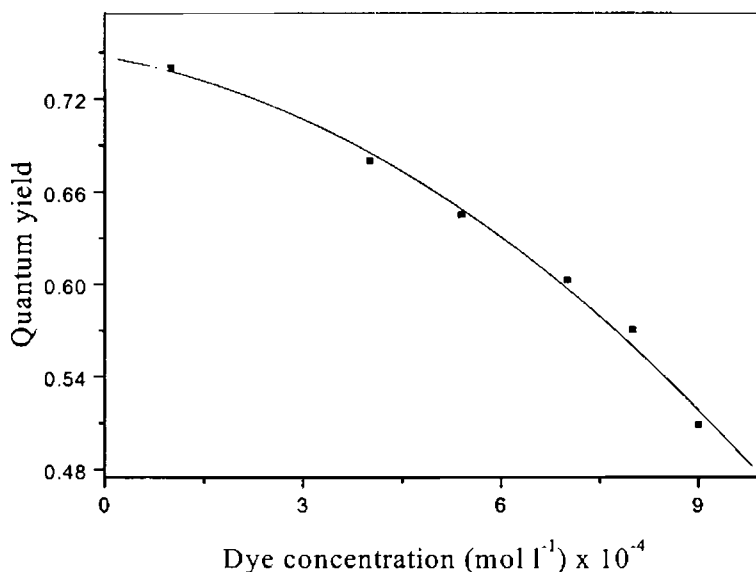

Figure 3.6 Variation of quantum yield of dye doped PMMA with concentration for a power of 5 mW.

The variation of quantum yield with concentration obtained using equation (3.13) is shown in figure 3.6. The laser power is kept constant at 5 mW in this experiment.

The quantum yield closely depends on the environment of the fluorescing molecule and on processes like internal conversion, intersystem crossing, solute-solute interaction [71,78 79-94] these parameters strongly depend on the excitation source, solvent characteristics and concentration of the dye.

The plot clearly reveals a decrease in fluorescence quantum yield at higher concentrations. This is a direct indication of the fact that nonradiative processes become significant at higher concentrations, which contribute to enhanced thermal lensing. One of the factors, which reduces fluorescence quantum yield is the re-absorption of emitted radiation by ground state molecules. This also enhances nonradiative relaxation processes between various vibronic levels of the dye molecules. Generation of dimers, excimers and other aggregates will also contribute to the decrease in fluorescence quantum yield. Dimers and higher aggregates can quench monomer emission by collisional or long-range nonradiative energy transfer [59,78, 79-94].

3.4.6 Conclusion

Since dye doped polymers are interesting for many optical applications including active medium for solid-state lasers, it is desirable to have a quantitative and accurate method to determine the absolute fluorescence quantum yield. Conventional fluorescence quantum yield measurements require the use of accurate luminescent standard samples and its comparison with a standard sample. In the present investigation quenched luminescent sample is used as the reference absorber since it has the same light absorption coefficient as the luminescent sample. In solid media, the rhodamine chromophore shows a

photophysical behavior similar to that in a liquid solution. Further more, this method is very sensitive and simple to perform. Where as recording fluorescence emission from samples of large dye concentrations is difficult. The TL technique is suitable for measurements even in the vicinity of complete fluorescence quenching.

3.5 Thermal diffusivity of rhodamine 6G doped polymer Matrix

3.5.1 Introduction

Thermophysical parameters such as thermal diffusivity, is a very important characteristic property of any material. Accurate values of thermal diffusivity of materials are crucial for practical engineering design as well as theoretical studies and analysis, especially in the fields of heat transfer and thermal processing. Since both thermal diffusivity and thermal conductivity are properties that characterize the heat transfer behavior of materials, applications including conduction and convection heat transfer, heat exchanger design, insulation problems, etc. rely heavily on these two parameters. Meanwhile, with the rapid development of numerical simulation techniques, thermal diffusivity and conductivity also play an important role in computational fluid dynamics as they appear in the governing equations that describe the flow and temperature distributions. Accurate measurement of these parameters is thus of primary importance to the heat transfer community.

The measurement of thermal diffusivity (D) was vigorously pursued in the 1950's and 1960's by various researchers. All these techniques, however, usually made direct use of the transport equations by measuring physical quantities such as heat flux and temperature gradients. These measurements are rendered difficult due to heat losses at boundaries and convective or

radiative effects in the test liquid, which are the main sources of error. A technique related to the present work was reported by Kim and Irvine [95] (1991), in which the thermophysical properties of liquids were determined using a thermal pulse technique. The time for thermal energy from a multilayer-heating element to traverse a known distance between two points in the liquid was measured by monitoring temperature peaks at the two points using thermocouples. However, this technique is limited by the finite size of the thermocouple, which causes uncertainties in the temperature measured at the two points.

The transient hot-wire technique [96,97] which is a typical method, has been widely used to measure liquid thermal conductivity and thermal diffusivity. A thin wire, usually platinum, is immersed in the test liquid. The wire is electrically heated and the heat is then radially conducted into the liquid. The time variation of temperature of the wire depends on the properties of the surrounding liquid. Thermal conductivity and thermal diffusivity of the liquid are then determined by measuring the temperature change history of the wire. Although hot-wire method has been widely used in practice, it has some shortcomings that are very difficult to overcome. One major difficulty is the effect of natural convection which occurs due to buoyancy effects as the wire is continuously heated. In addition, temperature variation of the wire is measured using a bridge circuit in which the wire acts as one bridge. Accuracy in temperature measurement is decreased by electrical noise and drift problems within the bridge circuit. The lack of precision in the determination of heating time also contributes to measurement errors.With the invention of laser in 1960, further research on liquid thermophysical properties has been accomplished with the development of many new techniques by taking advantages of the unique characteristics of laser light.

Compared with conventional experimental methods, laser-based techniques are fast, easy to operate, and have high sensitivity [98-100].

A laser flash method introduced first by Parker *et al.* (1961)[101] has been widely applied for the measurement of thermal diffusivity of solids. A high-energy pulsed laser beam strikes the front surface of a specimen and energy is absorbed. Thermal diffusivity of the specimen is determined by measuring the time-dependent temperature variations at the back surface [102]. But heat loss in the test liquid container, which could not be completely avoided, makes this assumption invalid and appears to be a major disadvantage of this method.

Opto-thermal methods are devoid of these difficulties. Calmettes and Laj [103] measured thermal diffusivity of certain liquids and solids using single beam TL technique. Gupta et al [104] developed double beam TL technique for measuring D of transparent solids and liquids. Bailey [105] successfully introduced TL technique for the determination of D of liquids. Bindhu et al [106, 107] using pulsed TL technique calculated D values of certain organic solvents and carried out the thermal diffusivity measurements in sea water.

The details of the experimental setup are same as that used for the measurement of quantum yield. Instead of the chopper a high-speed shutter is used in the measurement of thermal diffusivity. The signal output from PMT is processed using a digital storage oscilloscope. The concentration of dye in the matrix is $4 * 10^{-4}$ mol l^{-1} and this trace amount of dye enhances absorption.

3.5.2 Theory

The magnitude of the effective thermal lens produced by propagation of a cw Gaussian laser beam of spot size ω is governed by the steady state balance between laser heating and solvent or matrix heat dissipation. If the beam is suddenly turned on at time *t=0,* the lens approach to steady state governed by

$$f(t) = f_\infty(1 + t_c / 2t),$$ (3.14)

and the steady state focal length f_∞ of such a lens is derived as [108]

$$f_\infty = \frac{\pi k \omega^2}{PA(dn/dt)}$$ (3.15)

where k is the thermal conductivity (W cm^{-1} K^{-1}), P is the laser power (W), A is the sample absorbance, dn/dt is the refractive index change with temperature and t_c is the time response to attain the steady state focal length given by

$$t_c = \frac{\omega^2}{4D}.$$ (3.16)

from which D can be calculated. The thermal diffusivity in the sample is detected by its effect on the propagation of the probe laser beam aligned with the centre of the lens. If, after passage through the sample, the laser beam intensity is sampled in a small spot at the centre, the intensity observed is inversely proportional to the beam area. The expression relating the intensity as a function of time is given as [75,108, 109]

$$I_{(t)} = I_{(0)}\left[1 - \frac{\theta}{1 + t_c/2(t)} + \frac{\theta^2}{2(1 + t_c/2(t))^2}\right]$$ (3.17)

We have modified this equation for cw laser source as

$$I_{(t)} = I_{(0)}\left[1 - \frac{\theta}{1 + t_c/2(t - t_0)} + \frac{\theta^2}{2(1 + t_c/2(t - t_0))^2}\right]^{-1}$$ (3.18)

where t_0 is the time at $t=0$, θ is directly proportional to P_{th} by the relation

$$\theta = \frac{P_{th}(dn/dT)}{\lambda k}$$ (3.19)

where P_{th} is the laser power degraded to heat and λ is the laser wavelength. For a given solvent or matrix the experimental parameter of interest is θ, which may be obtained from the initial intensity I_0 and the intensity after the steady state has been established, I_∞, so that [75]

$$\theta = 1 - (1 + 2I)^{1/2}, \tag{3.20}$$

$$I = \frac{I_0 - I_\infty}{I_\infty} \tag{3.21}$$

The initial slope m of the decay curve $m = \dfrac{2\theta}{I_0 t_c}$ (3.22)

from which the value of t_c and hence D is calculated.

3.5.3 Results and Discussion

The dye doped polymer in the form of disc is placed at one confocal distance past the beam focus in order to get maximum signal. When the shutter is open

the pump beam generates thermal lens in the medium and as a consequence the probe beam through it expands. The probe beam centre at far field is coupled to the digital oscilloscope through monochromator-PMT assembly. The TL signal is recorded from which the relative change in intensity and initial slope is measured. The value of θ and t_c are determined and hence D is calculated. We have verified the measured t_c with theoretical fit obtained from Eqn. 3.18 and figure 3.7 shows TL decay curve of the sample. The solid curve represents the theoretical fit and points represent the experimental data. As can be seen from the figure, the agreement between the theoretical and experimental data is good (Table 3.1) [110,111].
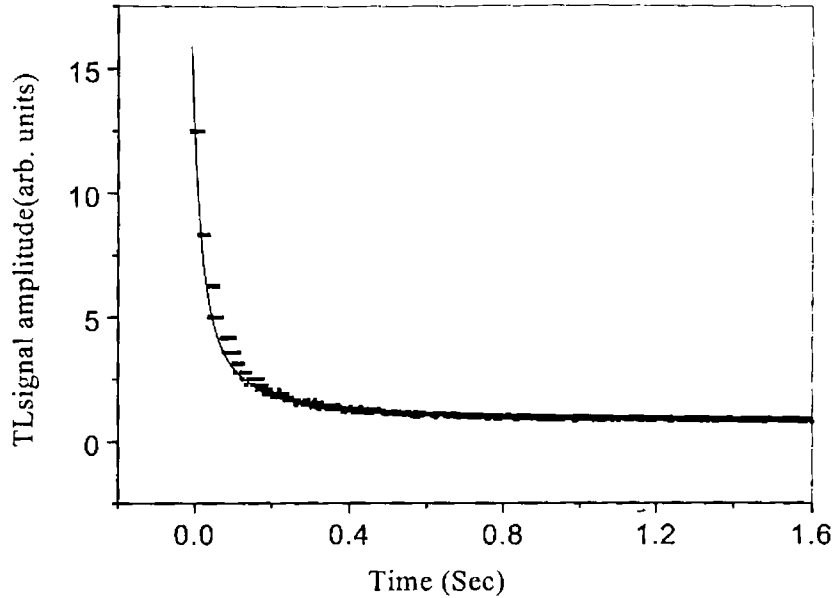
Figure 3.7 Decay curve for solid sample for a power of 30 mW. The solid curve represents the theoretical fit obtained using the eqn. (3.19) and the points represent the experimental data.

To eliminate the uncertainty in the determination of beam radius, a reference sample with known D is used to determine the diffusivity of the sample. In the present experiment, water is used as the reference sample. Therefore,

$$D = D_{water} \frac{t_c^{water}}{t_c} \qquad (3.23)$$
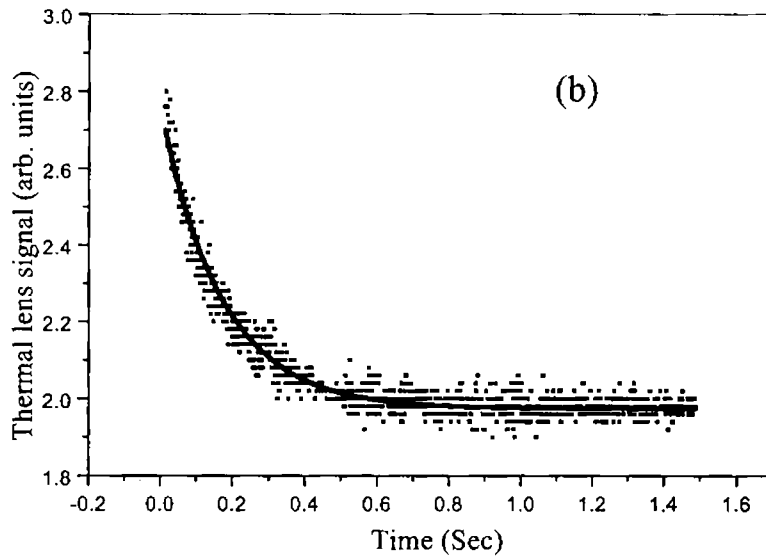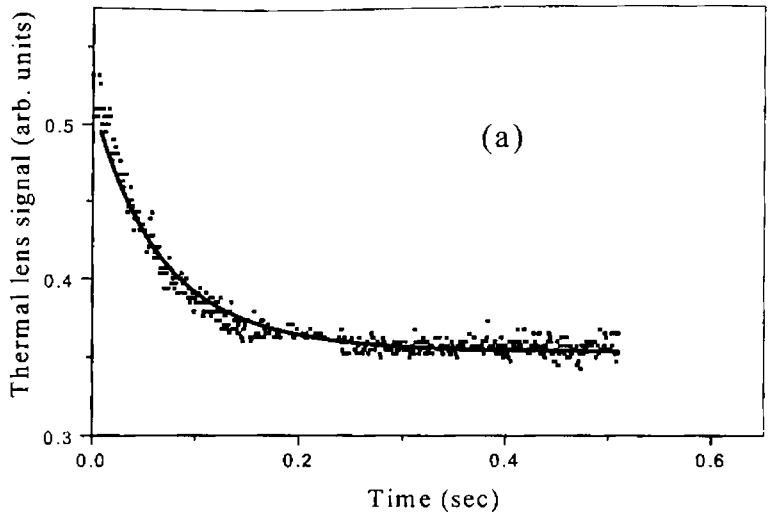
Figure 3.8 Decay curve for (a) MMA and (b) Water

In order to verify this method of calculation of D, we have conducted the experiment in MMA and water. Trace amount of rhodamine 6G is added (4 x 10^{-4} mol l^{-1}) to increase the absorption. Figure 3.8 (a)and (b) shows the decay curve for MMA and water respectively. The D value obtained for PMMA using the present setup is 15-20% less than the literature value where single beam TL technique was used.However, Nonell et al [70] reported results that substantiate our observed values. These observations help us to conclude that thermal diffusivity has only weak dependence on matrix in polymer state. Table 3.2 shows the variation of TL time constant as a function of pump power. Results show that time constant is independent of pump power.

Table 3.1 Thermal diffusivity values for different organic liquids studied using dual beam cw thermal lens technique. Reported values are also given.

Sample	t_c (s)	Value of D (cm/sec^2) Calculated using TL technique	Literature value [110,111]
Water	0.16±0.01		1.43*10^{-3}
Acetone	0.22±0.01	1.07±0.01*10^{-3}	1.07*10^{-3}
MMA	0.20±0.01	1.18±0.01*10^{-3}	
PMMA	0.26±0.04	0.90±0.04*10^{-3}	1.08*10^{-3} (34)

Table 3.2 Thermal lens time constant (t_c) values for different pump powers.

Power (mW)	t_c (s)
8	0.25±0.02
10	0.30±0.01
14	0.25 ± 0.02
20	0.29±0.01
25	0.30±0.01

3.5.4 Conclusion

Analyses of the results lead to the conclusion that the thermal diffusion coefficient of the sample calculated using TL technique is comparable with the reported literature value. The D value is essentially independent of the polymer matrix as well as the power of the pump laser source.

3.6 Photochemical stability of rhodamine 6G molecules in polymer matrix.

3.6.1 Introduction

Apart from using as active laser media dye doped polymer composites have been considered as candidates for new electro-optic materials, logic gates, photo-detectors, holographic recording and solar concentrators [37-44]. In this regard it is highly desirable to study the photostability of doped sample. The study of photochemical stability of rhodamine 6G doped polymer using TL technique is discussed in this section. Investigations are carried out using both

cw and pulsed laser sources at different pump intensities. The effect of concentration of the dye on photostability is also studied using this technique.

During the last two decades several studies on photo-induced bleaching of organic dyes embedded in solid matrices have been reported [24, 25, and 27,112-114]. Several theoretical models have been developed to explain photo-bleaching of the dye under pulsed and continuous-wave irradiation. Dyumaev et al [14] have developed a theoretical model for the photo-destruction of lasing dyes by correlating the dye concentration and photostability. Newell et al [115] have developed a model to explain their observation on dye photo-bleaching using transmission studies under cw irradiation.

The experimental setup is similar to that used for quantum yield measurements. In order to record the photostability of the sample, radiation at 532 nm wavelength from a Diode Pumped Nd: YVO_4 laser is used as the pump beam. The pump beam is intensity modulated using a chopper. For pulsed experimental studies, the laser source used is the 530 nm radiation from Optical Parametric Oscillator (OPO). The probe used in both cases is the 632.8 nm wavelength from an intensity stabilized He- Ne laser. For cw experimental setup, lock-in amplifier is used for recording the spectrum. But in pulsed setup, digital oscilloscope is used.

3.6.2 Results and discussion

Figures 3.9 and 3.10 describes the time evolution of TL signal for cw and pulsed excitation sources respectively. The variation of thermal lens signal with time for excitation laser powers ranging from 3mW to 42 mW is shown in figure 3.9. Increase in TL signal at low powers (3 and 6 mW) is due to residual thermal lens signal of the previous cycles of intensity modulation.The lens decay during previous cycle is not completed due to characteristic signal response time t_c. The

characteristic time constant for the sample is ≈260 ms.The time dependent decrease in the TL signal (figure 3.9 and 3.10) is obviously due to the photo-induced chemical changes in the present sample. It can be seen that the dye molecules embedded in the PMMA matrix does not undergo any change in its chemical properties at very low laser powers such as 3 mW and 6 mW (figure 3.9). But the gradual decrease in the TL signal for laser powers of 15 mW and above reflects the photodegradation of rhodamine 6G molecules. From the figures (3.9 and 3.10) it is very clear that the rate of this reaction increases with increase in pump power.
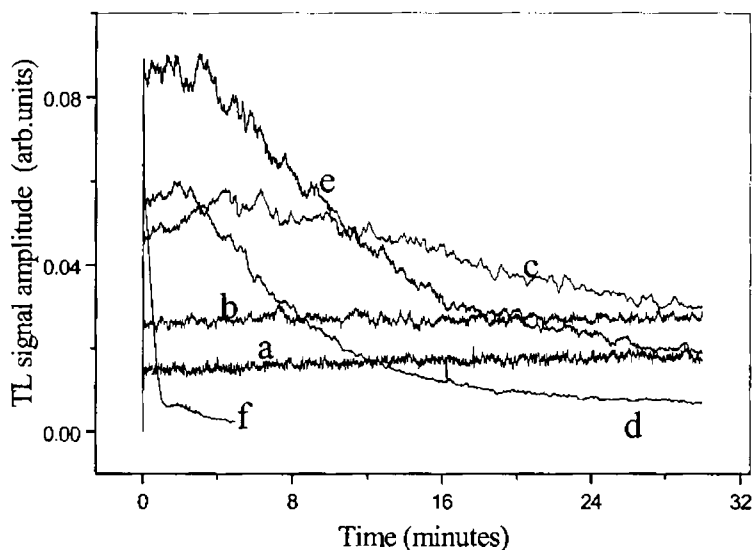

Figure 3.9 The variation of thermal signal strength with time for cw) laser powers in mW (a) 3 (b) 6 (c) 15 (d) 20 (e) 28 (f) 42. The concentration of the sample is 1.5×10^{-3} mol l^{-1}

This is in accordance with the earlier reported photoacoustic measurements on dye doped PMMA [118]. The saturation in the TL signal is an indication of complete destruction of the dye molecules in the pump beam path. Absorption spectrum also confirms this result (fig. 3.11). The photobleaching of the dye results in a permanent colour change, which indicates that the reaction is an irreversible one. The completely bleached portion of the sample is almost transparent as an undoped PMMA sample (figure 3.11).

This implies that the photochemical reaction product of rhodamine 6G does not absorb in the visible region. The photochemical degradation of rhodamine 6G occurs only in the presence of a suitable optical radiation, which produces large local increase in temperature and thermal destruction of the dye molecules. Again, laser power, used for the present study, will excite the molecules only to their first excited singlet or triplet states.
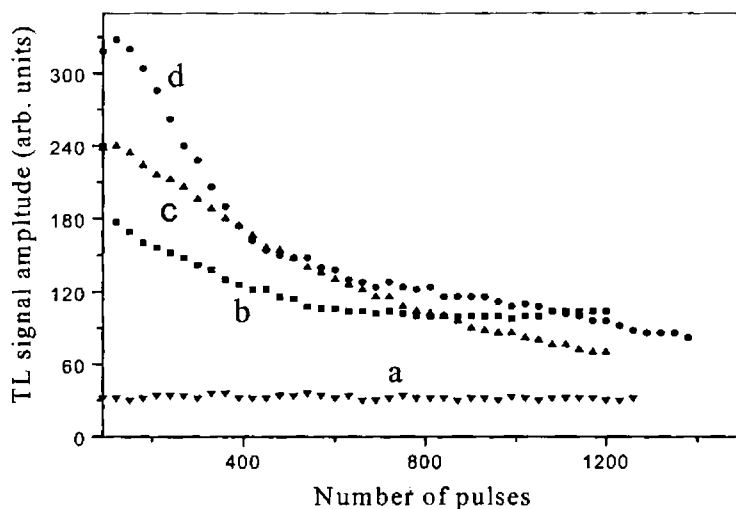

Figure 3.10 Normalized TL output as a function of the number of pump pulses for a power in mW (a) 1 (b) 7 (c) 13.5 (d) 21.5

Although there is no general consensus concerning the mechanism responsible for laser damage of polymeric materials, there is already enough evidence to establish that the laser damage of polymers is energy dependent and that the viscoelastic properties of the matrix determine damage resistance [31]. The variation of photobleaching with concentration of the dye molecules is studied at four different concentrations and is shown in figure 3.12. In all these measurements the laser power is kept constant at 10 mW and from the observation it is clear that no photobleaching has occurred at this laser power.

Pure polymers with saturated chains do not absorb in ultraviolet-visible region of the spectrum (300-700nm) (figure 3.11).
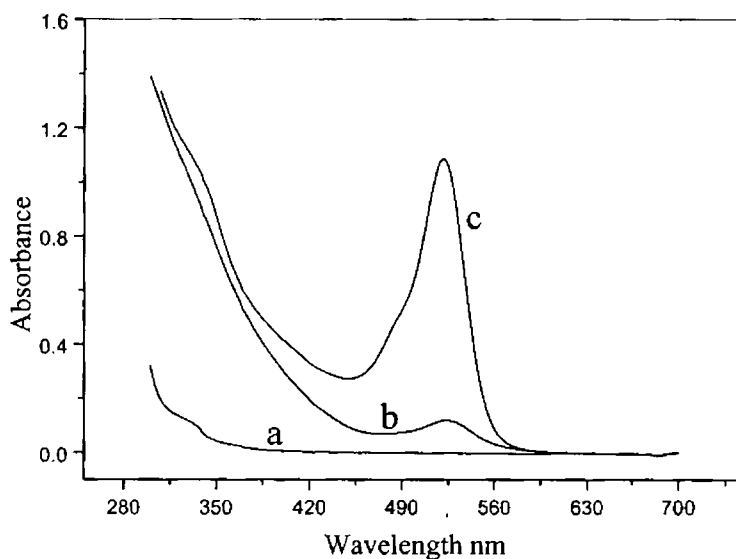
Figure 3. 11 Absorption spectra of rhodamine 6G doped PMMA sample
(a) plain PMMA (b) after bleaching (c)before bleaching

Hence it is evident that the impurities act as photo sensitizers. It is believed that the dye molecules in any of these excited states react with the polymer molecules, or with the free radicals or with any other impurities in the sample (traces of transition metals, hydroperoxides, etc.), which are introduced during the synthesis or processing to give a colourless product. Dissolved oxygen and concentration of dye in the sample may also contribute to the reaction [21].
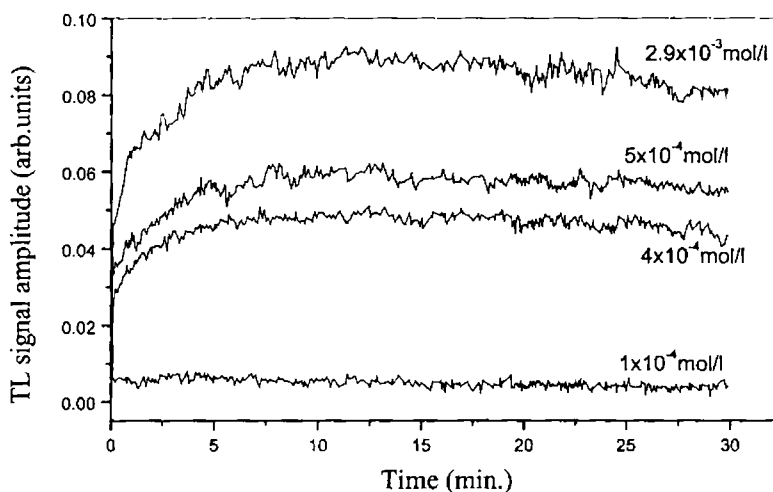
Figure 3.12 Plot of TL signal versus time for different dye concentrations

3.6.3 Conclusion

From our experimental results we can conclude that the rate of photo-bleaching is directly proportional to the incident power and it decreases with increase in the concentration of the dye molecules. The intermolecular interaction of the dye with polymer plays a significant role in the process responsible for photostability.

A solid host for lasing dyes is an attractive alternative to their liquid solutions, with obvious technical advantages such as compactness,

manageability, lack of toxicity and flammability, suppression of flow fluctuations, solvent evaporation etc. The two main problems found in polymeric solid-state dye lasers are usually the low laser damage threshold of the material compared to other solid state laser media and photodegradation of the dye. If these problems are properly addressed, the above mentioned advantages would make polymers very attractive as host materials in solid state dye lasers.

References

1. F. J. Duarte, and L. W. Hillman, (Eds), *Dye laser principles,* Academic Press, New York, (1990).
2. F. P. Schafer, Principles of *Dye Laser Operation in: Topics in applied physics, Dye Lasers,* Vol. 1 (Springer-Verlag, 1989).
3. B. H. Soffer and B. B. McFarland, *Appl. Phys. Lett.* 10, 266 (1967).
4. O. G. Peterson and B. B. Snavely, *APPL. Phys. Lett.* 12, 238 (1968).
5. H. Wang and L. Gampel, *Opt. Commun.* 18, 444 (1976).
6. M. L. Lesiecki and J. M.Drake, *Appl.. Opt.* 21, 557 (1982).
7. K. M. Dyumaev, A. A. Manenkov, A. P. Maslyukov, G. A. Matyushin, V. S. Nechitailo and A. M. Prokhorov, *Sov. J. Quantum Electron,* 13, 503 (1983).
8. D. Anvir, D. Levy and R. Reisfeild, *J. Phys. Chem.* 88, 5956 (1984)
9. D. Anvir, D. Levy and R. Reisfeild, *J. Non –Cryst. Solids.* 74, 395 (1985).
10. D. A. Gromov, K. M. Dyumaev, A. A. Manenkov, A. P. Maslyukov, V. S. Nechitailo and A. M. Prokhorov, *J. Opt. Soc. Am. B* 2, 1028 (1985).
11. V. V. Rodchenkova, S. A. Tsogoeva, T. M. Muraveva, L. K. Denisov and B. M. Uzhinov, *Opt. Spectrosc* (USSR), 60, 35 (1986).
12. R. Reisfeld, R. Zusman, Y. Cohen and M. Eyal, *Chem. Phys. Lett.* 147, 142 (1988).
13. G. R. kumar, B. P. Singh and K. K. sharma, *Opt. Soc. Am. B* 8, 2119 (1991).
14. K. M. Dyumaev, A. A. Manenkov, A. P. Maslyukov, G. A. Matyushin, V. S. Nechitailo and A. M. Prokhorov, *J Opt. Soc. Am. B* 9, 143 (1992).
15. R. E. Hermes, T. H. Allik., S. Chandra, and J. A. Hutchiston, *Appl. Phys. Lett.* 63, 877 (1993).
16. F. J. Duarte, *Appl. Opt.,* 33, 3857 (1994).
17. F. Tang, C. Zhu and F. Gan, *J. Appl. Phys.* 78, 5884 (1995).
18. A. Costela, F. Florido, I. Garcia-Moreno, R. Duchowiz, F. Amat-Guerri, J. M. Figuera and R. Sastre, *Appl. Phys. B* 60, 383 (1995).
19. M. Rodriguez, A. Costela, F. Florido, I. Garcia-Moreno, J. M. Figuera and R. Sastre, *Meas. Sci. Technol.,* 6, 971 (1995).

20. M. D. Rahn and T. A. king, *Appl. Opt.* 34, 8260 (1995).
21. A. Maslyulov, S. Sokolov, M. Kaivola, K. Nyholm and S. Popov, *Appl. Opt.* 34, 1516 (1995).
22. R. Sastre and A. Costela, *Adv. Mater.* 7, 198 (1995).
23. R. M. Balachandran, D. P. Pacheco and N. M. Lawandy, *Appl. Opt.* 35, 640 (1996).
24. A. Costela, I. Garcia-Moreno, J. M. Figuera, F. Amat-Guerri, R. Mallavia, M. D. Santamaria and R. Sastre, *J. Appl. Phys.* 80, 3167 (1996).
25. A. Costela, I. Garcia-Moreno, J. M. Figuera, F. Amat-Guerri, J. Barroso and R. Sastre, *Opt. Commun.* 130, 44 (1996).
26. W.H holzer, A. Penzkofer, S. Gong, A. Blever and D. C. Bradlev, *Adv. Mater.* 8, 974 (1996).
27. A. Costela, I. Garcia-Moreno, H. Tian, J. Su, K. Chen, F. Amat-Guerri, M. Carrascoso, J. Barroso and R. Sastre, *Chem. Phys. Lett.* 277, 392 (1997).
28. N. D. Kumar, J. D. Bhawalkar and P. N. Prasad, *Appl. Phys. Lett.* 71, 999 (1997).
29. W. J. Wadsworth, S. M. Giffin. I. T. Mckinnie, J. C. Sharpe, A. D. Woolhouse, T. G. Haskell and G. J. Smith, *Appl. Opt.* 38, 2504 (1999).
30. A. Costela, I. Garcia-Moreno, J. Barroso and R. Sastre, *Appl. Phys. B* 67, 167 (1998).
31. A. Costela, I. Garcia-Moreno, J. M. Figuera, F. Amat-Guerri and R. Sastre, *Laser Chem.* 18, 63 (1998).
32. J. Huang. V. Bekiari, P. Lianos and S. Couris, *J. Lumin.* 81, 285 (1999).
33. G. Somasundaram and A. Ramalingam, *J. Photochem. Photobio.* 125, 93 (1999).
34. A. V. Deshpande and E. B. Namdas, *J. Lumin.* 91, 25 (2000).
35. W. Holzer, H. Gratz, T. Schmitt, A. Penzkofer, A. Costela, I. Garcia-Moreno, R. Sastre and F. J. Duarte, *Chem. Phys.* 256, 125 (2000).
36. E. Yariv, S. Schultheiss, T. Saraidarov and R. Reisfeld, *Opt. Mater.* 16, 29 (2000).
37. H. Franke, *Appl. Opt.* 23, 2729 (1984).
38. D. J. Welker and M. G. Kuzyk *Appl. Phys. Lett.* 69, 1835-1836 (1996).
39. A. Suzuki, T. Ishii and Y. Maruyama, *J. Appl. Phys.* 80, 131 (1996).
40. M. A. Diaz-Garcia, F. Hide and B. J. Schwartz, *Appy. Phy. Lett.* 70, 3191 (1997).
41. I. Riess and D. Cahen, *J. Appl. Phys.* 82, 3147 (1997).
42. S. Berleb, W. Brutting, M. Schwoerer, R. Wehrmann and A. Elschner, *J. Appl. Phys.* 83, 4403 (1998).
43. Magda A.El-Shahawy, *Polymer Testing* 19, 821-829 (2000).
44. Yono Hadi Pramono, Masahiro Geshiro, Toshiaki Kitamura and Shinnosuke Sawa, *IEICE TRANS. ELECTRON* Vol. E83-C, 1755 – 1762 (2000).
45. J. M. Kauffman, Appl. Opt. 19, 3431 (1980).
46. H. Kuhn, *Chimica*, 9,237 (1955).
47. P.P. Sorokin, J. R. Lankard, V. L. Morczzi and E. C. Hammond, *J. Chem. Phys.* 48, 4726 (1968).
48. J. E. Selwyn and J. I. Steinfeld, *J. Phys. Chem.* 76, 762 (1978).
49. C. V. Shank, *Reviews Mod. Phys.* 47,649 (1975).
50. A. D. Britt and W.B. Moniz, IEEE. *J. Quantum Electron,* 913 (1972).
51. K. A. Selanger, J. Faines and T. Sikkeland, *J. Phys. Chem.* 81, 1960 (1977).
52. V. E. Korobov, V. V. Shubin and A.K. Chibisov, *Chem. Phys. Lett.* 45, 498 (1977).
53. V. E. Korobov and A.K. Chibisov, *J. Photochem.* 9, 411 (1978).

54. F. L. Arbeloa, I. L. Gonzalez, P. R. Ojeda and I. L. Arbeloa, *J. Chem. Soc. Faraday Tran. 2*, 78, 989 (1982).

55. A. V. Aristov and V. S. Shevandin, *Opt. Spectrosc (USSR)* 58,337 (1985).

56. F. L. Arbeloa, T. L. Arbeloa, E. G. Lage and I. L. Arbeloa, *J. photochem. Photobiol. A: Chem.* 56, 313 (1991).

57. J. C. Mialocq. P. Hebert, X. Armand, R. Bonneau and J. P. Morand, *J. photochem. Photobiol. A: Chem.* 56, 323 (1991).

58. D. Magde, G. E. Rojas and P. G. Seybold, *Photochem. Photobiol.* 70, 737 (1999).

59. D. Magde, R. Wong and P. G. Seybold, *Photochem. Photobiol.* 75, 327 (2002).

60. G. G. Guilbault, *Practical fluorescence* (Marcel Dekker, INC, New York, 1973.

61. S. I. Vavilov, *Z. Phys.* 22,226 (1924).

62. D. M. Hercules and H. Frankel, *Science*, 131, 1611 (1960).

63. G. Weber and F. W. J. Teale, *Trans. Faraday Soc.* 54,649 (1958).

64. J. N. Demas and J. A. Crosby, J *Phys. Chem.* 75, 991 (1971).

65. I. O. Starobogatov, *Opt. Spectrosc.* 42, 172 (1977).

66. W. Lahmann and H. J. Ludewig, *Chem. Phys. Lett.* 45, 177 (1977).

67. R. S. Quimby and Yen, *Opt. Lett.* 3, 181 (1978).

68. P. Sathy, R. Philip, V. P. N. Nampoori and C. P. G. Vallabhan, *Pramana-J. Phys.* 34, 585 (1990).

69. C. V. Bindhu, S. S. Harilal, R. C. Issac, V. P. N. Nampoori and C. P. G. Vallabhan, Modern *Phys. Lett.* B 10, 1103 (1996).

70. S. Nonell, C. Marti, A. Costela, I. Garcia-Moreno and R. Sastre, *Appl. Phys. B* (DOI) 10.1007/s003400100481 (2001).

71. A. Chartier, J. Georges and J. M. Mermet, *Chem. Phys. Lett. 171*, 347 (1990).

72. R. D. Snook and R. D. Lowe, *Analyst*, 120, 2051 (1995).

73. J. Georges, N. Arnaud and L. Parise, *Appl. Spectrosc.* 50, 1505 (1996).

74. C. V. Bindhu, S. S. Harilal, *Analytical Science*, 17, 1, 2001.

75. J. H. Brannon and D. Magde, *J. Phys. Chem.* 82,705,1978.

76. J. Shen and R. D. Snook, *Chem. Phys, Let.*155, 583 (1989).

77. F. R. Grabiner, D. R. Siebert and G. W. Flynn, *Chem. Phys. Lett.* 17,189 (1972).

78. Achamma Kurian, K. P. Unnikrishnan, Pramod Gopinath, V. P. N. Nampoori and C. P. G. Vallabhan, *J. Nonlinear Opt. Phys. & Mats.* 10, 415 (2001).

79. R. E. Sah, *J. Lumin.* 24/25, 861 (1989).

80. F. L. Aarbeola, T. L. Arbeola I. L. Arbeola A. Costela I. G. Moreno, J. M. Figuera, F. A. Guerri and R. Sastre, *Appl. Phy. B*, 63, 651, 1997.

81. C. V. Bindhu, S. S. Harilal, G. K. Varier, R. C. Issac, V. P. N. Nampoori and C. P. G. Vallabhan, *J. Phys. D: Appl. Phys.* 29, 1074 (1996).

82. C. V. Bindhu, S. S. Harilal, V. P. N. Nampoori and C. P. G. Vallabhan, Pramana, 52, 435 (1999)

83. K. H. Derxhage, *Laser Focus*, 9, 35 (1973 a).

84. T. G. Pavlopoulos and P. R. Hammond, *J. Am. Chem. Soc.* 96, 21 (1974).

85. M. I. Snegov, I. I. Reznikova and A. S. Cherkasov, *Opt. Spectrosc.* 36, 55 (1974).

86. C. Bojarski and G. Obermller, *Acta Phys. Pol.* A50, 389 (1976).

87. T. Urisu and K. Kajiyama, *J. Appl. Phys.* 47, 3559 (1976).

88. A. K. Chibisov and T. D. Slavnova, *J. Photochem.* 8, 285 (1978).

89.   Y. Lu and A. Penzkofer, *Chem. Phys.* 107, 175 (1986).
90.   J. E. Sabol, *J. photochem. Photobiol. A: Chem.* 40 245 (1987).
91.   O. V. Aguilera and D. C. Neckers, *Acc. Chem. Res.* 22, 171 (1989).
92.   F. Ammer, A. Penzkofer and P. Weidner, *Chem. Phys.* 192, 325 (1995).
93.   J. Georges, *Spectrochimica Acta A*, 51, 985 (1995).
94.   M. Fischer and J. Georges, *Spectrochimica Acta A*, 53, 1419 (1997).
95.   S. G. Kim, T. F. Jr. Irvine, *Proceedings of the Second World Conference on Experimental Heat Transfer, Fluid Mechanics and Thermodynamics*, Dubrovnik,Yugoslavia, Elsevier Science Company, 1991.
96.   Y. Nagasaka, , and A. Nagashima, *Review of Scientific Instruments*, Vol. 52, pp. 229–232, 1981.
97.   J. J. Healy, J. J. de Groot and J. Kestin, *Physica C*, 82, 392 (1976).
98.   S. S. Raman, V. P. N. Nampoori, C. P. G. Vallabhan, G. Ambadas and S. Sugunan, Appl. Phys. Lett. 67, 2939 (1995).
99.   M. L. Baesso, J. Shen and R. D. Snook, *Chem. Phys. Lett.* 197, 255 (1992).
100. S. M. Lima, J. A. Sampaio, T. Catunda, R. Lebullenger, A. C. Hernandes, L.Basso, A. C. Bento and F. C. G. Gandra, *J. Non-cryst. Solids*, 256/257, 337   (1999).
101. W. J. Parker, R. J. Jenkins, C. P. Butler and G. L. Abbot, *J. Appl. Phys.* 32, 1679 (1961).
102. H. W. Deem and W. D. Wood, Rev. Sci. Instrum. 33, 1107 (1962).
103. P. Calmettes and C. Laj, *J. de physique*, C1, 125 (1972)
104. M. C. Gupta, S. Hong, A. Gupta and J. Moacanin, *Appl. Phys. Lett.* 37, 505 (1980).
105. R. T. Bailey, F. R. Cruickshank, D. Pugh, S. Guthrie, A. Moleod, W. S. Foulds, W. R. Lee

      and. Venkatesh, Chem. Phys. 77, 243 (1983).

106. C. V. Bindhu, S. S. Harilal, V. P. N. Nampoori and C. P. G. *Vallabhan, Opt. Eng.*

      37,(1998).

107. C. V. Bindhu, S. S. Harilal, V. P. N. Nampoori and C. P. G. *Vallabhan* , Current Sci. 74,764 (1998).
108. J. R. Whinnery, *Acc. Chem. Res.* 7, 225 (1974).
109. N. J. Dovichi amd J. M. Harris, *Anal. Chem.* 52, 2338(1980).
110. K Raznjevic, *Handbook of Thermodynamic Tables and Charts*, Hemisphere pub. Corporation, Washington (1976).
111. C. R. C. Weast, *CRC handbook of Chemistry and Physics,* CRC press. inc. Florida (1987).
112. I. Rosenthal, *Opt. Commun.* 24, 164 (1978).
113. E. T. Knobbe, B. Dunn, P. D. Fuqua, and F. Nishida, *Appl. Opt.* 29, 2729 (1990).
114. A. Onu, M. Palamaru, E. Tutovan and C. Ciobanu, *Polymer degradation and stability,* 60,465 (1998).
115. J. C. Newell, L. Solymar and A. A. Ward, *Appl. Opt.* 24, 4460 (1985).
116. N. A. George, B. Aneeshkumar, P. Radhakrishnan and C. P. G. Vallabhan, *J. Phys. D: Appl. Phys.* 32, 1745 (1999).

4

Energy transfer mechanism in dye mixtures using Thermal lens technique

Transfer of excitation energy between molecules is an important controlling factor in various fields, ranging from radiation physics to biology. For example photosynthetic process in plants takes place through electronic energy transfer between macromolecules. The energy transfer study has become a powerful spectroscopic tool for obtaining information about molecular excited states not obtainable by conventional spectroscopic methods. Almost all the works reported earlier analyzed the mechanism of energy transfer in mixtures by using fluorescence measurement method. This chapter describes the usefulness of thermal lens technique to study the electronic energy transfer in two types of organic dye mixtures viz., fluorescein- rhodamine B in ethanol using an Optical Parametric Oscillator and rhodamine 6G-rhodamine B in methanol using Ar ion laser as the excitation source. pH dependence of fluorescence quantum yield of fluorescein dye is also investigated, results of which are included in this chapter.
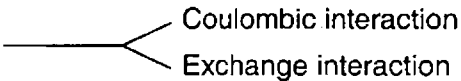
4.1   Introduction

When a molecule is excited to higher energy levels, energy transfer (ET) is one of the different ways to divest itself of its excess energy. ET between similar molecules in liquid solutions results in the depolarization and self-quenching of the fluorescence of such solutions. Between unlike molecules, the corresponding transfer process results in the quenching of the fluorescence of one species and the sensitization of the fluorescence of the other. The first observation of energy transfer was made by Cario and Frank in 1923 [1]. In their experiments on sensitized fluorescence of a mixture of mercury and thallium vapour, when irradiated with the light of mercury resonance line (2537Å), showed the emission spectra of both atoms. Since thallium atoms do not absorb the exciting light, it gets excited only indirectly by an excitation transfer from mercury atoms. Since the transfer of energy by reabsorption is impossible and hence this transfer may be non-radiative with a mercury atom as the donor or sensitizer and the thallium atom as the acceptor.

Even though first observation of sensitized fluorescence in solution was made by Perrin and Choucroun in 1929 [2] only recently have extensive discussions of its applications to various fields such as photodynamics of multichromophoreic assemblies [3, 4], interlayer and intralayer excitation transport in langmuir-Blodgett films [5], storage and migration of energy in photosynthetic systems [6] determination of molecular architecture [7] been published. Most of the works published earlier analyzed the energy transfer effect in mixtures by fluorescence resonant energy transfer. We have demonstrated the usefulness of thermal lens technique to study the energy transfer mechanisms in fluorescein-rhodamine B and rhodamine 6G–rhodamine B mixture. This chapter

deals with the detailed description of this method to study ET in these dye mixtures.

4.2 Phenomenological description of electronic energy transfer in solutions.

Intermolecular energy transfer between two molecular species separated by a distance in the condensed phase has been observed in numerous molecular systems [8-34]. Main mechanisms involved in the electronic energy transfer in molecular systems are

- Radiative or trivial transfer
- Nonradiative energy transfer ———< Coulombic interaction
Exchange interaction
- Excitation migration

4.2.1 Radiative transfer

In radiative transfer of electronic energy the light emitted by the excited state donor (D^*) travels through the solution and is absorbed by the acceptor (A). The process requires two steps with the intermediacy of a photon

$$D^* \rightarrow D + h\nu \qquad (4.1)$$

$$h\nu + A \rightarrow A^* \qquad (4.2)$$

No direct interaction of the donor and acceptor is involved. Obviously only energies corresponding to that part of the emission spectrum of the donor which overlaps with the absorption spectrum of the acceptor can be transferred. The efficiency of the transfer is governed by the Beer-Lambert law. This transfer can occur over very large distances (relative to molecular diameters) and the

probability that an acceptor molecule reabsorbs the light emitted by a donor at a distance R varies as R^{-2}. Radiative energy transfer is characterized by the invariance of the donor emission lifetime and a change in the emission spectrum of the donor [35, 36]. The transfer efficiency does not depend upon the viscosity of the medium.

4.2.2 Nonradiative energy transfer

The radiationless energy transfer from excited state donor molecule can occur due to Coulombic and / or electron exchange interaction between D^* and A. Nonradiative transfer of electronic energy involves the simultaneous de-exciation of the donor and the excitation of the acceptor, a one step process that does not involve the intermediacy of a photon. In the mechanism of radiationless excitation transfer close resonance between the initial $(D^* + A)$ and final $(D + A^*)$ states is required.
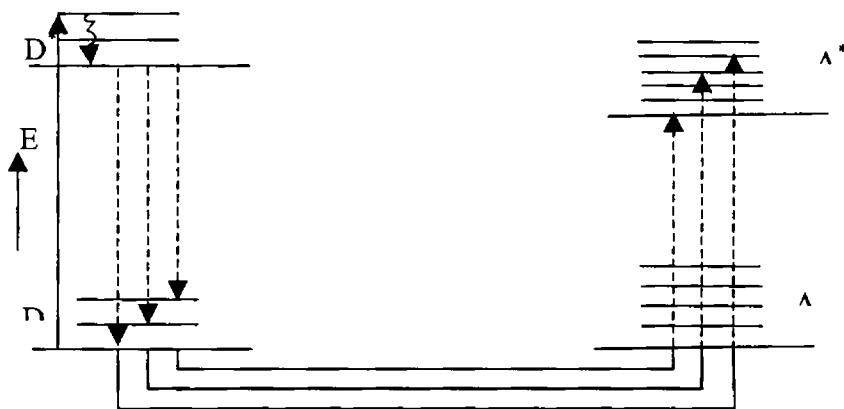

Figure 4.1 Coupled or resonant transition for a donor-acceptor pair.

This condition is fulfilled if the transfer in the donor $(D^* \rightarrow D)$ and the transition in the acceptor $(A^* \rightarrow A)$ involve the same energy, the excitation transfer being the simultaneous occurrence of the two coupled or resonant transitions as shown in figure 4.1 [36- 38]. Several theories have been established to explain the energy transfer phenomenon. Forster [38] was the first to develop a theory of ET, taking into consideration of dipole-dipole interaction between molecules. Later on Dexter [39] developed a theory of sensitized luminescence in solids and discussed dependence of transfer efficiency in donor and acceptor concentrations and temperature. Robinson and Frosch [40] pointed out the similarities and differences among the various types of radiationless transitions which can occur in a dense medium. Inokuti and Hirayama [41] generalized Forster's theory and applied it to the case of multiple and exchange interactions. In these theories, molecule is assumed to be stationary during its excited state. Yokota and Tanimoto [42] explained diffusion effect on energy transfer process. Briks and Georghiou [43] discussed the Forster kinetics and Stern-Volmer kinetics and developed an intermediate kinetics, which obey partial mixing of excited state donor and acceptor by diffusion during the energy transfer. Burshtein [44] gave a theory to explain the effect of rapid energy migration on energy transfer process and Loring [45] et al has given one of the most general theories of transport and trapping of excitation energy. Blumen and Klafter [46] explained the restricted geometries on the direct energy transfer. In all these theories the conditions necessary for nonradiative energy transfer are

- the donor molecule must be a fluorophore which has sufficiently long fluorescence lifetime.
- the emission spectrum of the donor and the absorption spectrum of the acceptor must overlap partially.

- the transition dipole moments must have a suitable orientation to each other.

- the distance between the donor and the acceptor must be within a limiting range (usually smaller than 10 nm).

4.2.2.1 Coulombic interaction- Froster kinetics

The Coulombic interaction represents a classical interaction between charged particles and electric field. In the Coulombic mechanism an excited molecule (an oscillating dipole) may cause the electrons of a given ground state molecule to oscillate in the same way as does the electric field of a light wave. For light absorption the resonance condition is $\Delta E(A \rightarrow A^*) = h\nu$ and for energy transfer the resonance condition is $\Delta E(D^* \rightarrow D) = \Delta E(A \rightarrow A^*)$. In the case of light, the coupling occurs between the electrons of A and the oscillating electric field of the light wave. In the case of energy transfer, the coupling occurs between the oscillating electrons of D^* and the electrons of A. Coulombic resonance energy transfer occurs via electromagnetic field and does not require physical contact of the interacting partners and is dependent on the inverse sixth power of the intermolecular separation [38]. The probability of such transfer is large if the emission spectrum of the donor overlaps with the absorption spectrum of the acceptor partially.

Forster had developed a quantitative expression for the rate of electronic energy transfer due to dipole-dipole interaction as [38]

$$K = \frac{9000 \ln 10 k^2}{128\pi^6 NR^6 \tau} \int_0^\infty F_D(\nu)\varepsilon_A(\nu) \frac{d\nu}{\nu^4} \qquad (4.3)$$

The spectral overlap integral is given as [36, 38, 47]

$$J = \int_0^\infty F_D(v)\varepsilon_A(v)dv \tag{4.4}$$

in which $F_D(v)$ is the spectral distribution of the donor emission, $\varepsilon_A(v)$ is the spectral distribution of the acceptor absorption, v is the wave number of the excitation radiation, N is the Avogadro's number, τ is the intrinsic or radiative lifetime of the excited sensitizer, n is the refractive index of the solvent, k^2 is the orientation factor and R is the mutual distance between both molecules.

The efficiency of Forster-type energy transfer is expressed in terms of critical radius R_0, the distance of separation of donor and acceptor at which the rate of intermolecular energy transfer is equal to the sum of the rates for all other de-excitation processes [38]. The expression for R_0 is given as

$$R_0^6 = \frac{9000\ln 10 k^2 \Phi_D}{128\pi^6 N R^6 v^4} \int_0^\infty F_D(v)\varepsilon_A(v)dv \tag{4.5}$$

A useful relation between the radius of the quenching sphere R and the concentration of the acceptor is given by

$$R_0(\text{Å}) = \frac{7.35}{(c_0)^{1/3}} \tag{4.6}$$

where c_0 is the critical concentration at which the transfer is 50% efficient (the donor fluorescence is half quenched) and R_0 and C_0 do not depend on the donor transition strength.

4. 2.2.2 Exchange interaction - Stern-Volmer kinetics

The exchange interaction is a diffusion controlled collisional transfer that requires close approach of the donor and acceptor, which is of the order of collisional diameters [36-38] (5-10 A°). This mechanism is dependent on solvent viscosity and temperature. The theory of energy transfer by electron exchange was worked out by Dexter [39] that considered transfer to nearest acceptor molecule only. The application of this method of obtaining bimolecular fluorescence quenching constants has been provided by Stephenson and co-workers [48].

The rate of change of concentration of D^* is given by [47]

$$\frac{d[\mathrm{D}*]}{dt} = fI - k_1[\mathrm{D}*] - k_2[\mathrm{D}*] - k_3[\mathrm{D}*].[A]$$ (4.7)

$$fI = (k_1 + k_2 + k_3[A])\mathrm{D}*$$ (4.8)

where $[D^*]$ is the concentration of the excited state solute D, I is the intensity of radiation and f is the efficiency of light absorption, k_1, k_2 and k_3 are the rate constants for decay of D^* by fluorescence, by quencher A and all other processes other than fluorescence and quenching by quencher A.

The fluorescence quantum yield in the presence of quencher is [47]

$$\phi_A = \frac{k_1\mathrm{D}*}{fI} = \frac{k_1}{(k_1 + k_2 + k_3[A])}$$ (4.9)

and in the absence of quencher

$$\phi_0 = \frac{k_1}{(k_1 + k_2)}$$ (4.10)

$$\frac{\phi_0}{\phi_A} = 1 + \left[\frac{k_3}{k_1 + k_2}\right][A]$$ (4.11)

$$\frac{\phi_0}{\phi_A} = 1 + k_3[A]\tau$$ (4.12)

where $\tau = \dfrac{1}{(k_1 + k_2)}$ is the lifetime of D^* in the absence of quencher. Eqn (4.12) is called Stern-Volmer expression [49].

4.2.3 Excitation migration

Radiative migration is due to the absorption of a fraction of (D^*) fluorescence by other molecules of the same species [47]. Radiative migration is of particular importance in concentrated solutions and its presence modifies the fluorescence spectrum, fluorescence quantum yield, the fluorescence lifetime and its influence on the efficiency of any competing radiationless processes [47].

4.3 Fluorescein-Rhodamine B system

The study of energy transfer is important owing to the numerous applications in biochemical research, especially because of the dependence of transfer rates on the distance between the donor and the acceptor. The mechanism of energy transfer in laser dye mixtures is also used to improve the efficiency and to broaden its spectral range of dye lasers [15, 25-27, 32, 50]. Fluorescence Energy

transfer is a technique now widely applied to probe biological and other complex systems for the determination of fluorophore separation and structure [51]. In this technique donor molecules are excited in the presence of acceptor molecules and the luminescence yield of donor and or acceptor are measured as a function of concentration.

However, photothermal methods measure the photon energy which has been converted into heat while fluorescence observes the re-emitted photons and hence both thermal and fluorescence spectroscopy are complementary to each other. Except the work of Rai et al (photoacoustic method) [52] not much works have been reported in which energy transfer phenomenon is monitored using nonradiative measurement techniques. During the last three decades energy transfer mechanism using numerous donor-acceptor organic dye pairs have been reported by various investigators [53-60]. In this chapter TL method is used to determine the distances within and between molecules in fluorescein-rhodamine B system at different rhodamine B concentrations. The thermal lens signals, which arise due to the nonradiative de- excitation of donor and / or acceptor, are measured.

Optical characterization of dyes depends on various factors like chemical environment, concentration of the dye etc. One of the important parameter, which influences fluorescence quantum yield, is the pH value of the dye solution. Dependence of pH on fluorescence quantum yield for fluorescein has been studied. Details are given in section 4. 5 of this chapter.

4.3.1 Experimental

An accurately weighed amount of rhodamine B is dissolved in spectroscopic grade ethanol to give a concentration of 1.79 m mol l^{-1}. From this stock solution, sample solutions with different concentrations ranging from 1.79 m mol l^{-1} to 0.0798 m mol 1^{-1} are prepared. Donor (fluorescein) having a concentration of 0.24m mol l^{-1} is mixed with the different concentrations of rhodamine B (acceptor).

The experimental setup is same as pulsed thermal lensing method described in chapter 2. The excitation radiation employed in the present investigation is 470 nm radiation from an Optical Parametric Oscillator with tunable output in the range 450-650 nm. This wavelength of excitation is used since it lies widely separated from the absorption spectrum of the acceptor molecules. Radiation of wavelength 632.8 nm from a low power (1.5 mw) intensity stabilized He-Ne laser source is used as the probe beam. Samples in a quartz cuvette (1 mm) are kept one confocal length past the beam waist. TL signal is processed using a digital storage oscilloscope. The present work is done at a temperature of 26 ° C. The absorption and fluorescence spectrum of the sample are recorded.

4.3.2 Results and discussion

Forster showed that electronic excitation transfer by dipole-dipole interaction is diffusive at all times. Recently Haan and Zwanzig [61] considering the effect of disorder, found that the transfer is nondiffusive at early times in dilute solution and conjectured that diffusive behavior is attained only at long times or at higher concentrations. Stern-volmer eqn., (4.12) modified by Inokuti and Hirayama [41] can be written as

$$\frac{\phi}{\phi_0} = \left(1 + \frac{c}{c_0}\right)^{-1} \qquad\qquad (4.13)$$

This eqn. can be rewritten as $\dfrac{\eta_L^{\;o}}{\eta_L^{\;A}} = 1 - \dfrac{c}{c_0}$ $\qquad\qquad (4.14)$

where $\eta_L^{\;o}$ is the thermal lens signal measured for donor alone, $\eta_L^{\;A}$ is the TL signal in the presence of acceptor and c_0 is an arbitrary reference concentration. Substituting the value of c_0 in the eqn (4.6) the distances between the molecules for each acceptor concentration are evaluated. Figure 4.2 gives the absorption spectrum of fluorescein at a concentration of 0 .24 m mol l^{-1}.
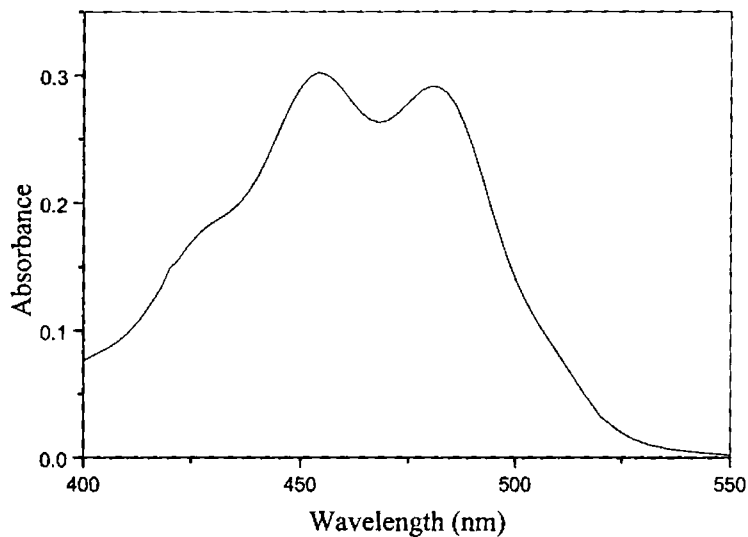

Figure 4.2   Absorption spectrum of fluorescein.

The emission spectrum of fluorescein (donor) and absorption spectrum of rhodamine B (acceptor) in ethanol is shown in figure 4.3.

Considerable overlap between emission of donor and absorption of acceptor is evident. The excitation wavelength, $_{ex}$ = 470 nm, is practically not absorbed by rhodamine B. The absorption spectrum shows twin peak since fluorescein can exist in different ionic forms. Florescence spectra of fluorescein (concentration 2.4×10^{-4} mol l^{-1}) in presence of various concentrations of rhodamine B (concentration varying from 7.98 $\times 10^{-5}$ mol l^{-1} to 1.79×10^{-3} mol l^{-1}) are shown in figure 4.4.

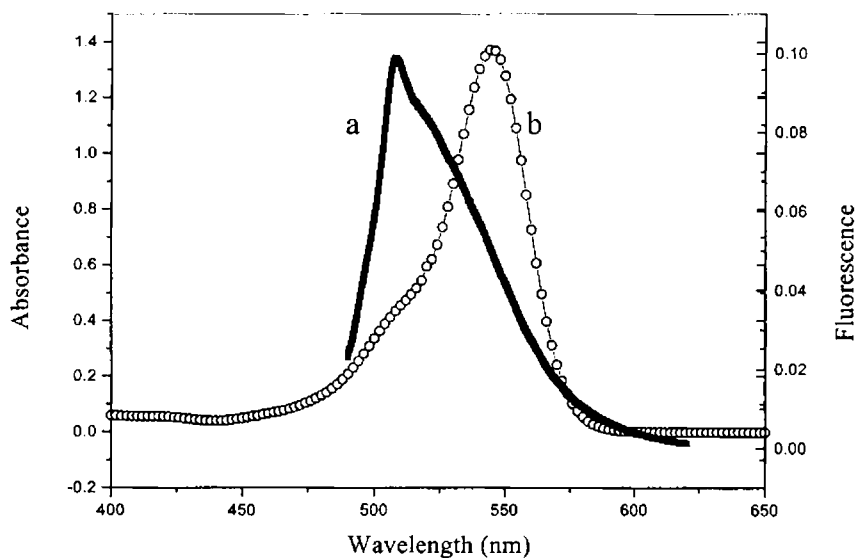*Figure 4.3 Emission spectrum of fluorescein (a) and absorption spectrum of rhodamine B (b).*

The successive quenching of fluorescein emission accompanied by enhancement in the intensity of rhodamine B fluorescence is due to energy transfer from fluorescein to rhodamine B, since contribution to acceptor fluorescence due to direct excitation is very small as can be seen from figure 4.3. The observed red shift in the acceptor fluorescence with increasing acceptor

concentration is due to Stoke's shift and also may be due to radiative migration among acceptors [47].
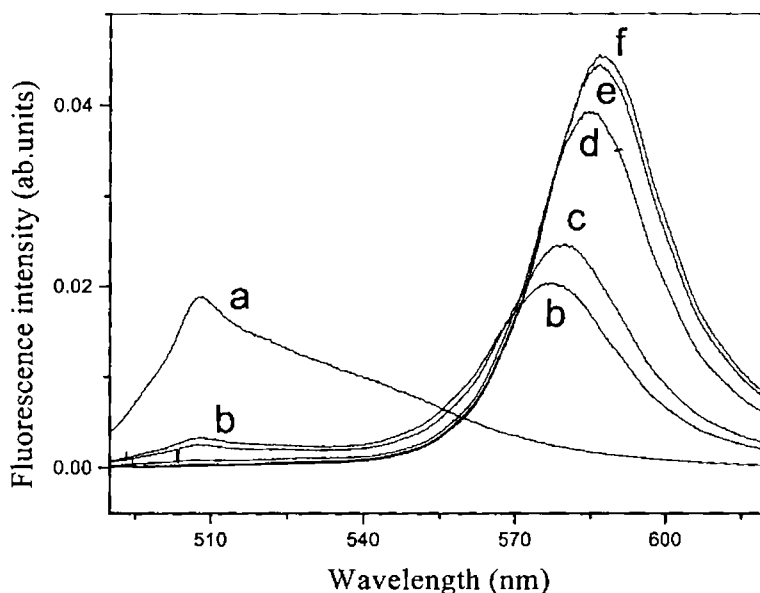

Figure 4.4 Variation of fluorescence intensities of fluorescein–rhodamine B system in ethanol. Fluorescein concentration is fixed at 2.4×10⁻⁴ mol l⁻¹ (a) and rhodamine B concentrations in m mol l⁻¹ are (b) 0.0798 (c) 0.120 (d) 0.449 (e) 1.20 (f) 1.79

At low acceptor concentration (below 4.49×10^{-4} mol l^{-1}) due to fast donor-donor transport/ translational diffusion, donor fluorescence decay is exponential. Decay of fluorescein (concentration 2.4×10^{-4} mol l^{-1}) in presence of acceptor concentration higher than 4.49×10^{-4} mol l^{-1} deviate from exponential behavior (Forster kinetics). Various observed energy transfer parameters, reduced concentration and distance between the molecules (R_0) for each acceptor concentration calculated using eqn. 4.6 are given in table 4.1.

Table 4.1 Observed values of reduced concentrations and distances between the molecules at different acceptor concentrations.

Acceptor concentration (mol l^{-1})	TL-Ratio	Reduced concentration c_0 (m mol l^{-1})	R_0 Å
7.98×10^{-5}	0.504	0.161	135
1.20×10^{-4}	0.435	0.218	123
4.49×10^{-4}	0.206	0.565	89
1.20×10^{-3}	0.172	1.446	65
1.79×10^{-3}	0.153	2.119	57

The higher calculated valued of R_0 is due to the influence of diffusion on direct energy transfer [43,57,58]. When the distance between the molecule is, $R_0 = 57$ Å, long-range dipole-dipole interaction (Forster kinetics) is the dominating mechanism and at this acceptor concentration (1.79 m mol l^{-1}) the fluorescence of donor is completely quenched. When fluorescein is excited with blue light (470

nm), it will normally give off green light. However, if fluorescein is in close proximity to rhodamine B (57 Å), it will transfer its total energy to the rhodamine B in a radiationless transfer. Now rhodamine B will give off red fluorescence. TL measurement method is an effective tool to measure the distance between the non-fluorescent molecules.

4.4 Rhodamine 6G – Rhodamine B system

Rhodamine 6G and rhodamine B are xanthene derivatives that cover the wavelength region from 460-700 nm. These dyes have excellent lasing results in dye laser applications.

4.4.1 Experimental

The experimental setup is the same as that given in 4.2.1. For the present work, 488 nm radiation from an Ar-ion laser is used as the pump beam to generate the thermal lens in the medium. Radiation of wavelength 632.8 nm from a low power (1.5mW) intensity stabilized He-Ne laser source is used as the probe beam. Solution of the mixture in a quartz cuvette (3mm) is kept in the pump beam path. The absorption spectra of donor, acceptor and their mixture in methanol are recorded with a UV-VIS-IR spectrophotometer. Fluorescence spectra of donor, acceptor and their mixture are recorded using the technique described in chapter 2 section 2.5.3.

An accurately weighed amount of rhodamine 6G (Exciton) was dissolved in spectroscopic grade methanol to give a concentration of 4.1×10^{-3} mol l^{-1}. From this stock solution, sample solutions with different concentrations ranging from 1.3×10^{-3} mol l^{-1} to 4.1×10^{-5} mol 1^{-1} were prepared. The different concentrations of rhodamine B in the same range were also prepared. Donor (rhodamine 6G)

having a concentration of 4.1 x 10^{-4} mol l^{-1} was mixed with the different concentrations of rhodamine B (acceptor). TL measurements are carried out with donor alone and mixture with the acceptor concentration ranging from 4.1x 10^{-5} mol l^{-1} to 1.3 x 10^{-3} for different excitation powers. The same measurement was performed by keeping rhodamine B constant at 4.1 x 10^{-4} mol l^{-1} and donor concentration varied

4.4.2 Results and discussion

The energy transfer by exchange interaction has been neglected in the present case because (a) no new fluorescence peak were detected in the mixture to indicate any fluorescence exciplex formation, (b) the concentrations of donor and acceptor were taken to be less than 2 x 10^{-3} mol l^{-1} and hence collisional encounter due to short range would be very rare [36-38]. In the concentration range we used, the dependence of quantum efficiency of radiationless transfer from D* to A* on acceptor concentration is insensitive to the kinetics (Forster and Stern-Volmer) [58]. Since the intensity of fluorescence is

proportional to ϕ_f, eqn. (4.12) can be rewritten as

$$\frac{I_f^0}{I_f^A} = 1 + K_f \tau [A] \qquad (4.15)$$

I_f^0 and I_f^A are the fluorescence intensities in the absence and presence of acceptor respectively. Since $I_f^0 < I_f^A$, their ratio increases with $[A]$ as is clear from eqn. (4.15). Thermal lens method measures directly the nonradiative decay of excited species and the TL signal, η, is complementary to that of fluorescence signal. Hence, equation (4.15) can be modified for TL signal as

$$\frac{\eta_L^{\,o}}{\eta_L^{\,A}} = 1 - K_L \tau [A] \qquad (4.16)$$

where $\eta_L^{\,o}$ and $\eta_L^{\,A}$ are the TL signals for donor alone and with the acceptor respectively.

Theory and experiment have shown that the various mechanisms involved in energy transfer in mixtures may be distinguished by evaluating the energy transfer rate and critical transfer radius [38,47]. Figure 4.5 Shows the absorption and emission spectra of donor and acceptor. The figure clearly shows the overlap between emission spectrum of rhodamine 6G (b) and absorption spectrum of rhodamine B (c) in methanol which satisfies the important condition necessary for the electronic energy transfer.
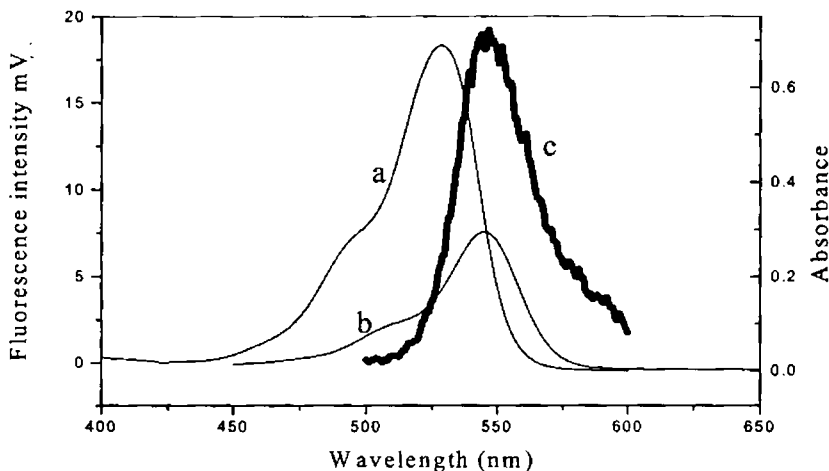

Figure 4.5 Absorption and emission spectra of donor and acceptor. (a) and (b) absorption and emission spectrum of donor (c) absorption spectrum of acceptor.

Figure 4.6 shows the absorption spectra of the mixture with acceptor being kept at a constant concentration while donor concentration is varied. (Figure 4.6) shows blue shift to the shorter wavelength side of the absorption peak in the visible region.
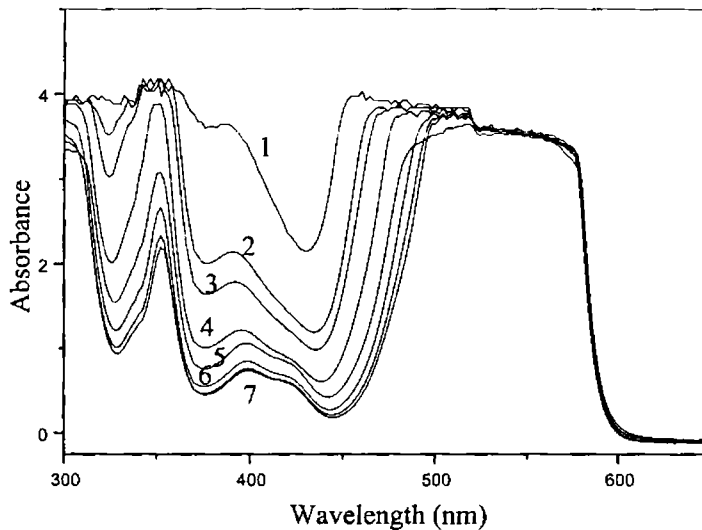

Figure 4.6 Absorption spectra for constant acceptor concentration and concentration of donor varied in m mol l^{-1} (1) 4.1 (2) 1.3 (3) 0.75 (4) 0.42 (5) 0.(6) 0.07 (7) 0 .04.

This is due to the enhanced excitation of the rhodamine 6G molecules as the donor concentration is increased. This is also evident from figure 4.8, in which When donor is kept constant and acceptor varied the absorption shows a red shift. This is due to enhanced optical absorption in the acceptor molecules as the concentration of the acceptor concentration is increased.
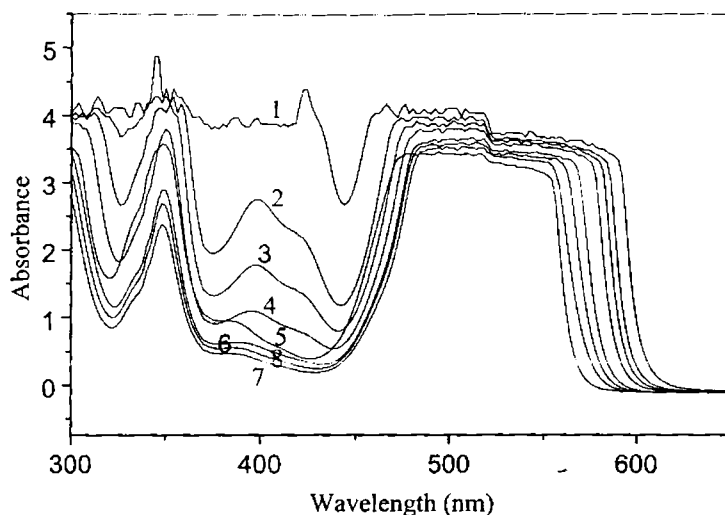
Figure 4.7 Absorption spectra for constant donor concentration at 0. 24m mol l^{-1} and concentration of acceptor varied in m mol l[-1](1)4.1 (2)1.3(3) 0.75 (4) 0.42(5)0.13 (6) 0.07(7) 0 .04 (8) 0.013

Figure 4.9 describes the variation of peak fluorescence wavelength with concentration, when the concentration of the donor is kept constant while varying the acceptor concentration. Peak fluorescence wavelength follows a similar profile ie. red shifted. the peak fluorescence wavelength shows a blue shift. Figure 4.7 shows the absorption spectra of the mixture with donor concentration is kept constant and the concentration of the acceptor is varied.
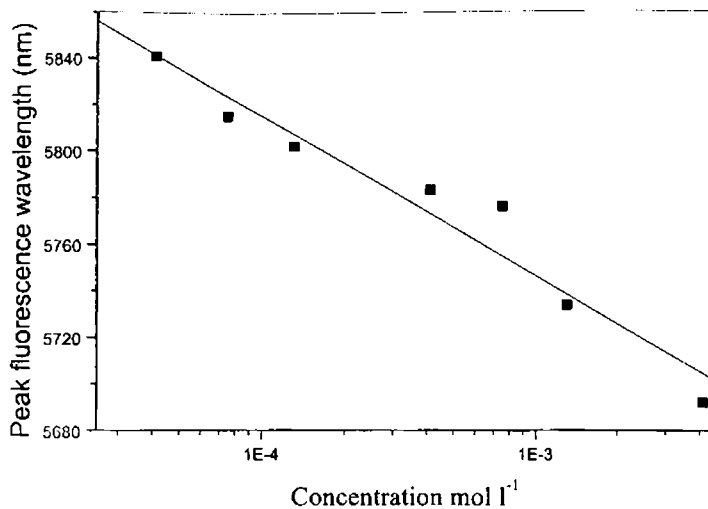
Figure 4.8 Variation of peak fluorescence wavelength:
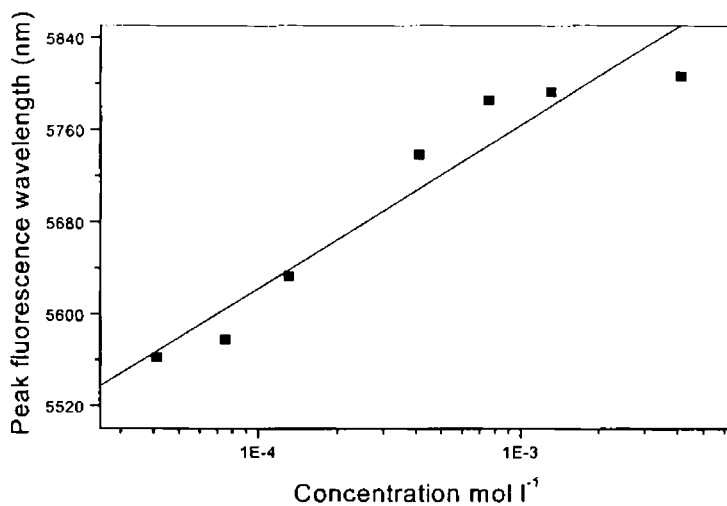*acceptor concentration constant and donor concentration varied.*

Figure 4.9 Variation of peak fluorescence wavelength:donor constant,acceptor varied.

In order to calculate the energy transfer rate constants in the mixture, the ratio of the TL signal of donor alone at a concentration of 4.1×0^{-4} moll $^{-1}$ to the TL signal of the mixture with acceptor concentration ranging from 4.1×10^{-5} mol l $^{-1}$ to 1.3×10^{-3} mol l $^{-1}$ are investigated (figure 4.10). The plot is a straight line obeying Stern-Volmer equation, and from the slope, the value of K_L is determined. By considering the lifetime τ of the excited donor in the absence of acceptor [62] as ~ 3.7 ns, the value of K_L is obtained as 1.44×10^{11} l mol $^{-1}$ s $^{-1}$ [63] which is in good agreement with the results obtained by earlier workers [19,24,55,59]. We have also calculated the nonradiative energy transfer rate using equation (4.15).
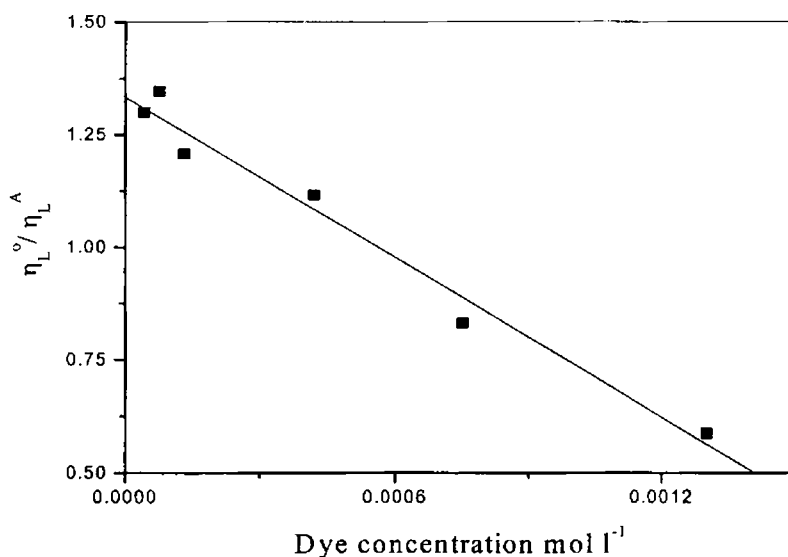

Figure 4.10. The Stern–Volmer plot for rhodamine 6G – rhodamine B pair

Figure 4.11 shows the variation of the ratio of the fluorescence intensity of donor in the absence and in the presence of acceptor with latter concentration ranging from 4.1 x 10^{-5} mol l^{-1} to 1.3 x 10^{-3} mol 1^{-1}. The results obey Stern-Volmer equation and from the slope we have calculated the transfer rate as 1.7 x 10^{11} l mol^{-1} s^{-1} [63] and which is in close agreement with value obtained using TL technique. The Value of K_L calculated using TL technique is slightly lower than that from fluorescence studies. This is because, apart from energy transfer process, TL signal can also be arised due to direct excitation – deexcitation process of acceptor.
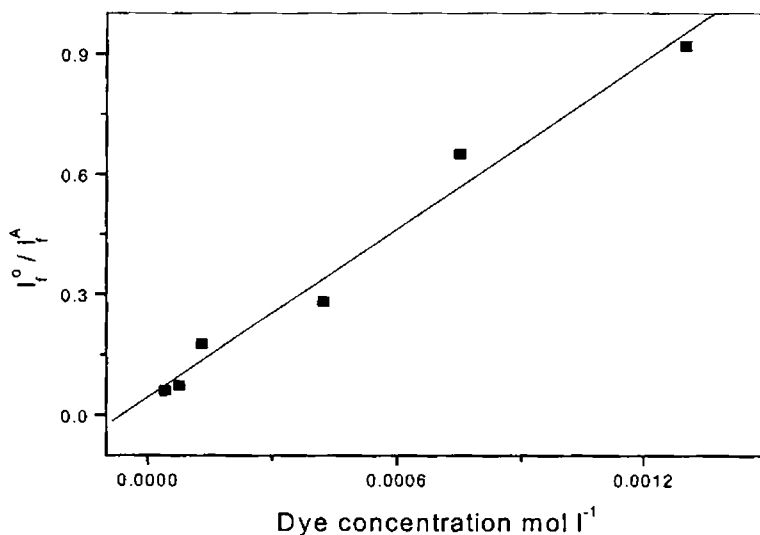

Figure 4.11 The Stern–Volmer plot using fluorescence measurement method.

From figure (4.10) and (4.11) the value of R_0, the critical transfer radius, is calculated using the eqn (4.6) $R_0 = 7.35([A]_{1/2})^{-1/3} \overset{0}{A}$, where $[A]_{1/2}$ is the half quenching concentration of the acceptor at which $I_f^A = \frac{1}{2} I_f^o$ or $\eta_L^A = \frac{1}{2} \eta_L^o$.

Thus the calculated value obtained is $62\overset{0}{A}$ and $65 \overset{0}{A}$ respectively [63]. The observed value agrees well with that obtained in resonance transfer for other donor-acceptor pairs reported earlier using other techniques [18, 24, 56, 64-66]. Using this technique we concluded that although radiative and collisional processes probably contribute to the energy transfer in the rhodamine 6G-rhodamine B laser dye mixture, resonance transfer due to long range dipole-dipole interaction is the dominating mechanism responsible for the efficient excitation transfer.

4.5 Study of fluorescence quantum yield of dyes

This section describes the use of TL technique to study fluorescence quantum yield of dyes taking fluorescein as the representative dye because it is one of the most commonly used fluorescent dye today. It is an important xanthene dye with large variety of technical applications. It has a very high molar absorptivity in the visible region, a large fluorescence quantum yield and a high photostability making it very useful in applications where high sensitivity is needed. Furthermore, due to the availability of a variety of chemistries that can be used to conjugate it to functional biomolecules, fluorescein is widely used as fluorephore in the biosciences [67]. Recently it is also employed to label primers used in automated DNA sequencing [68]. It can be effectively used in energy transfer measurements to determine distances within and between molecules [64, 69].

Because of these reasons it is desirable to study the effect of environment on the fluorescing efficiency of this dye.

Fluorescence quantum yield (ϕ_f), one of the important photophysical parameters, is a measure of the rate of nonradiative transitions that compete with the emission of light. The application of TL effect for the measurement of quantum yield was first introduced by Brannon and Magde [70]. Since then, the technique has been used to determine this parameter in fluorescent solutions [71] and in fluorescent polymers [72]. Usually fluorescence quantum yield is measured by comparing the relative fluorescence intensity of the sample under study with a standard reference sample, for which the fluorescence quantum yield is known. In this kind of measurement it is necessary to introduce corrections for the spectral sensitivity of the detection system. Even after the various corrections for system geometry, re-absorption, polarization etc, the accuracy of the quantum yield values obtained from photometric measurements is rather poor [73]. In order to evaluate the absolute quantum efficiency both the radiative and non-radiative relaxation processes taking place in the medium are considered. Since the contribution from non-radiative processes is not directly measurable using the traditional optical detection methods, thermo-optic methods have been adopted for this purpose. In this section, we describe the use of thermal lens method to study the variation of fluorescence quantum yield of fluorescein as a function of pH and concentration of the dye.

The fluorescence quantum yield ϕ_f is given by [70]

$$\phi_f = \left(1 - \frac{A^r \eta^s}{A^s \eta^r} \right) \frac{\lambda_f}{\lambda} \qquad (4.19)$$

The ratio of the peak fluorescence wavelength λ_f to the excitation wavelength λ takes account of Stokes shift. η^r and A^r corresponds to the TL signal and absorbed power respectively for the sample pH at which the fluorescence intensity is quenched completely. The thermal lens signal η^s has been measured as the variation of light intensity at far field at the centre of the probe beam and A^s corresponds to the absorbed power of the sample.

4.5.1 Experimental

The experimental setup of dual beam thermal lens technique employed in the present investigation is shown in chapter 2. Laser radiation at 488 nm wavelength from an Argon-ion laser (Lyconix) is used as the pump beam to generate the thermal lens in the medium. Radiation of wavelength 632.8 nm from a low power (1mw) intensity stabilized He-Ne laser source was used as the probe beam. The pump beam was intensity modulated at 7 Hz using a mechanical chopper (EG&G 192). Sample in a quartz cuvette (3mm) was kept in the pump beam path.

First, the sample pH was adjusted to 2 using conc. H Cl and then an accurately weighed amount of fluorescein was added to make the concentration to be 2.4×10^{-4} mol l^{-1}. Then samples having different pH ranging from 4 to 9 were prepared by adding appropriate amount of Na OH solution. This procedure was repeated for another concentration of 1.59×10^{-4} mol l^{-1}. pH of the solution was measured using pH-meter (pH scan Merck)with accuracy of ± 0.2. Ethanol was used as the solvent since it has no absorption in the specified wavelength region.

4.5.2 Results and discussion

Figure 4.12 depicts the absorption spectrum of fluorescein at different pH values using spectrophotometer. Fluorescein exists in several ionic and neutral forms such as (a) cationic (b) neutral (c) monoanionic and (d) the dianionic (figure 4.14) [74-76]. At each pH chosen, one particular form of the dyes predominates. In acidic solutions cation is present. Around neutral pH the mono- and dianionic species are present and they have quiet different spectroscopic properties.
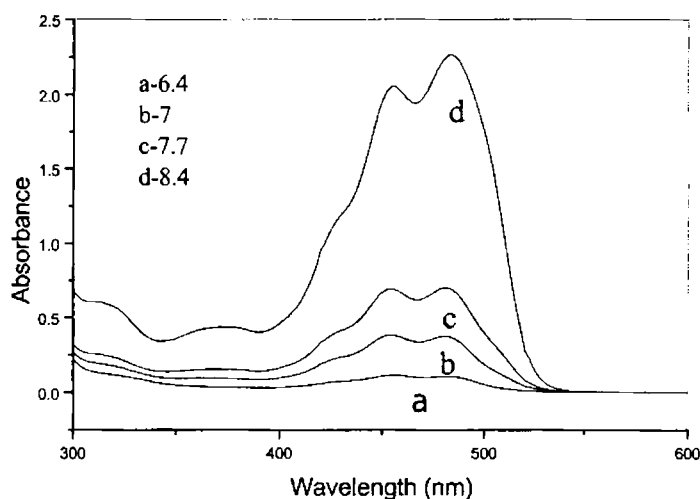
Figure 4.12   Absorption spectra of fluorescein, for different pH values for a concentration of 2.4 x 10⁻⁴ mol l⁻¹

The monoanion absorbs at 454 nm and 472 nm and dianion absorbs at 490 nm [74, 75]. In the molecule of fluorescein the carboxyl phenyl is almost

perpendicular to the xanthene ring and therefore is not conjugated to the xanthene group.

Figure 4.13 Variation of peak absorption as a function of pH. Dye shows enhanced absorption in the alkaline media.
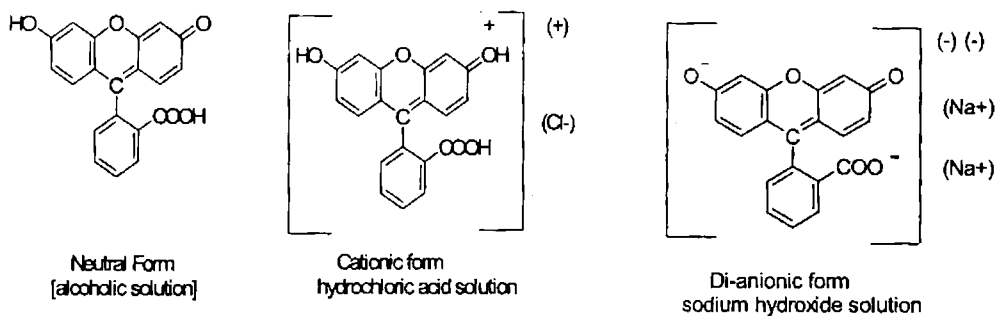
Figure 4. 14 Different protolytic forms of fluorescein

Thus the ionization and alkylization of the carboxyl is not expected to influence the absorption spectrum in the visible region.
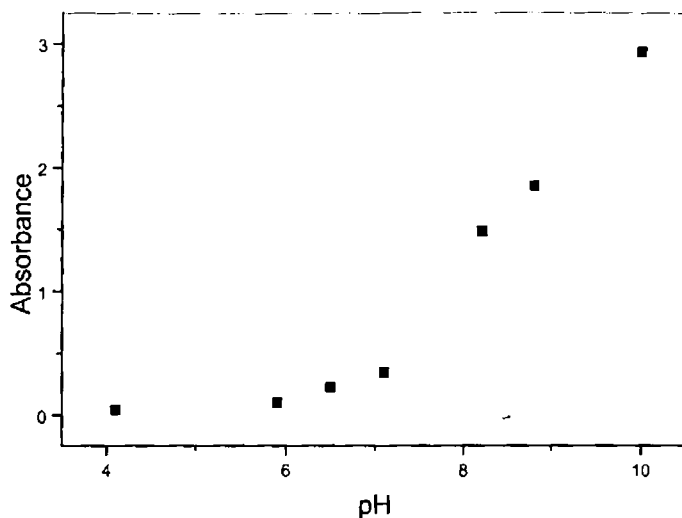
Figure 4.15 shows the variation of TL signal amplitude with pH for different excitation powers. The figure indicates that nonradiative de-excitation is enhanced as the medium becomes more and more basic. Martin and Lindqvist [75] argued that hydrogen bonding plays a central role in the nonradiative deactivation of fluorescein and that equilibrium is established in the excited state between fluorescent H- bonded dyes and nearly non-fluorescent free dyes. Figure 4.16 represents the peak fluorescence wavelength as a function of pH. The auxochrome ⁻OH attached to the chromophore shifts the peak fluorescence wavelength to longer wavelength.
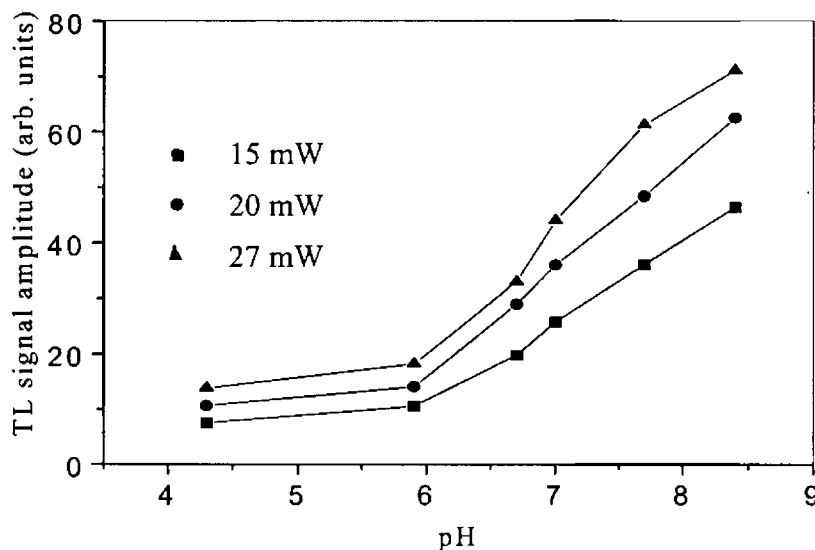
Figure 4.15 Variation of TL signal amplitude with pH for three different powers
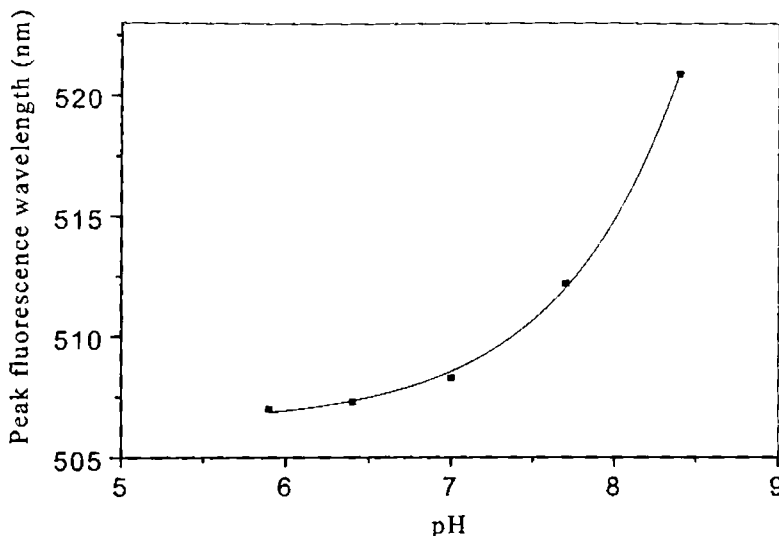
Figure 4.16 pH dependence of peak fluorescence wavelength of fluorescein for a concentration of 2.4 x 10^{-4} mol l^{-1}

The variation of quantum yield with pH is shown in Figure 4.17. Fluorescein dissolves in alkali to give a reddish brown solution, which on dilution gives a yellowish-green fluorescence. Following the absorption of radiation, the relaxation process of each form occurs mainly by vibrational relaxation, internal conversion and fluorescence. The various forms may also undergo intersystem crossing to the triplet state, but this process can be neglected owing to the low quantum yield. Bowers and Porter [77] found the triplet yield to be $\phi_T = 0.05$ and Soep et al [78] found it to be $\phi_T = 0.03$.

The low fluorescence yield of fluorescein in neutral and slightly acidic solutions is due to the formation of lactonic form of the dye from the excited state

of the quinonoid form which does not absorb in the visible [74, 75, 79, 80]. Drexhage [81] reported that the fluorescence efficiency depends on the character of the end groups of the chromophore and in alkaline medium the anionic form attains the rigidity introduced by O⁻ bridge makes the molecule highly fluorescent.
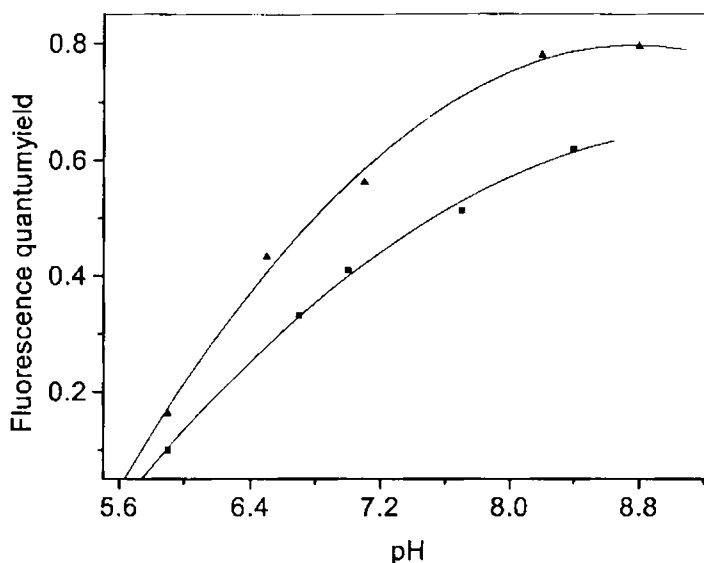
Figure 4.17 Variation of quantum yield of fluorescein with pH corresponding to two concentrations (2x 10⁻⁴ mol / l, 1.5x 10⁻⁴ mol/ l).

The plot clearly reveals a decrease in fluorescence quantum yield at higher concentrations. This is a direct indication that non-radiative processes become significant at higher concentrations and contribute to enhanced thermal lensing [82]. Internal conversion rate is said to depend exponentially on the S_1-S_0

energy gap [83]. The Forster type energy transfer between fluorescein molecules results in the depolarization and self-quenching of its fluorescence [84]. Innerfilter effect can be expected to result in the decrease of quantum yield with increasing concentration. Dimers or higher aggregates formation can be neglected since we have used low concentration of the dyes.

4.6   Conclusion

The thermal blooming technique offers a novel method for the investigation of the energy transfer in organic molecules. We have evaluated the energy transfer rate and critical transfer radius for Rhodamine 6G-Rhodamine B mixture. Using this technique we confirmed that resonance transfer which takes place between two well separated dye molecules due to Froster type dipole-dipole interaction is the dominating mechanism responsible for the efficient excitation transfer.   In the case of fluorescein – rhodamine system, at low acceptor concentration diffusive mechanism dominates while at higher concentration energy transfer takes place through Forster type dipole-dipole mechanism. The technique is simple and its high sensitivity indicates that it can be applied for a wide range of non-fluorescent materials.

A dual beam TL technique was successfully employed for the determination of the absolute value of the fluorescence quantum yield for different pH values. The photophysical parameters of fluorescein strongly depend on its environment. In different media, fluorescein exists in different structure forms and / or gives varied absorption spectra, fluorescence spectra and quantum yield. The variation of quantum yield with the concentration of the dye solution showed a decreasing tendency irrespective of the pH of the solution used.

References

1. G. Cario and J. Franck, *Z. Physik,* 17, 202 (1923).
2. J. Perrin and Choucroun, *Acad. Sci.* 189, 1213 (1929).
3. M. N. Berberan-Santos, P. Choppinet, A. Fedorov, L. Jullien and B. Valeur, *J. Am. Chem. Soc.* 121, 2526 (1999)
4. Harriman, M. Hissler, O. Trompette and R. Ziessel, *J. Am. Chem. Soc.* 121, 2516 (1999).
5. K. Sienicki, *J. Chem. Phys.* 94, 617 (1991).
6. P. Allcock, R. D. Jenkins and D. L. Andrews, *Phys. Rev. A,* 61, 023812-1 (2000).
7. C. G. Dos Remedios and P. D. J. Moens, *J. Stru. Biol.* 115, 175 (1995).
8. L. N. M. Duyesns, *Nature,* 168, 548 (1951).
9. E. J. Bowen and B. Brocklehurst, *Trans. Faraday Soc.* 49, 1131 (1953).
10. E. J. Bowen and R. Livingston, *J. Am. Chem. Soc.* 76, 6300 (1954).
11. E. J. Bowen and B. Brocklehurst, *Trans. Faraday Soc.* 51,774 (1955).
12. R. Livingston, *J. Phys. Chem.* 61, 860 (1957).
13. R. Hardwick, *J. Chem. Phys.* 26, 323 (1957).
14. R. G. Bennet, *J. Chem. Phys.* 41, 3037 (1964).
15. C. E. Moeller, C. M. Verber and A. H. Adelman, *App. Phys. Lett.* 18, 278   (1971).
16. V. L. Pugachev and A. K. Chibisov, *Optical society of America* 34, 284 (1973).
17. B. Berlman, M. Rokni and C. R. Goldschmidt, *Chem. Phys. Lett.* 22, 458 (1973).
18. C. Lin and A. Dienes, *J. Appl. Phys.* 44 , 5050 (1973).
19. T. Urisu, K. Kaajiyama, *J. Appl. Phys.* 47, 3563 (1976).
20. E. Weiss and S. Speiser, *Chem. Phys. Lett.* 40, 220 (1976).
21. Y. Kusumoto, H. Sato, K. Maeno and S. Yahiro, *Chem. Phys. Lett.* 53, 388 (1978).
22. M. Kleinerman and M. Drabrowski, *Opt. Commun.* 26, 81 (1978).
23. S. Speiser, *Opt. Commun.* 29, 213 (1979).
24. S. Muto and C. Ito, *Jpn. J. Appl. Phys.,* 20, 1591 (1981).
25. J. Cox and B. K. Matise, *Chem. Phys. Lett.* 76, 125 (1980).
26. T. G. Pavlopoulos, *Opt. Commun.* 38, 299 (1981).
27. E. G. Marason, *Opt. Commun.* 40, 212 (1982).
28. N. Sugimoto, S. Takezawa and N. Takeuchi, *Jap. J. Appl. Phys.* 21, 1536 (1982).
29. S. Muto, H. Nagashima and C. Ito, *Elect. And Commun. Jap.* 66-c, 104 (1983).
30. M. Terada and Y. Ohba, *Jap. J. App. Phys.* 22, 1392 (1983).
31. M. I. Savadatti, S. R. Inamdar, N. N. Math and A. D. Mulla, *J. Chem. Soc.* 82, 2417 (1986).
32. B. Panoutsopoulos, M. Ali and S. A. Ahmed, *Appl. Opt.* 31, 1213 (1982).
33. J. R. Coppeta and C. B. Rogers, *Am. Inst. Aeronautics and Astronautics, (1994).*
34. J. R. Coppeta and C. B. Rogers, *Am. Inst. Aeronautics and Astronautics* (1995).
35. F. Wilkinson , *Luminescence in Chemistry,* E. J. Bowen (Ed.), Van Nostrand, Princeton, (1967).
36. A. A. Lamola and N. J. Turro, *Energy transfer and Organic Photochemistry,* in: Technique of organic chemistry, vol. 14, P. A. Leermakers and A. Weissberger (Ed.), Interscience (1969).
37. J. Turro, *Modern molecular photochemistry,* Benjamin\Cummings publishing company, California pp. 317-319 (1978).
38. Th. Forster, *Discuss. Faraday Soc.* 27, 7 (1959).

39. D. L. Dexter, *J. Chem. Phys.* 21, 836 (1953).
40. G. W. Robinson and R. P. Frosch, *J. Chem. Phys.* 38, 1187 (1963).
41. M. Inokutti and F. Hiryama, *J. Chem. Phys.* 43, 1978 (1965).
42. M. Yokota and O. Tanimoto, *J. Phys. Soc.Jap.* 22, 779 (1967).
43. J. B. Briks and S. Georghiou, *J. Phys. B 1,* 958 (1968).
44. Burshtein, *Sov. JETP Phys.* 35, 882 (1972).
45. R. F. Loing, H. C. Anderson, M. D. Fayer, *J. Chem. Phys.* 76, 2015 (1982).
46. A. Blumen and J. Klafter, *J. Phys. Chem.* 84, 1397 (1986).
47. J. B. Birks, *Photophysics of aromatic molecules,* J. B. Birks (Ed.), Wiley- Interscience, London (1969).
48. L. Stephenson, D. G. Whitten, G. F. Vesley and G. S. Hammond, *J. Am. Chem. Soc. 88, 3665 (1966).*
49. Stern and M. Volmer, *Phyzik Z.* 20, 183 (1919).
50. P. J. Sebastian and K. Sathianandan, *Opt. commun.* 32, 422 (1980).
51. R. M. Clegg, A. I. Murchie, A. Zechel and D. M. J. Lilley, *Proc. Natl. Acad. Sci. USA* 90, 2994 (1993).
52. V. N. Rai, S. N. Thakur and D. K. Rai, *Pramana* 23, 215 (1984).
53. A. Dienes and M. Madden, *J. App. Phys.* 44, 4161 (1973).
54. P. Y. Lu, Z. X. Yu, R. R. Alfano and J. I. Gersten, *Phys. Rev. A* 26, 3610 (1982).
55. P. Y. Lu, Z. X. Yu, R. R. Alfano and J. I. Gersten, *American phys.l soc.* 27, 2100 (1983).
56. M. B. Levin, M. G. Rova, V. V. Rodchenkova and B. M. Uzhinov, Sov. J. *Quantum Electron.* 17, 14 (1987).
57. K. K. Pandey and T. C. Pant, *Chem. Phys. Lett.* 170, 244 (1990).
58. R. D. Singh, A. K. Sharma, N. V. Unnikrishnan and D. Mohan, *J. Mod. Opt.* 37, 419 (1990).
59. G .A. Kumar and N. V. Unnikrishnan, *J. Photochem. Photobio.* 144, 107 (2001).
60. R. K. Swank and W. L. Buck, *Phys. Rev.,* 91,927 (1953).
61. S. W. Hann and R. W. Zwanzig, *J. Phys. Chem.* 68, 1879 (1978).
62. K. A. Selanger, J. Faines and T. Sikkeland, *J. Phys. Chem.,* 81, 1960 (1977).
63. A. Kurian, K. P. Unnikrishnan, P. Gopinath, V. P. N. Nampoori and C. P. G. Vallabhan, *J. Nonlinear Opt. Phys. Mat.* 10, 415 (2001).
64. S. Sanghi, D. Mohan and R. D. Singh, *Spectrochimica Acta Part A* 53, 713 (1997).
65. V. Misra, H. Mishra, H. C. Joshi amd T. C. Pant, *Sensors and Actuators B* 63,18 (2000).
66. N. V. Unnikrishnan, S. H. Batti and R. D. Singh, *Opt. Acta* 31, 983 (1984).
67. R.Sjoback, J. Nygren and M. Kubista, *Spectrochim. Acta. A* 51, L7, 1995.
68. Y. Cheng, and N. J. Dovichi, *Science,* 242, 562 (1988).
69. M. Voicescu, M. Vasilescu and A. Meghea, *J. Fluore.* 10, 229 (2000).
70. J. H. Brannon and D. Magde, *J. Phys. Chem.* 82,705(1978).
71. J Shen and R. D. Snook, *Chem. Phys, Let.*155, 583(1989).
72. M. L. Lesiecki and J. M.Drake, *Appl.. Opt.* 21, 557(1982).
73. J. N. Demas and J. A. Crosby, *J Phys. Chem.* 75, 991(1971).
74. L. Landqvist, *Ark. Kem.* 16, 79 (1960).
75. M. M. Martin and L. Lindqvist, *J. Lumin.*10, 381 (1975).
76. Finar I. *Organic Chemistry- fundamental principles,* vol. 1, 6th Ed. pp. 868, Longman, Singapore (2000).

77. P. G. Bowers and G. Porter, *Porc. . R. Soc.* (Lond.) A, 299, 348 (1967).
78. B. Soep, A. Kelliman, M. Martin and L. Lindqvist, *Chem. Phys. Lett.* 13, 241(1972).
79. A. Chartier, J. Georges and J.M. Mermet, *Chem. Phys. Let.* 171, 347,1990.
80. A. Song, J. Zhang, M. Zhang, Tao Shen and J. Tang, *colloids and Surfaces A; Physicochem. & Eng. Aspects,* 167, 253 (2000).
81. Drexhage K. H. *Dye lasers*, ed. Schafer F. P., Springer, Berlin (1989).
82. C. V. Bindhu, S. S. Harilal, *Analytical Science*, 17, 1 (2001).
83. D. Magde, G. E. Rojas and P. G. Seybold, *Photochem.Photobiol.*70, 737 (1999).
84. Th .Forster, *Discuss. Faraday Soc.*, 27, 7 (1959).

5

Thermal lens spectra of aniline and certain organic dyes

Thermal lens spectra of aniline and certain organic dyes are described in this chapter. Two photon absorption spectrum of aniline are recorded using thermal lens technique with Optical Parametric Oscillator as the pump source. The C-H and N-H stretching overtones of aniline in liquid phase are investigated using this technique. A local mode model based on uncoupled, anharmonic X-H oscillators is used to analyze the observed spectra. The wavelength dependence of thermal lens signal of organic dyes such as rhodamine B and crystal violet are also recorded using this technique and details of which are given in this chapter.

5.1 Two photon absorption spectrum of aniline

5.1.1 Introduction

Albert Einstein in his famous discovery of the photoelectric effect reasoned that photons might ionize an atom only if they had energy greater than a particular threshold energy corresponding to the ionization energy of the atom. In 1931, Maria Göppert-Mayer [1] predicted theoretically that an atom or a molecule might absorb two or more photons simultaneously, thus allowing an atom or a molecule to be excited to states unreachable by single photon absorption. Since any observable effect of this phenomenon of multiphoton absorption could not be possible without a very intense beam of radiation, her prediction could not be investigated in detail until the invention of the first laser in 1960. Again it received relatively little consideration for practical applications because of the relatively small size of the effective cross-sections of the phenomenon for available materials. The interaction of intense monochromatic laser radiation with atoms and molecules opened a new field viz., nonlinear optical absorption spectroscopy. Two-photon absorption (TPA) is one of the important nonlinear optical phenomena which helps us in obtaining details about the excited states of molecules which are unobservable in one photon absorption (OPA) process. In this process a molecule absorbs two photons instantaneously and achieves an excited state that corresponds to the sum of the energy of the incident photons. There need not be an intermediate state for the atom to reach before arriving at the final excited state (as if it were moving up two stair steps by stepping one at a time). Thus through two-photon absorption one can populate high energy levels that are otherwise unreachable by single photon transitions from the ground state.

Kaiser and Garrett in 1961 [2] first observed TPA from Eu^{2+} by monitoring fluorescence emission resulting from radiative relaxations by excited state

molecules. An important step in this regard made by Cagnac et al [3] in 1973 showed that TP excitations can be induced by relatively low power but narrow line lasers. Numerous investigations of TPA in various samples using fluorescence measurement method have been published [4-8]. Recently Brich (2001) published an excellent review on multiphoton excited fluorescence spectroscopy of bimolecular systems [9]. However, this method cannot be applied for molecules, which are nonfluorescent or those with low fluorescence quantum yield. Studies using the observation of direct optical absorption by molecules [10, 11] are also not a viable method since the magnitude of TPA cross-section is very small as compared to that in one photon absorption (OPA). Recent advances in synthesis and design of TPA materials and the advent of pulsed high power lasers have motivated a great deal of research into new technologies based on TPA induced processes [12-19]. Johnson and coworkers studied TP spectrum of substituted benzene using multiphoton ionization [20-25]. Recently Fisher and Tran reported the two photon induced fluorescence of dyes using cw TL technique with IR radiation from Ti: sapphire laser [26]. But there is serious drawback that all most all the solvents for the laser dyes have absorption in the near IR region.

Measurements using thermo-optic effect is an alternate method to identify multiphoton phenomena in nonlinear media where nonradiative de-excitation is monitored. Of the various thermo optic phenomena, optoacoustic spectroscopy and thermal lens spectroscopy are the two widely employed tools to detect very weak absorption processes [27-31].TL effect is reported to be advantageous for investigating multiphoton absorption processes in liquids since (1) this method is very accurate in measuring weak absorption in solution (2) analysis can be done for light scattering liquids also. TL method to study TP absorption was first used by Twarowoski and Kliger to record the TL spectrum of benzene [32. 33]. Thermal lens effect has also been used to detect TPA in laser dyes by monitoring TL signal at a fixed pump beam

wavelength [34, 37]. In certain cases, TP spectra were recorded using tunable dye lasers but each dye has only a narrow tuning range of about 5 to 20 nm in the visible part of the spectrum. [38-42].

Vibrational overtone spectrum of molecules involving X- H stretching vibrations (X=N, O, Cl etc) is now a well-established tool for information regarding molecular structure, dynamics and higher vibrational states in polyatomic molecules. Several investigations of the overtone spectra of the N-H stretching in aniline using fluorescence measurement method have been reported in the literature [43-46]. Ellis [47] performed some of the earlier work in liquid benzene by photographing the absorption spectrum. Later Martin and Kalanter [48], Hentry and Siderband [49], and Hayward and Hentry [50] have investigated the overtone spectra of substituted benzene by conventional spectroscopic technique. However this technique failed to investigate the overtone spectrum of the higher order harmonics. A higher vibronic transition has been reported in gaeous benzene by Bray and Berry [27] and in solids by Perry and Zewell [51]. Burberry and co workers using the technique of TL have identified overtones in liquid benzene and aromatic liquids [52, 53]. Rasheed et al [54] recorded fifth CH overtone of some organic molecules using thermal lens method. This chapter describes the use of TL effect to record the TP induced thermal lens spectra of aniline using tunable radiation from Optical Parametric Oscillator (OPO) as the excitation source. Optical parametric devices provide wide and continuous wavelength coverage, easy and rapid wavelength tunability, high-energy output and the advantage of being all solid -state. The sensitivity of TL technique is suitable to investigate TP induced overtone spectra of substituted benzene like aniline, toluene etc.

5.1.2 Materials

Among the benzene derivatives, the simplest amine, the aniline molecule has received particular attention because its spectroscopy is well known. Organic compounds with simple or conjugated unsaturated groups like aniline ($C_6H_5NH_2$) show characteristic bands in the UV spectrum. NH2 group is planar with the benzene ring [55]. Electronic transitions in aniline are often affected by the change in the intermolecular hydrogen bonding in suitable solvents or at low temperature. Hydrogen bonding enhances internal conversion. It has been noted that interaction between lone pair electron of nitrogen atom in NH2 group with ring π-electrons imparts $n\pi^*$ character to excited electronic states and nonradiative processes like intersystem crossing are influenced by such interaction.

5.1.3 Theory- Two photon absorption-Local mode model

The process of TPA is similar to ordinary single photon absorption but the selection rule is different [56]. To an electric–dipole approximation, two photon transitions are allowed between states of same parity whereas single photon transitions are allowed between states of different parity
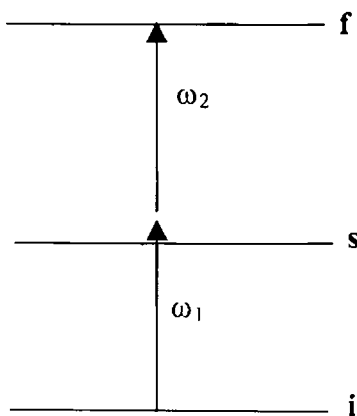

Figure 5.1 TP excitation of a system from i to f via virtual intermediate state s.

Various theories based on perturbation theory as well as tensor theory have been made for the TPA studies [56-61]. The transition probability of two photon process was first derived by Goppert-Mayer [1] using second order perturbation theory. The two photon propagating in a nonlinear absorbing medium have the attenuation governed by the equation [61]

$$\frac{dI_1}{dz} = -\omega_1 \gamma I_1 I_2 \qquad\qquad (5.1)$$

$$\frac{dI_2}{dz} = -\omega_2 \gamma I_1 I \qquad\qquad (5.2)$$

where two photon absorption coefficient γ and I_1 and I_2 are the beam intensities at ω_1 and ω_2 respectively.

The usefulness of the local mode (LM) model in describing the higher overtone hydrogen based vibrational stretching states of benzene and several other polyatomic molecules has been recognized by many workers [51-54, 62-65]. Progressions in the ground electronic state of overtones involving stretching motion of bonds containing hydrogen are seen to follow closely the one dimensional Birge-Sponer eqn for an anharmonic oscillator [66]. The transition energies for the prominent peaks in the overtone absorption spectra of molecules which contain X-H bonds are given as [51-53]

$$\Delta E_{0 \rightarrow v} = v(A - Bv) \qquad\qquad (5.3)$$

where $\Delta E_{0 \rightarrow v}$ is the observed energy difference between the ground state and v^{th} quantum level. A-B = X_1 is the mechanical frequency and B = X_2 is the anharmonicity of the X-H bond.

5.1.4 n − photon induced TL effect

Thermal lens is formed by the deposition of heat via a nonradiative decay process after laser energy has been absorbed by the sample and the focal length of the lens formed is given as [32,33]

$$\frac{1}{f} = \frac{1}{f_0}\left(1 + \frac{2nt}{t_c}\right)^{-2} \tag{5.4}$$

$$\frac{1}{f_0} = \frac{4lDN\sigma h \nu n^2 H}{kJ\omega^{2n+2}}\left(\frac{dn}{dT}\right)\left(\frac{2}{\pi}\right) \tag{5.5}$$

$$t_c = \frac{\omega^2}{4D}, \tag{5.6}$$

$$D = \frac{k}{\rho C_p}, \tag{5.7}$$

$$H = \int_0^t p(t)dt \tag{5.8}$$

where f is the time-dependent focal length of the thermal lens, f_0 is the focal length just after heating pulse, t_c is the characteristic time constant of decay, l is the sample length, D is the thermal diffusivity, N is the number of molecules, σ is the cross-section of absorption, ν is the frequency of the heating laser, h is the Planck's constant, n is the number of photons, H is the total output energy of the laser, k is the thermal conductivity, J is the Joule's constant, ω is the beam radius, ρ is the density, C_p is the specific heat and $P(t)$ is the intensity of the heating laser. The probe beam interacting with the TL will be affected and the TL signal is usually measured as the relative change in the intensity at the probe beam center and is given as [34]

$$\eta = \frac{I_{t=0} - I_{t=\infty}}{I_{t=0}} \qquad (5.9)$$

$$= S_p = S_{(t=0)}\left(1 + 2t/t_c\right)^{-2} \qquad (5.10)$$

where

$$S_{(t=0)} = \frac{5\ln(10)AE_0}{\omega^2\lambda\rho C_p}\frac{dn}{dT} \qquad (5.11)$$

For n photon process [32,33]

$$\eta = E^n \qquad (5.12)$$

where E is the energy of the incident photon n is the number of photons involved in the absorption process. A plot of log η vs log E will give n as its slope.

5.1.5 Thermal lens Spectrum of Aniline

5.1.5.1 Experimental

Experimental setup used for the recording of thermal lens spectrum of organic compounds like aniline and dyes are described elsewhere [67]. The pump beam used for the present study is the radiation from an Optical Parametric Oscillator with tunable output in the range 450-650 nm. Freshly distilled aniline (Merck) in a quartz cuvette (1 mm) is kept one confocal length past the beam waist. The TL signal output is processed using a digital storage oscilloscope. The present work is done at a temperature of 26 $^\circ$ C. The thermal lens spectra are normalized to account for the spectral profile of the OPO output. The absorption spectrum of the sample is recorded using a UV-VIS-IR spectrophotometer.

5.1.5.2 Results and discussion

The present studies deals with the two photon absorption process in liquid aniline using pulsed TL technique. Absorption spectrum of aniline in the UV-VIS region recorded using a UV-VIS-IR spectrophotometer is given in figure 5.2. The spectrum does not have any peak in the visible region indicating absence of any resonant OPA. Two prominent peaks in the UV region at 220 nm and 290 nm correspond to $S_0 \rightarrow S_2$ and $S_0 \rightarrow S_1$ related to $^1A_1 \rightarrow {}^1B_2$ and $^1A_1 \rightarrow {}^1B_1$ transitions respectively.

The TL spectrum of aniline is given in figure 5.3 which shows a sharp peak around 470 nm and prominent shoulder around 490 nm. In order to confirm the number of photons involved per absorption, log- log plot of TL signal strength to the pump laser power is made (figure 5.4).
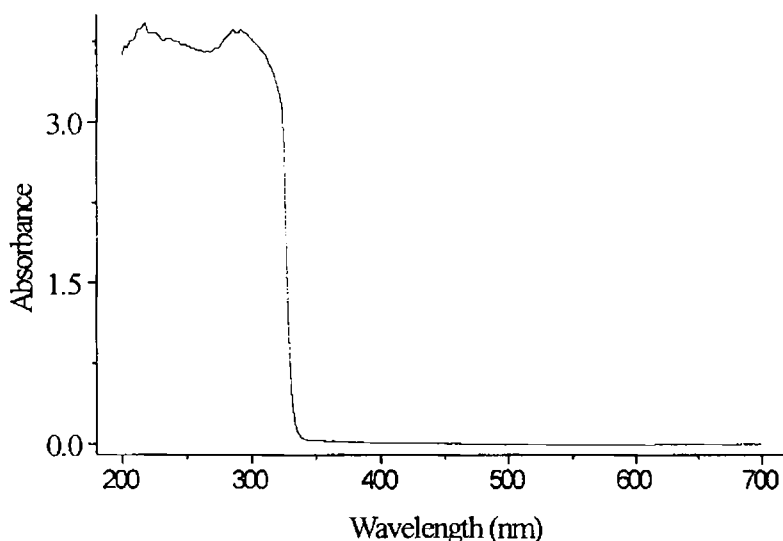

Figure 5.2. The absorption spectrum of aniline.

Log-log plot of TL signal, η vs E gives a slope n corresponding to the number of photons taking part in the multiphoton processes. At low pump power the

slope of log-log plot is around 1 while at higher laser power the slope is around 2. This means that at lower pump beam power, the phenomenon involved is OPA. However, spectrophotometric record shows absence of any such OPA processes. Hence only phenomemon responsible for OPA is overtone excitation.

Using data (Table 1) from a recent study of overtone absorption of aniline [68] it can be found that sixth and seventh overtones of ring CH stretching ($\Delta v = 7,8$) lie at 531 and 475 nm while $\Delta v = 7$ and $\Delta v = 8$ bands due to NH oscillator lie at 488 and 438nm. These overtone absorptions overlap with the wavelength region of TL spectrum recorded in the present experiment. Thus at lower laser power, overtone excitations corresponding to CH and NH oscillators lead to the TL spectrum in the 460-500 nm region.
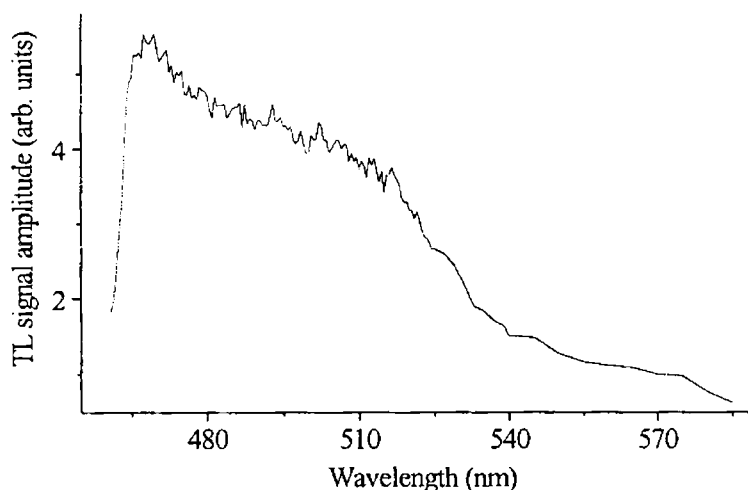

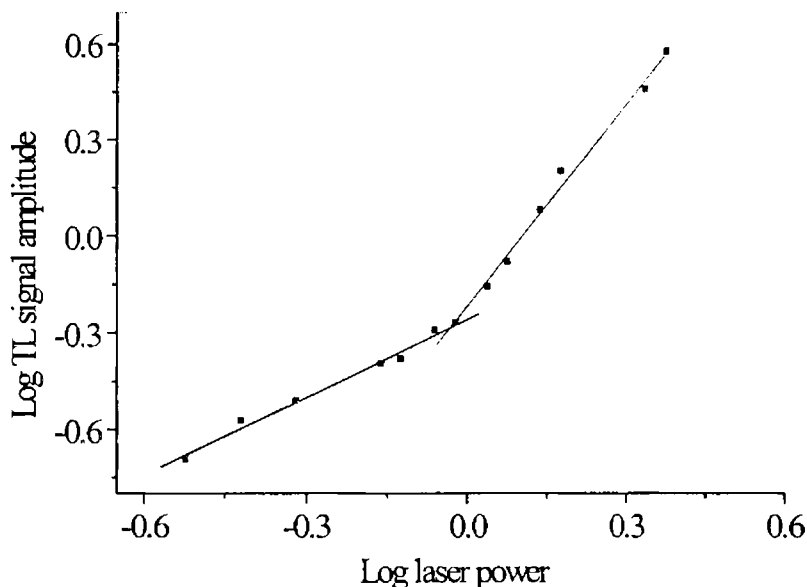*Figure 5.3. Thermal lens spectrum of aniline*

Figure 5.4 Log-log plot of thermal lens signal amplitude against laser power

At higher pump intensity, slope of log-log plot in figure 5.4 is around 2 indicating the existence of two photon absorption. The TL spectrum shows a sharp peak around 470 nm and prominent shoulder around 490 nm. As mentioned before, the absorption spectrum of aniline in the UV region (figure 5.2) shows two peaks at 200 - 250 nm and 250 - 350 nm regions matching to $S_0 \rightarrow S_2$ and $S_0 \rightarrow S_1$ transitions. TP absorptions corresponding to these transitions will be observed at 400-500 and 500-700 nm regions. Of these we get TL spectrum only in the 400-500 nm region equivalent to TPA corresponding to $S_0 \rightarrow S_2$ transitions. This means that transition $S_0 \rightarrow S_2$ corresponding to $^1A_1 \rightarrow {}^1B_2$ is TPA allowed while $^1A_1 \rightarrow {}^1B_1$ is not. This imply that $^1A_1$ and $^1B_1$ are of opposite symmetries and hence only OPA will be observed matching to $^1A_1 \rightarrow {}^1B_2$ transition. The fact that we get OP and TP absorptions corresponding to $^1A_1 \rightarrow {}^1B_1$ transition implies that $^1B_2$ will

also acquire certain symmetry characteristics of ^1A state through vibronic coupling [69-72].Results obtained are presented in the figure 5.5.

Table1. Local mode parameters and transition energies of the C-H and N-H oscillators in aniline [68]

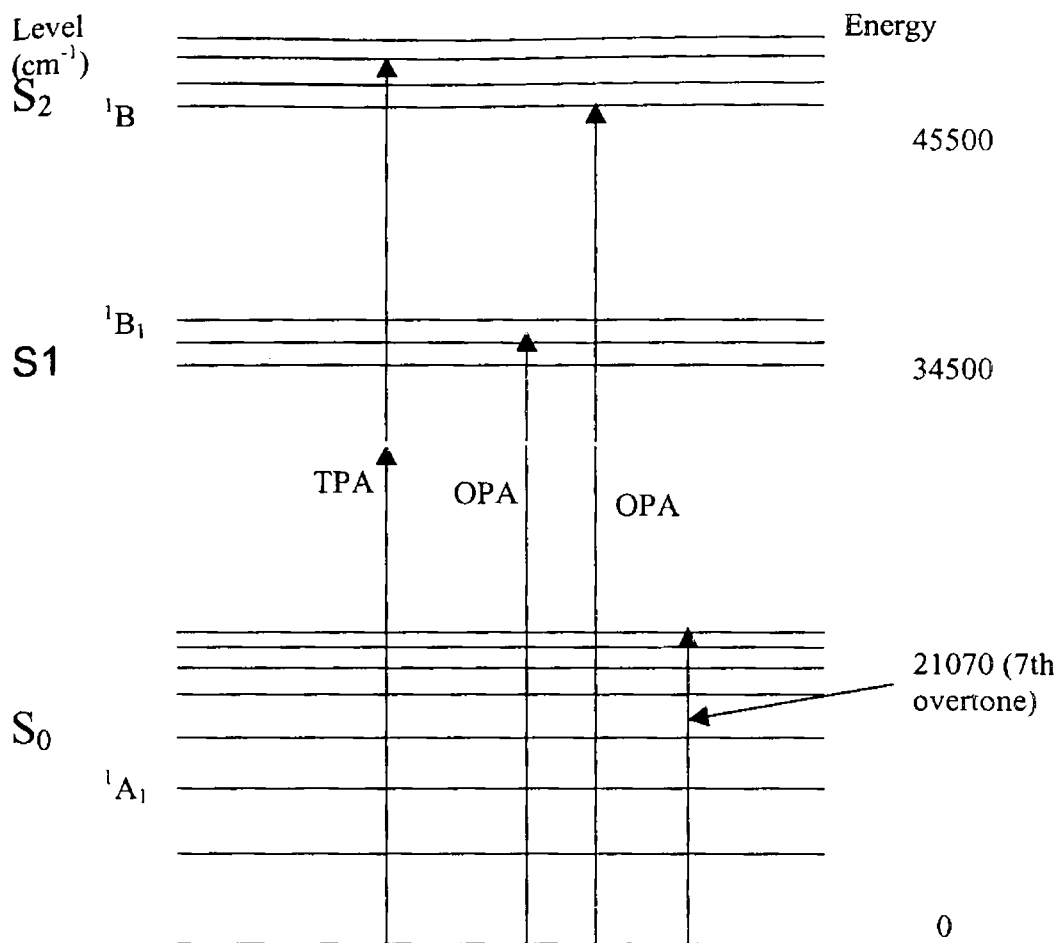| Local mode parameters	
C-H overtone	N-H overtones
(cm^{-1})	(cm^{-1})
$X_1 = 3136.33$	$X_1 = 3549.56$
$X_2 = -55.83$	$X_2 = -77.16$
(nm)	(nm)
$\Delta E_{0\rightarrow 6} = 607.1$	$\Delta E_{0\rightarrow 6} = 553.9$
$\Delta E_{0\rightarrow 7} = 531.1$	$\Delta E_{0\rightarrow 7} = 487.7$
$\Delta E_{0\rightarrow 8} = 474.6$	$\Delta E_{0\rightarrow 8} = 437.8$

Figure 5.5 Schematic energy level diagram showing relevant two photon and one photon absorptions (TPA, OPA) along with the overtone absorption in the case of Aniline. The level S_2 acquires the symmetry character of S_0 by vibronic coupling so that both OP and TP absorptions are possible.

5.2 Thermal lens spectrum of organic dyes using Optical Parametric Oscillator

5.2.1 Introduction

Eversince the discovery of photothermal lensing effect by Gordan et al [73] this technique of monitoring nonradiative relaxation in excited molecule has been refined by various researchers to suite for the study of various phenomena related to light-matter interactions [73-82]. Most important modification of the thermal lens technique is the dual beam method developed by Long et al [83] so that one can record the thermal lens spectrum of samples. Detection of thermal lens signal has been improved later on by incorporating optical fibre so as to introduce flexibility in the experimental configuration [84].

In this section we have studied the changes in the TL signal which results from the wavelength-dependent heating of the sample by absorption of the pump beam. A plot of these intensity changes therefore provides a characteristic signature of the absorption mechanism of the samples. Most of the studies reported earlier used tunable dye lasers as the pump beam. As mentioned before one of the drawbacks of dye lasers is the limited range of tunability. Recently Kawasaki et al recorded TL spectrum of NO_2 using OPO [85]. The present investigation describes the use of TL effect to record absorption spectrum of organic dyes in methanol using Optical Parametric Oscillator as the excitation source.

5.2.2 Materials and methods

Rhodamine B

Rhodamine B (RB) is a xanthene dye containing a carboxylic and quaternary ammonium group. RB is well known for their high fluorescence quantum

yields. This dye has been used in different solvents as an active medium for tunable lasers. Therefore, the optical properties of RB in solution have attracted great attention. Molecular structure and environmental effects such as nature of solvent, pH, temperature etc control the photophysical properties of organic dyes in solution [86-105]. This compound exists in a number of neutral and ionic forms [85]. Figure 5.6 shows the structure of RB.
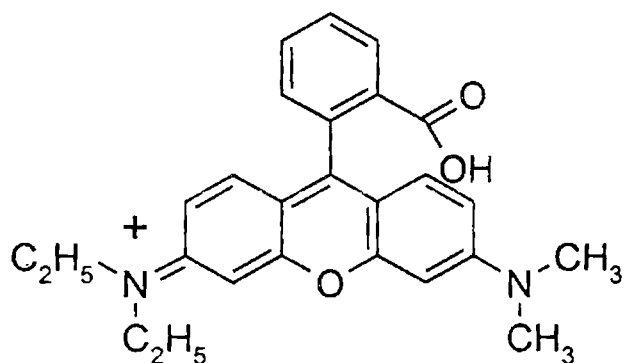
Figure 5.6 Structure of rhodamine B

The experimental setup is same as that used to record the TL spectrum of aniline. The absorption spectra of the sample having different concentration are recorded using a UV-VIS-IR spectrophotometer. Fluorescence spectra are recorded as described in chapter 2 section 2.5.3.

An accurately weighed amount of Rhodamine B is dissolved in methanol to give a concentration of 1.87 milli mol l^{-1}. From this stock solution, sample solutions with different concentrations ranging from 2.68 micro mol l^{-1} to 460 micro mol l^{-1} are prepared. Investigations were carried out in crystal violet dye also.

5.2.3 Results and discussion

The absorption, TL and fluorescence spectra of Rhodamine B in methanol at a concentration of 2.68 micromol l^{-1} are given in figure 5.7. Absorption spectrum shows the peak absorption at 18315 cm^{-1} and a shoulder at 19380 cm^{-1} which reveals two prominent vibronic levels at 546 nm (18315 cm^{-1}) and 516 nm (19380 cm^{-1}) with intensity variation as determined by Franck Condon principle. As is clear from the figure, TL spectral peak and absorption peak do not coincide. The fact that these peaks do not coincide reveals the unequal magnitudes of radiative and nonradiative transition probabilities from the excited vibronic levels.
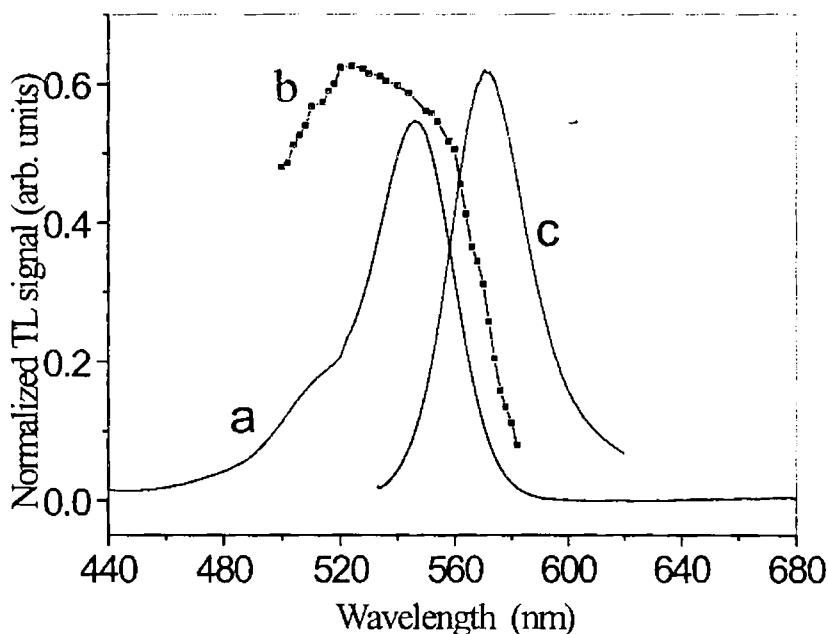

Figure 5.7 Spectra of Rhodamine B for a concentration of 2.68 micro mol l^{-1} in methanol (a) absorption spectrum (b) thermal lens spectrum (c) fluorescence spectrum.

Excitation to 19380 cm^{-1} level is followed by nonradiative de-excitations to a large number of low-lying vibronic levels. One can conclude that probability of nonradiative de-excitations from 19380 cm^{-1} is more than that from $18315 cm^{-1}$ level so as to get the TL spectral peak at 19380 cm^{-1}. This conclusion is also supported by the fact that fluorescence emission (and hence radiative relaxation cross-section) from this level is almost zero, as one would expect from the complementary nature of nonradiative and radiative relaxation processes. The fluorescence peak at longer wavelength accounts for the Stokes shift [90, 91]. Figure 5.8 shows the spectra of Rhodamine B in methanol at a concentration of 460 micro mol l^{-1}. As is evidently observed from the figure, at higher concentration there is a relative enhancement in the TL signal as compared to that in the fluorescence spectrum.
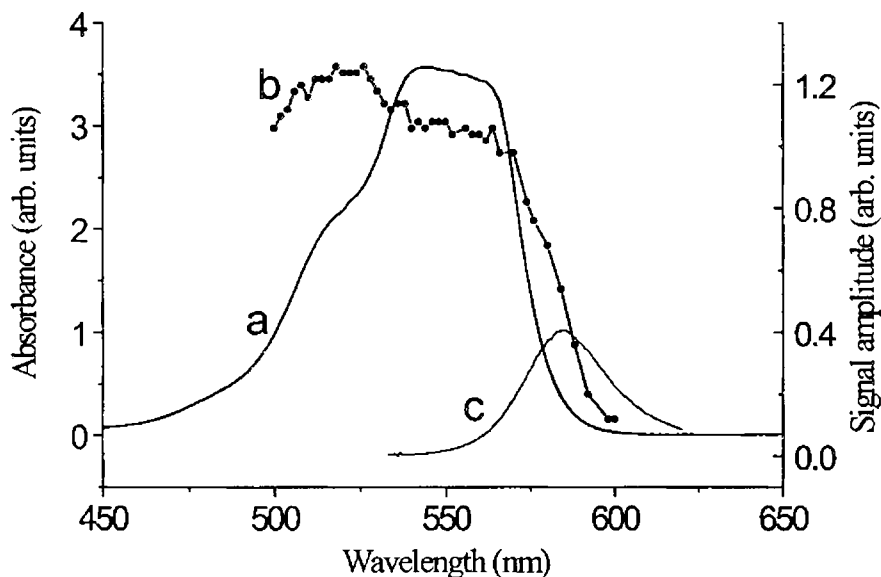
Figure 5.8 Spectra of Rhodamine B for a concentration of 460 micro mol l^{-1} in methanol (a) absorption spectrum (b) thermal lens spectrum (c) fluorescence spectrum.

Red shift in the fluorescence spectral peak at higher concentration is also observed in the figure. With increasing dye concentration the possibility of transfer of energy between molecules by collisional mechanism makes the nonradiative part to become more prominent. Hence it is obvious that fluorescence quantum yield decreases as the concentration increases [35]. Increased nonradiative de-excitation processes are revealed by the relative enhancement in the TL spectrum. Enhancement in nonradiative processes with increase in concentration will also take place due to reabsorption of fluorescence emission, thereby causing the red shift in the fluorescence peak (figure 5.9). Concentration dependence of TL signal (figure 5.10) from rhodamine B at various pump wavelengths also revealed same intensity results.
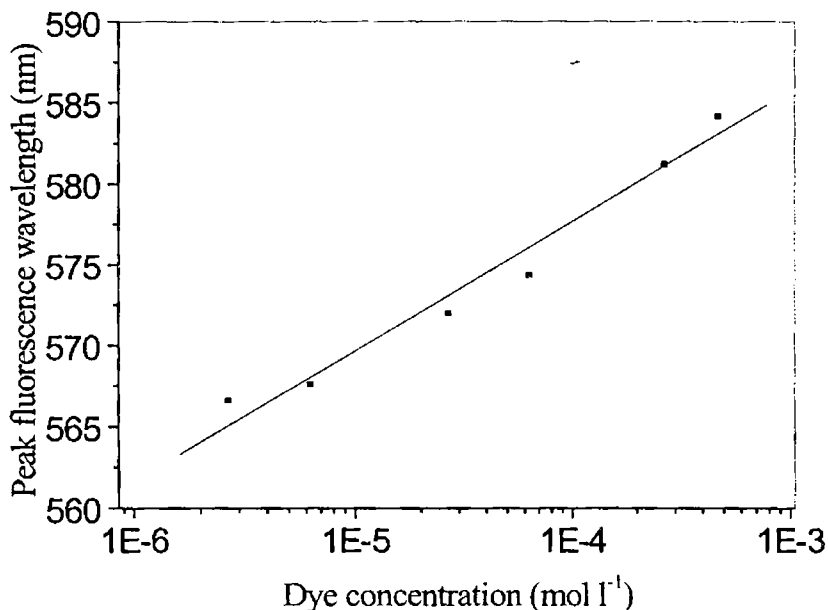
Figure 5.9 Concentration dependence of peak fluorescence wavelength of Rhodamine B.

In solutions of low concentration, dyes dissolve practically completely into monomers. It should be mentioned that basic dyes like Rhodamine B may dissociate at high dilutions into cations and anions [85]. The absorption spectra are determined by the intrinsic absorption of the dye molecules and the dye – solvent interaction. At this concentration dye-dye interaction is negligible because of the large average distance between them. The absorption spectra (figure 5.8) contain contributions from the monomers and the aggregates, which makes the spectrum broader at higher concentration. For highly soluble dye like rhodamine B the solute - solute interaction becomes prominent at high concentrations since the mean distance between them becomes small [35].

Figure 5.10 Variation of TL signal amplitude with concentration for different pump wavelengths in nm (■) 520 (●) 540 (▲) 560 (□) 570 (+) 574 and (▼)580.

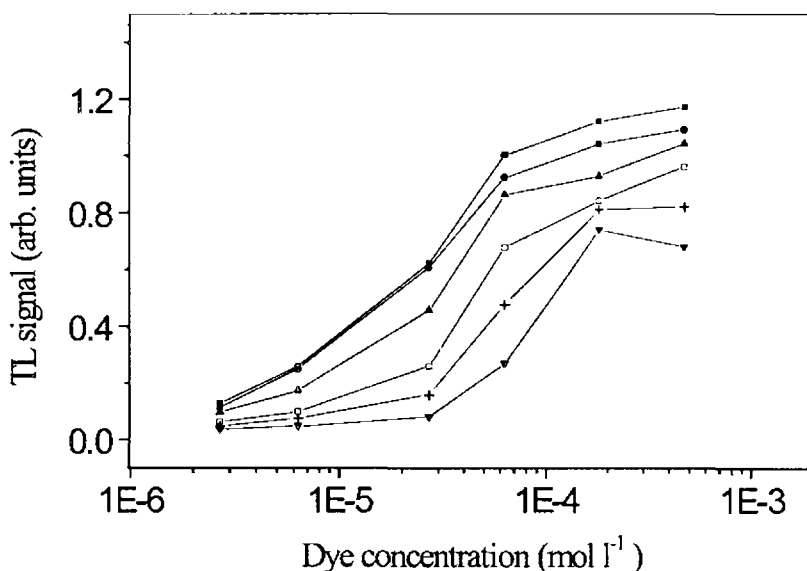On increasing the concentration of dye solution, the aggregate formation and reabsorption of fluorescence emission will result into the enhancement in absorption and nonradiative relaxations at higher wavelengths. This will enhance the TL signal.

5.3 Thermal lens spectrum of Crystal Violet (CV)

Crystal violet dye is derived from triphenylmethane are usually salts with OH or NH_2 in the pra positions with respect to the methane carbon. This dye is fairly reactive and can be easily converted to the free base on treatment with alkali or reduced to leuco form in a variety of ways. This dye is blue-violet in colour and broad absorption around 590 nm. The structure of the dye is shown in figure 5.11. This dye has many interesting features, which depends on its structure such as (1) the influence of concentration on the spectra and (2) the effect of interaction with a substrate and photochemistry. The absorption spectra of dilute aqueous solutions of CV (10^{-7} M) consists of a single absorption maximum around 594 nm (α band).
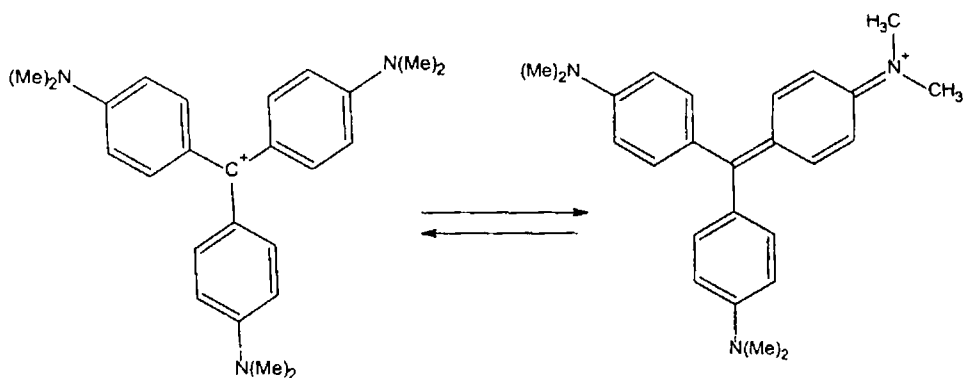
Figure 5.11 Structure of Crystal violet.
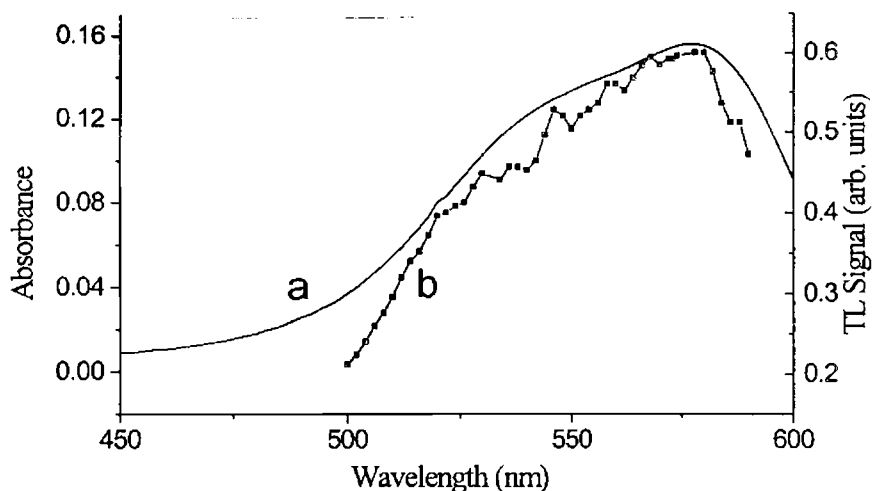
Figure 5.12 Absorption (a) and thermal lens (b) spectra of crystal violet for a concentration of 65 micro mol l^{-1}.

Figure 5.12 shows the absorption and TL spectrum of crystal violet dye. In contrast to the TLS of rhodamine B dye, absorption and the TL spectra of CV have the same profile and their peak coincides. This indicates that unlike in the case of rhodamine B, there are no intermediate vibronic levels from which nonradiative de-excitation becomes prominent. CV has very low fluorescence quantum efficiency so that the nonradiative relaxation is the major channel by which molecules relax to the ground state.

5.4 Conclusion

We have demonstrated the efficiency and usefulness of pulsed TL technique to study the multiphoton process in nonfluorescent materials. TL spectrum of aniline has been recorded in the 460-500 nm region using radiation from an OPO as the excitation beam. The C-H and N-H stretching overtones of aniline are investigated using this technique. Results show that $^1B_2$ acquires same

symmetry characteristics of $^1A_1$ through vibronic coupling. The nature of variation of TL signal amplitude with laser power clearly confirms the occurrence of two photon absorption in aniline. One of the important features of TL-based investigations is its effectiveness to study weak optical absorption arising due to weak phenomena like overtone absorption, singlet - triplet absorption, multiphoton absorption etc.

Our studies using optical parametric oscillator on organic dyes show that the simultaneous analysis of TL, absorption and fluorescence spectra will be helpful to understand relative magnitudes of nonradiative and radiative de-excitation probabilities from the excited states. TL signals from higher wavelength region (560-590 nm) get enhanced at higher concentration. This is due to increased nonradiative de-excitation probability on increasing the concentration.

References

1. M. Goppert-Mayer, *Ann. Phys.* 9,273, (1931).
2. W. Kaiser and G. B. Garrett, *Phys. Rev. lett.* 7,229 (1961).
3. B. Cagnac, G. Grynberg and F. biraben, *J. Phys.* 36,845 (1973).
4. S. Webman and J. Jortner, *J. Chem. Phys.* 50,2706 (1969).
5. R. M. Hochstrasser, H. N. Sung and J. E. Wessel, *J. Am. Chem. Soc.* 95:24, 8179 (1973).
6. T. W. Scott and A. C. Albrecht, *J. Chem. Phys.*74, 3807 (1981).
7. T. W. Scott, K. S. Haber and A. C. Albrecht, *J. Chem. Phys.*78, 150 (1983).
8. N. Mukherjee, A. Mukherjee and B. A. Reinnardt, *Appl. Phys. Lett.* 70, 1524 (1997).
9. D. J. S. Brich, *Spectrochim. Acta A* 57, 2313 (2001).
10. W. R. A. Greenlay and B. R. Henry, *J. Chem. Phys.* 69, 82 (1978).
11. M. J. Writh, A. C. Koskelo, C.E. Mohie and B. L. Sentz, *Anal. Chem.* 53, 2045 (1981).
12. P. K. Chowdhury, K. Sugawara, T. Nakanaga and H. Takeo, *J. Mol. Str.* 447, 7 (1998).
13. S. G. He, J. D. Bhawalker, C. Zhao and P.N. Prasad, *IEEE J. Quantum Electron,* 32,749 (1996).
14. R. P. Schmid, P. K. Chowdhury, J. Miyawaki, F. Ito, K. Sugawqrq, T. Nakanga, H. Takeo and H. Jones, *Chem. Phys.* 218, 291 (1997).
15. T. Nakanga and F. Ito, *Chem. Phys. Lett.* 348, 270 (2001).
16. T. Nakanga, K. Sugawqrq, K. Kawamata and F. Ito, *Chem. Phys. Lett.*267, 491 (1997).
17. T. Nakanga, F. lto, J. Miyawaki, K. Sugawara and H. Takeo, *Chem. Phys. Lett.*25, 414 (1996).

18. A. M. Bonch-Bruevich, T. K. Razumova and I. O. Starobogatov, *Opt. Spectrosco.* 42, 45 (1977).
19. G. S. He, K. Kim, L. Yuan, N.C Cheng and P. N. Prasad, *Appl. Phys. Lett.* 71, 1619 (1997).
20. P. M. Johnson, *Acc. Chem. Res.* 13, 20 (1980).
21. N. Mikami and M. Ito, *Chem. Phys. Lett.* 31, 472 (1975).
22. J. Murakami, K. Kaya and M. Ito, *J. Chem. Phys.* 72, 3263 (1980).
23. R. P. Rava, L. Goodman and K. Krogh-Jespersen, *J. Chem. Phys.* 74, 273 (1981).

24. L. Goodman and R. P. Rava, *J. Chem. Phys.* 74, 4826 (1981).
25. A. Sur, J. Knee and P. Johnson, *J. Chem. Phys.* 77, 654. (1982).
26. M. Fischer and C. D. Tran, *Appl. Opt.* 39, 6258 (2000).
27. R. G. Bray and M. J. Berry, *J. Chem. Phys* 71, 4909 (1979).
28. C. K. N. Patel, A. C. Tam and R. J. Kerl, *J. Chem. Phys.*, 71, 1470 (1979).
29. A.C. Tam and C.K.N. Patel, *Nature*, 280, 304 (1979).
30. A. V. Ravikumar, G. Padmaja, V.P. N. Nampoori and C. P. G. Vallabhan, *Pramana-J. Phys.* 33, L621 (1989).
31. P Sathy, R. Philip, V.P. N. Nampoori and C. P. G. Vallabhan, *J. Phys. D,* 27, 2019 (1994).
32. A. J. Twarowski and D. S. Kliger, *Chem. Phys.* 20, 253 (1977).
33. A. J. Twarowski and D. S. Kliger, *Chem. Phys.* 20, 259 (1977).
34. S. S. Harilal, R. C. Issac, C. V. Bindhu, G. K. Varier, V. P. N. Nampoori and   C. P. G Vallabhan, *Mod. Phys. Lett. B* 9, 871 (1995).

35. C. V. Bindhu, S. S. Harilal, R. C. Issac, G. K. Varier, V. P. N. Nampoori and C. P.G Vallabhan, *Mod. Phys. Lett. B*, 9, 1471 (1995).
36. R. C. Issac, S. S. Harilal, G. K. Varier, C. V. Bindhu, V. P. N. Nampoori and   C. P. G Vallabhan, *Opt. Eng.* 36, 332 (1997).
37. C. V. Bindhu, S. S. Harilal, Achamma Kurian, V P N Nampoori and C P G Vallabhan, *J. Nonlinear Opt. Phys. & Mats.* 7, 531 (1998).

38. D. R. Sibert, F. R. Grabiner and G. W. Flynn, *J. Chem. Phys.* 60, 1564 (1974).
39. R. L. Swofford , M. E. Long and A. C. Albrecht, *J. Chem. Phys.* 65, 179 (1976).

40. R. L. Swofford , M. E. Long, M. S. Burberry and A. C. Albrecht, *J. Chem. Phys.* 66, 664 (1977).

41. H. L. Fang and R. L. Swofford, *J. Chem. Phys.* 72, 6382 (1980).

42. H. L. Fang and R. L. Swofford, *J. Chem. Phys.* 73, 2607 (1980).

43. T. Nakanga, F. Ito, J. Miyawaki, K. Sugawara and H. Takeo, *Chem. Phys. Lett.* 267, 491 (1997).
44. K. Kawamata, P. K. Chowdhary, K. Sugawara and T. Nkanaga, *J. Phys. Chem. A,* 102, 4788 (1998).
45. 45. Ch. Gee, S. Douin, C. Crepin and P. H. Brechignac. *Chem. Phys. Lett.* 338, 130 (2001).
46. K. Ohashi, Y. Inokuchi, H. Izutsu, K. Hino. N. Yamamoto, N. Nishi and H. Sekiya, *Chem. Phys. Lett.* 323, 43 (2000).
47. J. W. Ellis, *Trans. Faraday Soc.* 25, 888 (1929).
48. T. E. Martin and A. H. Kalanter, *J. Chem. Phys.* 49, 235 (1968).
49. B.R. Hentry and W. Siebrand, *J. Chem. Phys.* 49, 5369 (1968).
50. R. J. Hayward and B. R. Henry, *Chem. Phys.* 12, 387 (1976)

51. J. W. Perry and A. H. Zewail, , *J. Chem. Phys.* 79, 582 (1979).
52. M. S. Burberry and A.C. Albrecht, *J. Chem. Phys.* 70,147 (1979).
53. R. L. Swofford, M. S. Burberry, J.A. Morrell and A. C. Albrecht, *J. Chem. Phys.* 66, 5245 (1977).
54. T.M.A Rasheed, V. P. N. Nampoori and K. Sathianandan, *Chem. Phys. 108, 349 (1986).*
55. T. K. Pal, G. K. Mallik, S. Lalla, K. Chatterjee, T. Ganguly and S. B. Banerjee, *Spectrochim. Acta A*, 43, 853 (1987).
56. V. S. Letokhov and V. P. Chebotayev, *Nonlinear Laser Spectroscopy*, Springer-Verlag, New York (1977).
57. B. Honig, J. Jortnaer and A. Szoke, *J. Chem. Phys.* 47,2714 (1967).
58. Wm. M. McClain, *Acc. Chem.. Res.* 7, 129 (1974).
59. Y. Fujimura and S. H. Lin , *J. Chem. Phys.* 74, 3726 (1981).
60. B. Dick and G. Hohineicher, *J. Chem. Phys.* 76, 5755 (1982).
61. Y. R. Shen, *Principles of nonlinear optics*, John Wiley, Singapore (1991).
62. B. R. Henry and W. Siebrand, *J. Chem. Phys.* 49, 5369 (1968).
63. B. R. Henry, *Acc. Chem. Res.* 10, 207 (1977).
64. L. Wunsch, F. Metz, H. J. Neusser and E. W. Schlag, *J. Chem. Phys.* 66, 286 (1977).
65. C. Jaffe and P. Brumer, *J. Chem. Phys.* 73, 5646 (1980).
66. R.T. Birge and H. S. Sponer, *Phys. Rev.* 28,259 (1926).
67. A. Kurian, K.P. Unnikrishnan, P. Gopinath. S. D. George, V. P. N. Nampoori and C. P. G. Vallabhan, *Spectrochimica Acta* (in press).
68. S. Shaji and T. M. A. Rasheed, *Spectrochim. Acta A*, 57,337 (2001).
69. R. L. Fulton and M. Gouterman, *J. Chem. Phys.* 35, 1059 (1961).
70. R. L. Fulton and M. Gouterman, *J. Chem. Phys.* 41, 2280 (1964).
71. I. Abram, A. de Martion and R. Frey, *J. Chem. Phys.* 76, 5727 (1982).
72. L. Goodman and R. V. Rava, *Acc. Chem. Res.* 17, 250 (1984).
73. J. P. Gordon, R.C.C. Lelte, R. S. Moore and S. P. S. Porto, *J. Appl. Phys.* 36, 3 (1965).
74. C. Hue and J. R. Whinnery, *Appl. Opt.* 12, 72 (1973).
75. N. J. Dovichi and J.M. Harris, *Anal. Chem.* 51, 728 (1979).
76. M. L. Lesiecki and J. M. Drake, *Appl. Opt.* 21, 557 (1982).
77. M. Terazima. and T Azumi, *Chem. Phys. Lett.* 141, 237 (1987).
78. R. D. Snook and R. D. Lowe *Analyst* 120, 2051 (1995).
79. J. Georges and J. M. Mermet, *Spectrochimica Acta.* 49 A, 397 (1993).
80. S. E. Bialkowski, *Appl. Opt.* 24, 2792 (1985).
81. M. Franko, *Talanta*, 54,1 (2001).
82. A. Kurian, K. P.Unnikrishnan, Pramod Gopinath, V. P. N. Nampoori and C. P. G. Vallabhan, *J. Nonlinear Opt. Phys. & Mats* 10, 415 (2001).
83. M. E. Long, R. L. Swofford and A. C. Albrecht, *Science*, 191, 183 (1976).
84. B. S. Seidal and W. Faubel, *J. Chromatography* A 817, 223 (1998).
85. S. Kawasaki, R. J. Jane and C. L. Tang, *Appl. Opt.* 33, 993 (1994).
86. R. W. Ramette and E. B. Sandell, *J. Am. Chem.. Soc.* 78, 4872 (1956).
87. K. K. Rohatgi and G. S. Singhal, *J. Phys. Chem.* 70, 1695 (1966).
88. P. Peretti and P. Ranson, *Opt. Commun.* 3, 62, (1971).
89. A. D. Britt and W. B. Moniz, *J. Org. Chem.* 38, 1057 (1973).
90. J. Ferguson and A. W. H. Mau, *Aust. J. Chem.* 26, 1617 (1973).

91. A. Penzkofer, W. Falkenstein and W. Kaiser, *Chem. Phys. Lett.* 44, 82 (1976).

92. V. E. Korobov and A. K. Chibisov, *J. Photochem.* 9, 411 (1978).

93. P. J. Sadkowski and G. R. Fleming, *Chem. Phys. Lett.* 57, 526 (1978).

94. L. L. Arbeloa and P. Ruizojeda, *Chem. Phys. Lett.* 79, 347 (1981).

95. A. D. Obsborne and A. C. Winkworth, *Chem. Phys. Lett.* 85, 513 (1982).

96. M. J. Snare, F. E. Treloar, K. P. Ghiggino and P. J. Thistlethwaite, *J. Photochem.* 18, 335 (1982).

97. M. Vogel and W. Rettig, *Chem. Phys. Lett.* 147, 452 (1988).

98. L. R. Politzer, K. T. Crago, T. Hampton, J. Joseph, J. H. Boyer and M. Shah, *Chem. Phys. Lett.* 159, 258 (1989).

99. T. Chang and W. L. Borst, *J. Chem./ Phys.* 93, 4725 (1990).

100. F. L. Arbeloa,T. L. Arbeloa, I. L. Arbeloa,M. J. T. Estevez, *J. Phys. Chem.* 95, 2203 (1991).

101.F. L. Arbeloa,T. L. Arbeloa, I. L. Arbeloa, A. costela, I. G. Moreno, J. M.

102.Figuera, F. Amat-Guerri and R. sastre, *Appl. Phys.* B, 64, 651 (1997).

103.D. Magde, G. E. Rojas and P. G. Seybold, *Photochem. Photobio.* 70, 737 (1999).

104.D. Magde, R. Wong and P. G. Seybold, *Photochem. Photobio.* 75, 327 (2000).

105.M. Faraggi, P. feretz, I. R.senthal and D. Weinraub, *Chem. Phys. Lett*, 103, 310 (1984).

6

Realization of optical logic gates

using thermal lens effect

This chapter describes how Optical logic gates can be implemented using thermal lensing technique. A dual beam thermal lens method using low power cw lasers in a dye-doped polymer is used as an alternate technique to perform logical functions such as NAND, AND and OR employing appropriate modes of data deduction.

6.1 Introduction

Computers have modernized human life to a great extent. The first practical computer based on vacuum tubes was large in size but small in computing capacity. The invention of transistors in 1947 provided smaller, faster and more efficient circuit elements. The speed of conventional computer is achieved by the development of the Very Large Scale Integration Technology and this has revolutionized the electronics industry and established the 20th century as the computer age. But further miniaturization of lithography introduced several problems such as dielectric breakdown, hot carriers and short channel effects. Since electronic circuits reached this limit, the speed of computers has now become a pressing problem. The rapid growth of internet demands faster speeds and larger bandwidths than electronic circuits can provide. In this situation, optical interconnections and optical integrated circuits provide a way out of these limitations to computational speed and complexity inherent to conventional electronics [1-6].

Optical computing received a great advancement after the invention of lasers in 1960. The characteristics of this light source allowed numerous computations to be realized by optical means. Optical computing represents a very stimulating challenge for optics that is better suited than electronics for highly parallel computing. The fact is that through a large number of small optical processors tied together by a powerful connecting network, optical signals can travel as light rays in free space. Optical computers use photons instead of electrons to perform appropriate functions. Optical interconnections and optical integrated circuits have several advantages over their electronic counterparts. Optical computing has inherent advantages such as massive connectivity, fast

speed and freedom from electromagnetic interference over electronic computers. Optical components do not need insulators because they do not experience cross talk. They are free from electrical short circuits. They have low loss transmission and provide large bandwidth. They are compact, lightweight and inexpensive to manufacture and more facile with stored information than magnetic materials. Another benefit of optical methods over electronic ones for computing is that optical data processing can be done by much easier and less expensive methods. Another advantage results from the fact that photons are uncharged and do not interact with one another as in the case of electrons. Hence, unlike electrical signals, light signals can cross paths without affecting the information that is to be received at their destinations. Information can also be multiplexed, with possibly as many as 1,000 separate channels in a single pulse.

At present most of the photonic devices are based on hybrid technology, which is an amalgam of optical and electronic hardware components [7-11]. In a typical hybrid configuration, the optical system performs its function efficiently and all other decisions and interfacing are done by flexible electronic components. This will limit the capabilities of optical processors. Hence most of R & D activities are concentrated on identifying proper photonic materials and optical signal processing techniques to develop all-optic computing elements [12, 13].

According to their functionality, optical computing systems can be divided into two categories: special purpose analog and general purpose digital systems. Recently, digital optical computing has been emphasized more because of the advances in photonic materials, which make energy- efficient ultra fast digital switching. They are based on nonlinear optical effects and they mimic the existing electronic computers having logic gates and memory elements.

Logic operations are nonlinear and hence nonlinear optics plays a vital role in the realization of a digital optical computer. Availability of coherent optical sources along with the realization of various nonlinear optical phenomena has made it possible to implement optics based computing and memory elements. It is now possible to control a light beam with another using nonlinear optical effects. Usually the method of implementation of binary logic elements uses nonlinear effect, where the nonlinearity consists of a threshold located at some input level [14-17]. This has helped in developing various types of optical logic elements based on optical phase conjugation [18, 19], optical bistability [20-26], optical interference [27], image subtraction [28], shadow casting logic or Spatial light modulators [29], etc.

Logic elements built from a four-wave mixing optical phase conjugator are based on the dependence of the output on three input beams. Pump beams represent two inputs. The probe is the readout beam and its conjugate the output. The conjugate beam is created as a result of the interaction of all three input beams in a nonlinear medium.

Optical bistability characterizes an optical system with two possible output states for a single input. The phenomenon of changes in refractive index due to the variation of the intensity of light, have been used to fabricate optical bistable devices. They are of two types (1) all-optical type and (2) the hybrid type. In the former type of Fabry-Perot resonator bistable device a nonlinear optical material is placed in the cavity and refractive index varies as light intensity varies. When the intensity is increased, constructive interference takes place and the intensity buildup occurs inside the resonator cavity. Even if the intensity falls, the device again approaches the resonance condition and the intensity goes up which is the high transmission state. When the intensity is lowered it does not immediately affect the intensity buildup in the resonator. When the input intensity is lowered

far enough, the intensity in the resonator is not sufficient to maintain constructive interference, and there fore the intensity in the resonator decreases sharply and the system switches back to the low-transmission stable state. Since the nonlinear coefficient is too small, large optical power is required to confirm bistability. In the hybrid type configuration an electro-optic controlled element is inserted in a Fabry-Perot resonator and the transmitted optical power is converted into voltage through the optical detector. This type does not require large optical power. Recently nonlinear guided waves to obtain bistability has developed in which an optical waveguide can be considered as very thin resonant cavity whose thickness is of the order of light wavelength. Such optical devices that utilize intensity-dependent index changes are expected to operate at high bit rates not attainable by electronic elements.

Another way of implementing optical switches is to shift and combine optical interference fringes [30]. In these studies, nonlinear optical materials are utilized to generate necessary phase changes, which in turn induce the shifting operation and interference fringes. Unfortunately efficient nonlinear materials that can respond at low power levels are not presently available.

An alternate approach is the one that does not require nonlinear optical materials or shifting operation of interference fringes, but simply utilizes a well-known photothermal phenomenon called thermal lens (TL) effect, which introduces intensity dependent refractive index [31-33]. In TL effect, thresholding phenomenon [14] is achieved due to the aberration of thermal lens. Above a certain threshold laser intensity, refractive index gradient in the medium becomes so large that thermal lens is created and the probe beam through the lens gets diverged to form a bottle like shape [34] with a central dark region surrounded by bright regions as shown in the figure 6.1. The central rays are deflected more

than the peripheral rays. From the figure it is clear that the appearance of dark central part depends both on the pump power as well as the position of detector along the beam axis. In the present experiment, the position of detector is fixed so that the variable parameter is the pump power. Such modifications of the probe beam shape can be used to implement optical logic gates due to the existence of threshold like phenomenon. Changes in the optical intensity at the center of the probe beam at far field due to thermal lens effect can be used as the thermal lens signal. The exact level of the threshold determines which Boolean function appears at the output. One can modify the scheme of data detection to realize various types of logic gates. [35].
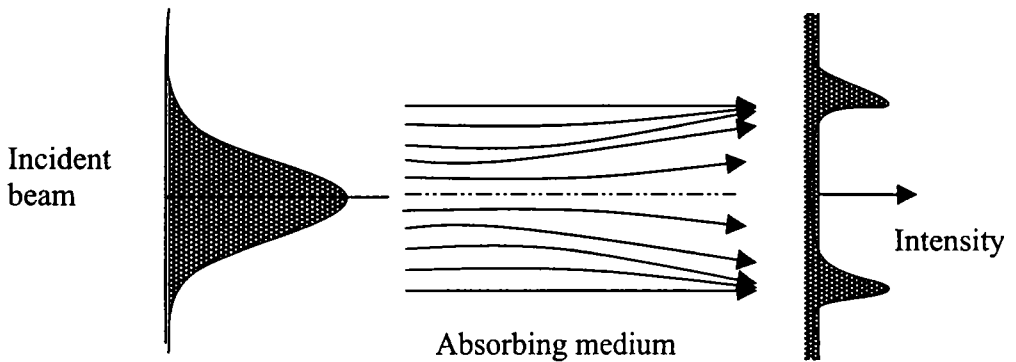

Figure 6.1 The ray diagram representing the distortion of beam cross-section due to thermal lens effect

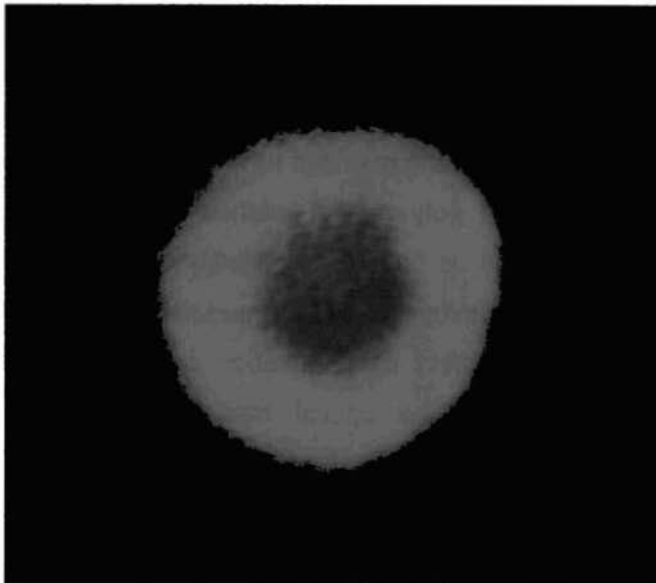Figure 6.2 Cross section of the probe beam showing TL for $I < I_{thresh}$

Figure 6.3 Cross section of the probe beam undergoing thermal blooming
for $I > I_{thresh}$

6.2 Materials

6.2.1 Polymers

Organic materials can perform functions such as switching, signal processing and frequency doubling using less power than inorganic materials. Polymers are familiar materials found throughout everyday life. Polymer molecules consist of many repeat units and the enormous range of possible repeat units give an almost unlimited variety of polymeric materials. This gives great diversity and applications of polymers, ranging from compact disks to car tyres. Biological polymers such as DNA, proteins and cellulose form the basis of life itself. Some other polymers show conducting or semiconducting electrical properties thus providing the basis for a new approach to electronics [35, 36]. One of the key reasons for the wide spread use of man-made polymers is the ease with which they can be processed into any desired shape or form. A further advantage of polymers is that modifying their chemical structure can control their properties. A number of solid organic polymeric matrices have been described in literature [37, 38]. Of these, the use of poly methyl methacrylate (PMMA) host presents additional advantages such as better compatibility with organic laser dyes and inexpensive fabrication techniques. These characteristics when combined with their lightweight would facilitate miniaturization and the design of integrated optical systems [23,39-42]. The optical medium selected for the present investigation is chemically stabilized Rhodamine 6G doped PMMA, due to its best optical transparency and resistance to laser damage [43-45]. Details of the method of preparation of the material are given elsewhere [46].

6.3 Experimental

The experimental setup for dual beam thermal lens method for realizing logic gates is shown in figure 6.4. Laser radiation at 532 nm wavelength from a Diode Pumped Nd: YVO_4 laser (Uniphase BWT-50) is split into two beams I_1 and I_2. These pump beams are later spatially overlapped in the medium and modulated using a chopper to generate thermal lens effect. The excitation beam was focused using a 400 mm focal length lens.

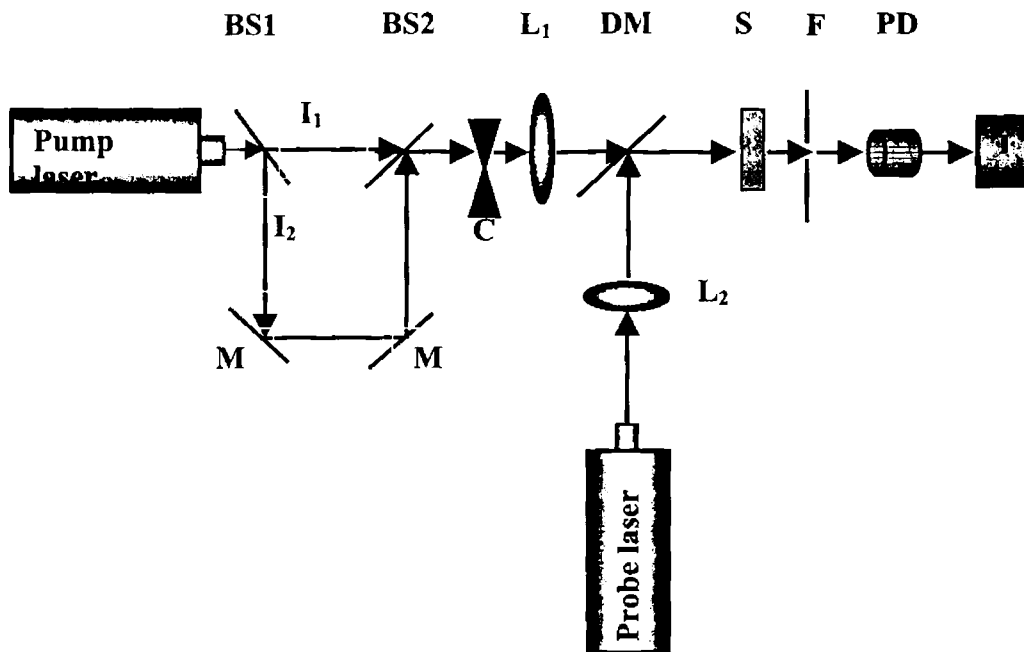*Figure 6.4 Schematic diagram of the experimental set up for realizing logic gates.*
BS1, BS2- *Beam Splitters,* **C** – *Chopper,* **L_1, L_2** – *Lens,* **DM** - *Dichroic Mirror,* **S** - *Sample,* **F**- *Filter,* **PD**-*Photodiode,* **D**-*Detector.*

A low power (1 mW) intensity stabilized He-Ne laser source of wavelength 632.8 nm is used as the probe beam which was focused by a 200mm focal length lens. Sample in the form of a disc (thickness 3 mm and 1 cm diameter), is kept in the path of the pump beam. The probe beam is made to pass collinearly through the sample using a dichroic mirror.

A filter is placed in the path of the emergent beams, which allows only the 632.8 nm wavelength to reach the photodiode. The signal is measured using a power meter (Liconix 55PM)

6.4 Results and discussion

For the realization of digital optical computing, the very basic building block is an optical gate capable of performing universal logic functions such as NAND, AND and OR gate.
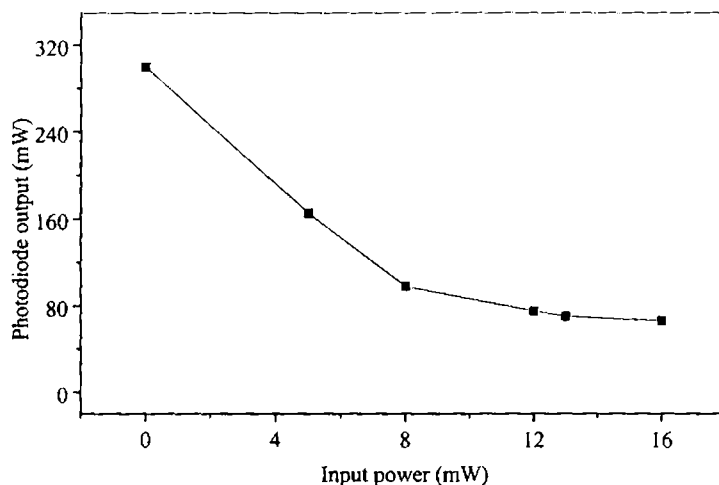

Figure 6.5 Power dependence of TL effect (sample concentration: 4 x 10^{-3} mol l^{-1})

All other functional devices can be built by employing different combinations of such basic gates. A simple implementation of these optical logic gates is achieved using nonlinear effect (TL effect), where the nonlinearity consists of a threshold located at some input level. The threshold like behavior of aberrated thermal lens effect monitored by the photodiode output is shown in the figure 6.5.

6.4.1 NANDgate

In the experiment to realize NAND gate, when the both pump beams (I_1 and I_2) are absent, the output corresponds to the intensity of probe beam itself. This is detected by the photodiode and is represented by the first condition in Table 1.

Table 1. NAND gate

(monitoring the photodiode output; I_1, $I_2 < I_s$, $I_1 + I_2 > I_s$,)

I_1 (input)	I_2 (input)	Photodiode output
0	0	1
0	1	1
1	0	1
1	1	0

If the input of either beam is below the threshold, there is a high output (second and third conditions of Table 1). If both inputs are present and the input is above threshold, thermal blooming is so strong that aberration of thermal lens takes place. In this condition, the output of photodetector is low, which is taken as zero. The input-output relations of the TL experiment, using the photodetector output as the signal, satisfy NAND gate type relation as shown in Table 1. Similar experimental setup using pthalocyanine film is described in a work done by NASA in 2000 [47].

6.4.2 AND gate

In order to implement AND gate, the thermal lens signal for different pump powers is obtained and is shown in figure 6.6.
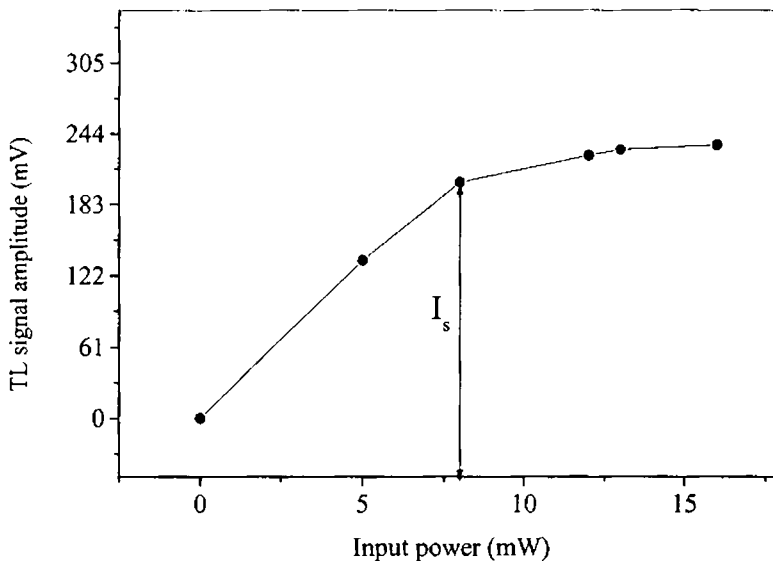

Figure 6. 6 Input-output characteristics for AND gate.

From the figure it is clear that when both pump beams (inputs) are absent, there occurs no thermal lens phenomenon, and hence the thermal lens signal is zero, which gives the first condition of Table 2. If the inputs are below the threshold I_s, i.e., either I_1 or I_2 is less than I_s, the thermal lens signal is low and can be considered as zero. I_1 and I_2 together produce aberrated thermal lens, which gives maximum thermal lens signal that corresponds to the last condition of Table 2. Saturation of intensity, I_s, depends on the concentration of the dye in the matrix.

Table 2. AND gate

(monitoring the TL signal; I_1, $I_2 < I_s$, $I_1 + I_2 > I_s$,)

I_1	I_2	TL output
0	0	0
0	1	0
1	0	0
1	1	1

6.4.3   OR gate

By adjusting the pump powers we can implement the OR gate also. When both the inputs are low, the TL signal is low. Adjust the inputs such that I_1 or I_2 is greater than I_s and the out put is high, as is evident from Table 3.

Table 3. OR gate

(monitoring the TL signal; I_1 & I_2 > I_{s},)

I_1	I_2	TL output
0	0	0
0	1	1
1	0	1
1	1	1

Absorbed power must not be so large to introduce photodegradation of the dye. It is a well-established fact that the PMMA matrix does not undergo any change in its chemical or any other physical properties at very low laser powers as we have used in the present investigation [45-47].

6.5 Conclusion

At present, all-optical digital computer is only at its infancy and there does not exist any complete systems. Intensive research is currently being pursued to attain this goal. Most of the optical devices and concepts of the present day are based on hybrid technology. Newer advances have produced a variety of thin films and optical fibers that make optical interconnections and devices practical. The thermal lens technique has been successfully implemented for realizing basic logic gates. The advantage of this technique is that basic logic gates can

be realized with optical beams of moderate intensity. In contrast to other optical logic gates, this method does not require any nonlinear optical materials, apart from being sensitive. The sample used for the present work is Rhodamine 6G doped PMMA, which is photochemically stable at moderate laser powers.

References

1. J. B. Flannery, *IEEE trans. Electron Devices ED*-20, 941 (1973).
2. A. W. Lohmann, *Nonlinear optics. & Optical. Computing*, (Ed. S. Martellucci and A. N. Chester, Plenum Press, New York, 1990).
3. H. Jerominek, F. Picard and D. Vincent, *Opt. Eng.* 32, 2092 (1993).
4. A. Niiyama and M. Koshiba, *J. Lightwave Tech.* 16, 162 (1998).
5. P. Mataloni, O. Jedrkiewicz, F. De Martini, *Phys. Lett. A* 243, 270 (1998).
6. A. J. Poustie, K. J. Blow, A. E. Kelly and R. J. Manning, *Opt. Commun.* 168, 89 (1999).
7. S. Yu and S. R. Forrest, *J. Lightwave Tech.* 11, 1659 (1993).
8. J. I. Song, Y. H. Lee, J. Y. Yoo, J. H. Shin A. Scherer and R. E. Leibenguth, *IEEE Photon Technol. Lett.* 5, 902 (1993).
9. A. G. Kirk, H. Thienpont, A. Goulet, P. Heremans, G. Borghs, R. Vounckx, M. Kuijk and I. Veretennicoff, , *IEEE Photon Technol. Lett.* 8, 467 (1996).
10. B. Lu, Y. Chen, J. Cheng, M. J. Hafich, J. Klem and J. C. Zolper, , *IEEE Photon Technol. Lett.* 8, 166 (1996).
11. A. V. Marquina, A. T. Jacome and F. R. Carrillo, *Opt. Eng.* 40, 2261 (2001).
12. T. Zhang, C. Zhang, G. Fu, Y. Li, Q. W. Song, B. parsons and R. R. Birge, *Opt. Eng.* 39, 527 (2000).
13. G. R. Collecutt and P. D. Drummond, *Opt. Commun.* 184, 237 (2000).
14. D.G. Feitelson, *Optical computing, A survey for computer scientists*, MIT Press, England page 168, 1992.
15. M. .H. Hassoun and R. Arrathoon, *Opt. Eng.* 25, 56 (1986).
16. S. L. Hurst, *Opt. Eng, 25, 44 (1986].
17. J. Fleuret, *Appl. Opt.* 23, 1609 (1984).
18. D. M. Pepper, *Scientific American.* 254, 56 (1986).
19. E. Abraham, C. T. Seaton and S. D. Smith, *Scientific American* 2489, 85 (1983).
20. H. Nishihara, M. Haruna and T. Suhara, *Optical integrated circuits* (McGraw Hill, New York 1987).
21. N. I. Ansari, S. Madhu, Athreya and S. V. R. Gutta, *IEEE Potentials*, 33 (1992).
22. D. J. Welker and M. G. Kuzyk, *Appl. Phys. Lett.* 69, 1335 (1996).
23. A. Suzuki, T. Ishii and Y. Maruyama, *J. Appl. Phys.* 80, 131 (1996).

24. *K. Sasalki and T. Nagamura, J. Appl. Phys.* 83, 2894 (1998).
25. . *Y. H. Pramono, M. Geshiro, T. kitamura and S. Sawa IEICE Trans.Electron, EB3-C,* !7, 55 (2000)
26. Y. Fainman, C. C. Guest and S. H. Lee, *Appl. Opt,* 25, 1598 (1986).
27. L. A. Wang, S. H. Chang and Y. F. Lin, *Opt. Eng.* 37, 1011 (1998).
28. H. Lee, H. Yau and N. Cheng, *Opt. Eng.* 37, 2156 (1998).
29. R. Giust, J. Goedgebuer and N. Butterlin, *Opt. Commun.* 181, 279 (2000).
30. P. W. Smith, *Opt. Engg.* 19, 456 (1980).
31. C. Hu and J. R. Whinnery, *Appl. Opt.* 12, 72 (1973).
32. H. L. Fang, R. L. Swofford, *The thermal lens in absorption spectroscopy,* in D. S. Kliger (Ed), *Ultra sensitive laser Spectroscopy.* Academic press, New York, 1983.
33. S. E. Bialkowski, *Photothermal spectroscopy methods for chemical analysis,* in; J. D. Winefordner (Ed), Chemical analysis, Vol 134, Wiley, New York, 1996, chapter 1.
34. H. Weichel, *Laser beam propagation in the atmosphere,* Ed. R. F. Potter, Spie Opt. Eng. Press. USA. (1990).
35. R. Friend, J. Burroughes and T. Shimoda, *Lasers and Optics,* 35 (1999).
36. I. D. W. Samuel, *Phil. Trans. R. Soc. Lond. A,* 358, 193 (2000).
37. A. Costela, I. Garcia-Moreno, J. M. Figuera, F. Amat-Guerri and R. Sastre, *Laser Chem.* 18, 63 (1998).
38. F. L. Arbeloa, T Lopez Arbeloa, I. Lopez Arbeloa, A. Costela, I. Garcia-Moreno, J. M. Figuera, F. Amat-Guerri and R. Sastre, *Appl. Phys. B* 64, 651 (1997).
39. A. Suzuki, T. Ishii and Y. Maruyama, *J. Appl. Phys.* 80, 131 (1996).
40. H. Franke, *Appl. Opt.* 23, 2729 (1984).
41. Magda A.El-Shahawy , *Polymer Testing* 19, 821 (2000).
42. M. Gupta, V. K. Sharma, A. Kapoor and K. N. Tripathi, *J. Opt.* 28, 37 (1997).
43. K. M. Dyumaev, A. A. Manenkov, A. P. Maslyukov, V. S. Nechitailo and and A. M. Prokhorov, *J Opt. Soc. Am. B* 9, 143, 1992.
44. F. Amat, A. Costela, J. M. Figuera, F. Florido and R. Sastre, *Chem. Phys. Lett.* 209, 352 (1993)
45. M. L. Ferrer,F. Amat, A. Costela, J. M. Figuera, F. Florido and R. Sastre, *Appl. Opt.* 33, 2266 (1994)].
46. A. G. Nibu, B. Aneeshkumar, P. Radhakrishnan and C. P. G. Vallabhan, *J. Phys. D: Appl. Phys.* 32, 1745 (1999).
47. H. Abdeldayem, D. O. Frazier, M. S. Paley and W. K. Witherow, *Recent Advances in Photonic Devices for Optical computing,(* NASA Marshall Space Flight Center, Space Sciences Laboratory, Huntsville, al 35812, 2000).

7

Kinetics of chemical reactions-An application of Thermal lens effect

This chapter explains the dual beam thermal lens technique employed to investigate reaction kinetics of chemical reactions in solutions. Concentration dependence of rate of reaction of potassium iodide and potassium dioxy persulphate is monitored using this technique. 532 nm radiation from a diode pumped Nd:YVO$_4$ (cw) is used as the excitation source to generate thermal lens in the medium and the lens is probed using 632.8 nm from a He-Ne laser. The time dependence of thermal lens signal strength provides the reaction rate. The rate of reaction is found to be proportional to the concentration of the reactants or products of the reaction. Studies show the enhancement of reaction speed with concentration of the reactants as is well known in the field of chemical kinetics.

7.1 Introduction

Kinetic studies provide very valuable information about reaction mechanisms and this subject includes empirical studies of the effects of reactants or products concentrations, temperature and hydrostatic pressure on reactions of various types. The first kinetic measurement was done by Wilhelmy in 1850 for the rate of inversion of sucrose. The important result to which he arrived was that the rate of reaction at any instant was proportional to the concentration of sucrose remaining at that time. A similar conclusion was reached by Berthelot and St. Gilles in 1862. In 1867 Harcourt and Eason investigated the reaction between potassium permanganate and oxalic acid.

Conventional techniques such as stopped flow and temperature jump are used to measure the kinetics of chemical reactions [1, 2]. These techniques are based on the measurement of the changes in the optical absorbance of the reactants or the products. The absorbance measured by conventional method, has relatively low sensitivity. To get a measurable signal, higher concentrations of the reagents are needed. The use of high concentration accelerates the rate of reactions.

Thermal lens effect which is one of the photothermal phenomena has been demonstrated to be a sensitive method for low absorbance measurements [3-8]. Haushalter et al demonstrated the usefulness of TL technique to study the reaction of the enzyme catalysed oxidation of dopamine by polypheneyl oxidase [9]. Franko and Tran [10-12] modified the theory of thermal lens effect and showed that TL technique can be effectively used for the study of slow as well as fast chemical reactions in liquids since the sensitivity of the technique is higher than that of the conventional optical transmission /reflection measurements because in the former case the absorbed energy is measured directly.

Let I_0 be the intensity of the incident radiation and I the intensity of the transmitted beam. Then the absorbed power is that degraded to heat, provided that there occurs no photochemical reaction and luminescence emission. We can write according to the principle of conservation of energy,

$$I_0 = I_{th} + I \qquad (7.1)$$

Absorbance is given by

$$= 1 - 10^{-A} \cong 2.303A \qquad (7.2)$$

In contrast to optical absorption, in which the time dependence of light absorption by a sample is monitored, thermal lens technique monitor the time dependence of heat evolution. As stated earlier TL effect is monitored as the far-field change in the probe beam spot size, by sampling the power of the probe beam that passes through a pinhole. The thermal lens signal is expressed as the relative change in intensity at the beam center as

$$S = \frac{I_0 - I}{I} = \frac{\Delta I}{I} \qquad (7.3)$$

where I_0 and I are the transmitted intensity before and after the formation of the thermal lens respectively.

Theory of TL effect gives

$$\frac{\Delta I}{I} = \frac{2.303 AP}{\lambda k} (-\frac{dn}{dT}) \qquad (7.4)$$

Above equation can also be written as

$$\frac{\Delta I}{I} = 2.303 AE \qquad (7.5)$$

$$E = \frac{P(-dn/dt)}{\lambda k} \qquad (7.6)$$

E represents the enhancement factor, A is the absorbance, P is the laser power,

λ is the pump laser wavelength, k is the thermal conductivity and $\dfrac{dn}{dT}$ is the

temperature coefficient of refractive index of the sample. For the same

absorbance, the relative variation of intensity $\dfrac{\Delta I}{I}$ is increased by a factor E,

called the enhancement factor [3]. Hence for low absorbance measurements this method has been demonstrated to be a sensitive technique.

7.2 Theory

The reaction rate of a chemical reaction is a quantity that defines how the concentration of a reactant or product changes with time. It may be expressed as

the rate of decrease of concentration C of reactants $(-\dfrac{dc}{dt}$), or as the rate of

increase of products of the reaction $(\dfrac{dx}{dt})$ where x is the concentration of the

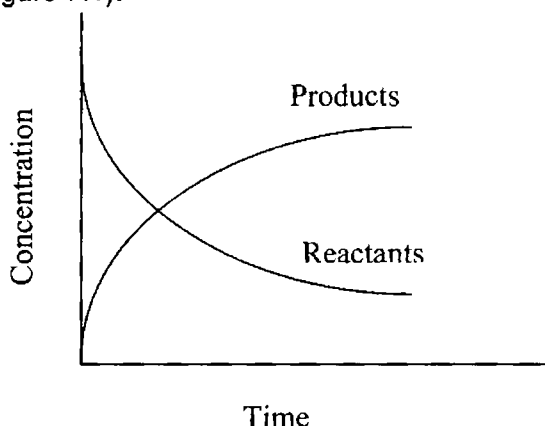products at time t (figure 7.1).

Figure 7.1 Reaction rate curve

From figure 7.1, one can write

$$C(t) = C_0 e^{vt} \qquad (7.7)$$

where v is the reaction rate.

In a kinetic study of a reaction there is no way of measuring the rate directly. Van't Hoff suggested the differential method in which the actual rate of reaction was determined by measuring the slope of concentration – time curve. The rate of reaction may be related to the concentration of a reactant by the equation [13]

$$v \alpha c^n \qquad \text{or} \qquad v = kc^n \qquad (7.8)$$

where k is the rate constant and n is the order of the reaction which is defined as the manner in which the rate of reaction varies with the concentration of the reacting substances or products of reaction. Thermal lens theories were derived on the assumption that the concentration of the species to be measured is constant with time [4, 14-17]. This is true for reactions whose rates are slow. Franko and Tran modified the theory of TL effect for fast reactions since changes in concentration are so large that they affect the thermal lens during excitation [11,12]. As is pointed out earlier TL signal strength is proportional to the concentration of the absorbing species in the medium. Hence, the time dependence of thermal lens signal strength will provide some information about the reaction rate.

7.3 Materials

An accurately weighed amount of potassium iodide is dissolved in water to give a concentration of 1×10^{-2} mol l^{-1}. From this stock solution, sample solutions with different concentrations ranging from 4.5×10^{-3} mol l^{-1} to 1×10^{-2} mol l^{-1} are

prepared. Potassium persulphate in water in the same concentration range is also prepared.

7.4 Experimental

Experimental setup is same as that described in chapter 2. The excitation beam from Nd:YVO$_4$ (cw) laser is modulated using a chopper. Equal concentration of 9.5*10^{-3} mol $^{-1}$1 of potassium iodide and potassium dioxy persulphate in water was made. 2ml of potassium iodide was taken in the cuvette (10mm thick) and 1ml of potassium dioxy persulphate is micropipetted into the cuvette. Following chemical reaction produces iodine

$$KI + K_2S_2O_8 \rightarrow I_2 + 2K_2SO_4 \qquad (7.9)$$

TL signal is monitored with respect to the concentration of iodine. Two drops of starch was added as indicator so as to enhance the absorption. During the reaction iodine is produced in the reaction cell. The absorption of 532 nm wavelength by the ground state iodine molecules brings them to their excited state from where several deactivation processes can take place during the excitation. Since the sample is nonfluorescent the entire electronic energy is converted into thermal energy, which is released in to the medium by nonradiative relaxation process. The density variation in the medium mimics the beam profile of the excitation beam and hence a refractive index gradient is created in the medium. This modification of refractive index leads to the growing of the effect of the virtual optical element called the TL. Since the lens formed is a divergent one, thermal blooming occurs. The propagation of the probe beam through the thermal lens results in spreading of the beam which causes the changes in the intensity at the centre of the probe beam. The probe beam is

coupled to a monochromator–PMT assembly using an optic fibre. The TL signal is detected as the relative change in the intensity of the probe beam centre at far field and data is detected and processed using a lock-in amplifier. The temperature is kept at 20°C through out the experiment since the rates of reactions are very sensitive to temperature.

7.5 Results and discussion

In the present study of the reaction between potassium iodide and potassium persulphate, as the concentration of iodine increases enhancement in the absorption of pump radiation is observed resulting in the increase in TL signal.

When the reaction is complete, no more iodine is liberated and hence the TL signal saturates. This is clear from the reaction rate curve shown in figure 7.2. It is obvious that the thermal lens signal strength is proportional to the concentration of the absorbing species in the medium. Since the concentration of the products formed is directly proportional to the reaction rate (eqn. 7.8), the time dependence of TL signal strength provides the reaction rate.

If C_I is the concentration of iodine liberated during the chemical reaction, TL signal at time t is

$$S(t) \propto C_I(t) \tag{7.10}$$

Or $\quad \dfrac{ds}{dt} \alpha \dfrac{dC_I}{dt}$

Initially $C_I(t) \propto t$

$\dfrac{dC_I}{dt}$ = a constant or $\dfrac{ds}{dt}$ = a constant K

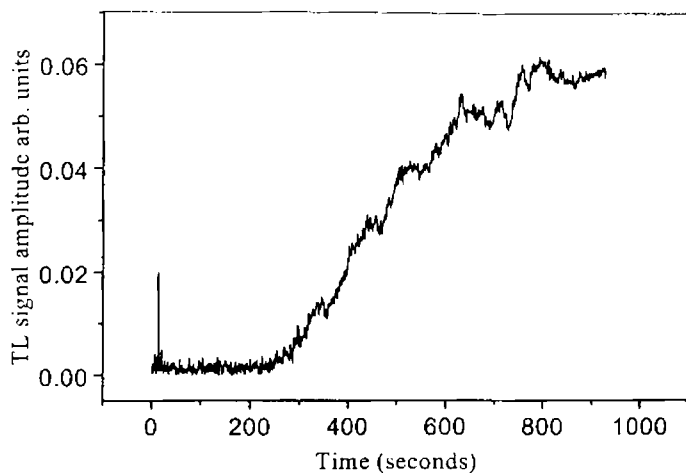*Figure 7.2 Thermal blooming curve for the reaction of potassium iodide and potassium persulphate of concentration 6.65x10^{-3} mol l^{-1}*
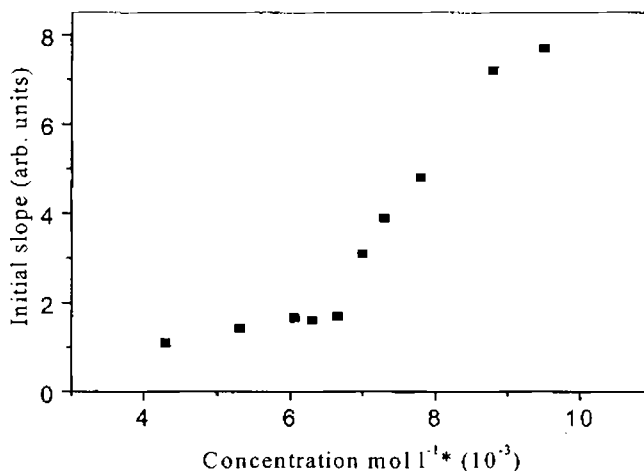

Figure 7.3 Plot showing the variation of initial slope with concentration of the reactants in the reaction cell. The plot shows the dependence of reaction rate K (arb. Unit/sec.)as function of reactant concentration.

At low concentration collision between the reactant molecules is low which leads to low reaction rate. An increase in the concentration of reactants results in enhanced collision probability between particles of the reactants. This results in the increase of the rate of reaction. Table shows the reaction rate at various reactant concentrations.

Concentration m mol l^{-1}	Initial slope
4.3	1.1
5.3	1.42
6.05	1.66
6.3	1.605
6.65	1.69
9.7	3.1
7.3	3.9
7.8	4.8
8.8	7.2
9.5	7.7

7.6 Conclusion

Compared to other conventional kinetic methods, the thermal lens technique provides kinetic results, which are not only accurate and precise but also can be obtained with reagents whose concentrations are about 100 times lower. The use of thermal lensing in chemical and analytical studies is still not a mainstream subject. However, it can be a very promising approach due to its special features

as a sensitive method of molecular spectroscopy. This may combine both basic and applied research, which undoubtedly expands the region of applications of thermo-optical spectroscopy. This ultra sensitive technique can be used for the kinetic determination of fast chemical reaction where reactants and or the products have low absorptivities.

References

1. Zuman P. and Patel R. *Techniques in organic Kinectics* (Wiley, New York,1984)
2. Frost A. A. and Pearson R. G. *Kinetics and Mechanism*, 2nd ed. (Wiley, New York, 1961)
3. N. J. Dovichi and J. M. Harris, Annal. Chem. 51,728 (1979).
4. Gordon J P, Lelte R C C, Moore R S and Porto S P S, *J. Appl. Phys.*36, 3 (1965).
5. C. Hue and J. R. Whinnery, *Appl.Opt.*12 (1973) 72.
6. A. Kurian, K. P. Unnikrishnan, P. Gopinath, V. P. N. Nampoori and C. P. G. Vallabhan, *J. Nonlinear Opt. Phys. & Mats* 10, 415 (2001).
7. C. V. Bindhu, S. S. Harilal, A. Kurian, V P N Nampoori and C P G Vallabhan,

    *J. Nonlinear Opt. Phys.& Mats.*7, 531 (1998).
8. H. L. Fang and R. L. Swofford, *J. Chem. Phys.*, 73, 2607 (1980).
9. J. P. Haushalter and M. d. morris, Appl. Spect. 34, 445 (1980).
10. M. Franko and C. D. Tran, Rev. Sci. Instrum., 62, 2430 (1991).
11. M. Franko and C. D. Tran, Rev. Sci. Instrum., 62, 2438 (1991).
12. M. Franko and C. D. Tran, Rev. Sci. Instrum., 67, 1 (1996)
13. K. J. Laidler, *Chemical kinetics*, Tata Mcgraw Hill Publishing (1990).
14. H. L. Fang and R. L. Swofford, J. Appl. Phys. 50,6609 (1979).
15. S. J. Sheldon, L. V. knight and J. M. Thorne, Appl. Opt. 21, 1663 (1982).
16. R. Vyas and R. Guptha, Appl. Opt., 27, 4701 (1988).
17. J. A. Sell, Photothermal investigations of solids and fluids, Academic press (1988).

8

Conclusions and Looking Forward

General conclusions and future scope of the work described in this thesis form the subject matter of this chapter

Previous seven chapters of the thesis described the use of thermal lens effect to characterize photonic materials. A schematic representation of the topics covered is given in fig 8.1
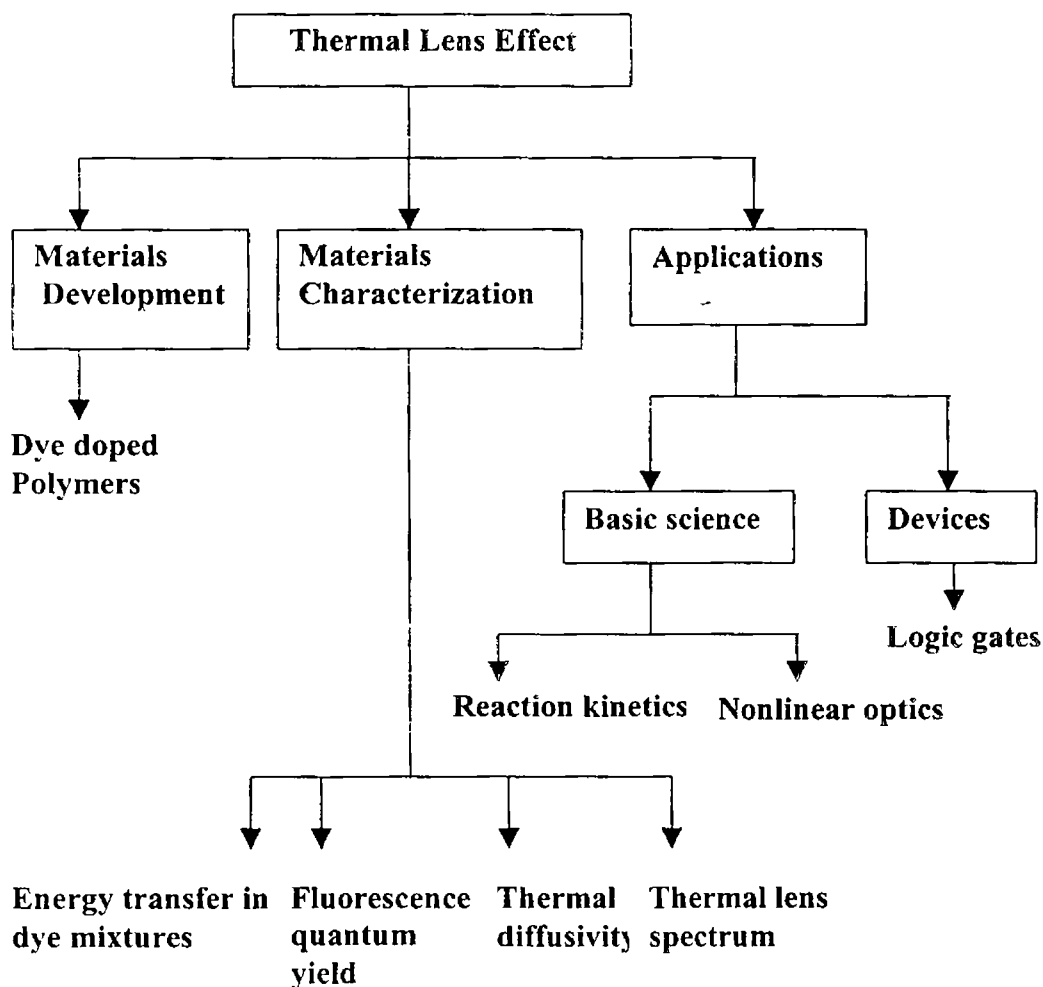

Fig 8.1 Schematic diagram of the work described in the present thesis

One of the important topics covered in the thesis is the preparation of dye doped polymers. Dye doped polymers are suitable for solid-state laser media. Dyes incorporated in solid matrices are also suitable for sensor applications. For example, pH values can be measured by monitoring the colour of the fluorescence light emitted by dye doped polymers. The effectiveness of thermal lens effect to evaluate fluorescence quantum yield and thermal diffusivity of such solid materials is discussed in this thesis. Energy transfer phenomena in dye mixtures are also described in detail.

It has been found that the study of thermal lens spectra of dyes in a broad spectral region can provide some information regarding the level selective nonradiative de-excitation processes. For example unlike in the case of crystal violet, rhodamine dye has a vibronic level from which nonradiatve relaxation is predominant. We also saw how the TL technique can be used to study two photon induces absorption using aniline as an example. Study of a time dependent chemical reaction using thermal lens effect is another topic, which is worth mentioning.

A work with an eye towards future viz., implementation of optical logic gates using thermal lens effect is an important contribution of the present thesis. Optical logic gates are essential components of optical computing and artificial neural network.

Future scope

What is described in the thesis is just an eye opener. Dyes incorporated in a matrix with appropriate physical, chemical and optical properties can be used to represent as artificial neurons to implement optical neural network. Learning mechanism can be incorporated by the proper choice of optical attenuators /

8 Conclusions

amplifiers so as to provide neural connection strength. Training of the neural network can be done by modifying the connection strengths. Such work will be

possible by a coherent mixing of diverse subjects like optics, electronics, chemistry, mathematics and information technology. Ability of free space connections between artificial neurons using light is an important advantage of optical neural network.

Another subject, which is worth pursuing, is the use of thermal lens spectroscopy to monitor time dependent chemical reactions. This will be helpful in understanding the kinetics of reaction as well as in identifying instabilities and chaos in complex chemical reactions.

Development of novel materials, both dyes as well as polymers, is another subject which will be of many applications in the field of Photonics. A field called Plastic Photonics has started to emerge. For example, plastic LEDs are already available commercially. Dye doped plastic fibres may work as fibre amplifier in the visible region.

Some of the above mentioned works have already got initiated in our laboratory. It is positive that there is the bright SUN in the horizon.